PAUL SCHERRER INSTITUT

M. Hildebrandt :: Group Detectors :: Paul Scherrer Institut

Gaseous Detectors and specific characteristics of Drift Chambers

PSI, LTP-Seminar, 08.05.2017

PAUL SCHERRER INSTITUT

Outline

introduction

- interaction of ionizing radiation with matter

part I

- fundamental processes in gaseous detectors
- operational modes

part II

- characteristics of drift chambers
- MEG and MEG II drift chambers

Interaction with Matter

Neutral and charged particles are detected through their interactions with matter:

- neutral particles $$I(x) = I_0 \cdot e^{-f(x)}$$
- charged particles $$E(x) = E_0 \cdot e^{-f(x)}$$

Interaction with Matter

- charged particles in gases : energy loss by ionization and excitation is described by Bethe-Bloch formula:

$$-\frac{dE}{dx} = 4\pi \cdot N_A \cdot r_e^2 \cdot m_e \cdot c^2 \cdot z^2 \cdot \frac{Z}{A} \cdot \frac{1}{\beta^2}\left[\ln \frac{2m_e \cdot c^2 \cdot \gamma^2 \cdot \beta^2}{I} - \beta^2 - \frac{\delta}{2}\right]$$

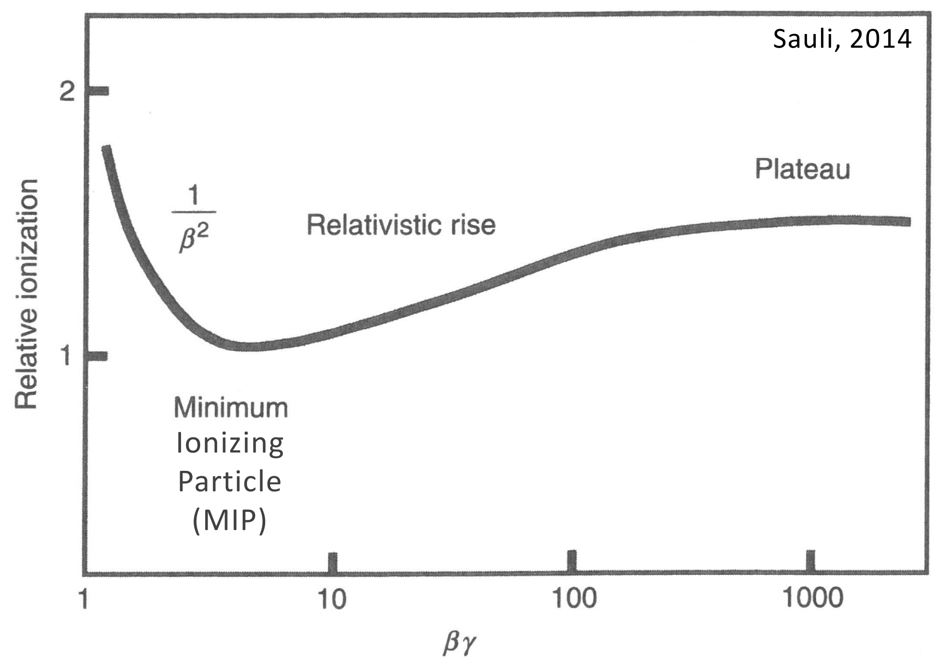

Interaction with Matter

- charged particles in gases : energy loss by ionization and excitation is described by Bethe-Bloch formula:

$$-\frac{dE}{dx} = \underbrace{4\pi \cdot N_A \cdot r_e^2 \cdot m_e \cdot c^2}_{} \cdot z^2 \cdot \frac{Z}{A} \cdot \frac{1}{\beta^2}\left[\ln\frac{2m_e \cdot c^2 \cdot \gamma^2 \cdot \beta^2}{I} - \beta^2 - \frac{\delta}{2}\right]$$

useful constant (and unit) from above:

$$4\pi \cdot N_A \cdot r_e^2 \cdot m_e \cdot c^2 = 0.3071 \frac{MeV}{g/cm^2}$$

→ energy loss $-\frac{dE}{dx}$ is usually given in units of $\frac{MeV}{g/cm^2}$ energy loss per surface mass density

→ energy loss *-dE* along track length *ds*

$$-dE = \frac{dE}{dx} \cdot \rho \cdot ds$$

ρ density $\left[\frac{g}{cm^3}\right]$

Interaction with Matter

Neutral and charged particles are detected through their interactions with matter:

- absorption or energy loss changes the properties of incident particle
- density ρ of detection medium influences the change of properties substantially

To follow a charged particle over a long track length, e.g. to measure

- bending radius of the particle trajectory in magnetic field to estimate the particle momentum

a low-density medium is required:

→ typical application of a gaseous detector

radiation length X_0: $E(x) = E_0 \cdot e^{-\frac{x}{X_0}}$ → $E(X_0) = \frac{1}{e} E_0$

→ filling gas has long radiation length

Radiation Length

radiation length X_0:

$$E(x) = E_0 \cdot e^{-\frac{x}{X_0}} \rightarrow E(X_0) = \frac{1}{e} E_0$$

material	Z	A	X_0[g/cm^2]	X_0/ϱ [cm]	E_c[MeV]
Hydrogen	1	1.01	63	700 000	350
Helium	2	4.00	94	530 000	250
Lithium	3	6.94	83	156	180
Carbon	6	12.01	43	18.8	90
Nitrogen	7	14.01	38	30 500	85
Oxygen	8	16.00	34	24 000	75
Aluminum	13	26.98	24	8.9	40
Silicon	14	28.09	22	9.4	39
Iron	26	55.85	13.9	1.76	20.7
Copper	29	63.55	12.9	1.43	18.8
Silver	47	109.9	9.3	0.89	11.9
Tungsten	74	183.9	6.8	0.35	8.0
Lead	82	207.2	6.4	0.56	7.40
Air	7.3	14.4	37	30 000	84
SiO_2	11.2	21.7	27	12	57
Water	7.5	14.2	36	36	83

Grupen, 1996

Characteristics of Gaseous Detectors

fundamental processes in gaseous detectors:

- creation of charge
- drift of charge
- amplification of charge
- detection of charge ("real" and induced)

Characteristics of Gaseous Detectors

fundamental processes in gaseous detectors:

- creation of charge
- drift of charge → gaseous electronics
- amplification of charge
- detection of charge ("real" and induced)

PAUL SCHERRER INSTITUT

Terminology – Gaseous Electronics

All relevant processes in the filling gas of the detector, in particular

- atomic / molecular physics, e.g.
  - scattering processes
  - rotational, vibrational, electronic excitations in meV – eV range,
  - ionisation, attachment and dissociation
- transport phenomena of charged particles in gases under the influence of electric or electric and magnetic fields, e.g.
  - drift velocity v_d
  - diffusion D_L, D_T
  - magnetic deflection angle $\alpha_{Lorentz}$

which are explored in

- kinetic theory and transport theory
- discharge physics and low energy plasma physics

are summarised under the expression "gaseous electronics".

Units in Gaseous Electronics

gaseous electronics scales with parameter E/N

reason: collision operator in Boltzmann transport equation is proportional to N

particle number density N

$$N = \frac{n}{V} = \frac{k_B \cdot T}{p}$$

→ E/N: 1 Townsend = 1 Td = 10^{-21} Vm^2
(Huxley, Crompton, Elford, 1966)

Sir J.S.E.Townsend
1868-1957

@ 20°C, 1 bar:

1 Td ≈ 250 V/cm

1Hx ≈ 0.025 T

→ B/N: 1 Huxley = 1Hx = 10^{-27} Tm^3
(Ness, 1991)
(Heylen, 1980: 10^{-23} Tm^3)

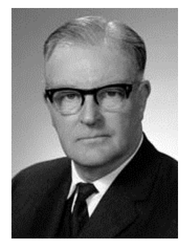

Sir L.G.H.Huxley
1902-1988

following units are often used:

- [E] = V/cm → T and p need to be defined
- [E/p] = V/(cm· torr), V/(cm·atm), V/(cm ·mmHg) → T needs to be defined
- [E/N] = V·cm^2

Primary Ionisation

creation of charge:

- charged and neutral particles dissipate part or all of their energy by generating electron-ion pairs
  - γ: point like
  - charged particle: along particle track

- primary ionisation n_0:
  - $n_0 = \Delta E / w$
  - w value: mean energy to produce electron-ion pair
  - w value > ionisation potential
    due to additional excitation of (inner shell) electronic, vibrational or rotational energy levels

separation of charge:

- electrical field to avoid recombination and to separate the electron-ion pairs

Primary Ionisation

Gas	Z	A	δ (g/cm^3)	E_{ex}	E_i (eV)	I_0 (eV)	W_i	dE/dx for MIP ($MeV/g\ cm^{-2}$)	dE/dx for MIP (keV/cm)	n_p (i.p./cm) a)	n_T (i.p./cm) a)
H_2	2	2	8.38×10^{-5}	10.8	15.9	15.4	37	4.03	0.34	5.2	9.2
He	2	4	1.66×10^{-4}	19.8	24.5	24.6	41	1.94	0.32	5.9	7.8
N_2	14	28	1.17×10^{-3}	8.1	16.7	15.5	35	1.68	1.96	(10)	56
O_2	16	32	1.33×10^{-3}	7.9	12.8	12.2	31	1.69	2.26	22	73
Ne	10	20.2	8.39×10^{-4}	16.6	21.5	21.6	36	1.68	1.41	12	39
Ar	18	39.9	1.66×10^{-3}	11.6	15.7	15.8	26	1.47	2.44	29.4	94
Kr	36	83.8	3.49×10^{-3}	10.0	13.9	14.0	24	1.32	4.60	(22)	192
Xe	54	131.3	5.49×10^{-3}	8.4	12.1	12.1	22	1.23	6.76	44	307
CO_2	22	44	1.86×10^{-3}	5.2	13.7	13.7	33	1.62	3.01	(34)	91
CH_4	10	16	6.70×10^{-4}		15.2	13.1	28	2.21	1.48	16	53
C_4H_{10}	34	58	2.42×10^{-3}		10.6	10.8	23	1.86	4.50	(46)	195

Sauli, 1977

a) i.p. = ion pairs

Primary Ionisation

Gas	Z	A	δ (g/cm³)	E_{ex}	E_i (eV)	I_0	W_i	dE/dx for MIP (MeV/g cm⁻²)	(keV/cm)	n_p (i.p./cm) a)	n_T (i.p./cm) a)
H_2	2	2	8.38×10^{-5}	10.8	15.9	15.4	37	4.03	0.34	5.2	9.2
He	2	4	1.66×10^{-4}	19.8	24.5	24.6	41	1.94	0.32	5.9	7.8
N_2	14	28	1.17×10^{-3}	8.1	16.7	15.5	35	1.68	1.96	(10)	56
O_2	16	32	1.33×10^{-3}	7.9	12.8	12.2	31	1.69	2.26	22	73
Ne	10	20.2	8.39×10^{-4}	16.6	21.5	21.6	36	1.68	1.41	12	39
Ar	18	39.9	1.66×10^{-3}	11.6	15.7	15.8	26	1.47	2.44	29.4	94
Kr	36	83.8	3.49×10^{-3}	10.0	13.9	14.0	24	1.32	4.60	(22)	192
Xe	54	131.3	5.49×10^{-3}	8.4	12.1	12.1	22	1.23	6.76	44	307
CO_2	22	44	1.86×10^{-3}	5.2	13.7	13.7	33	1.62	3.01	(34)	91
CH_4	10	16	6.70×10^{-4}		15.2	13.1	28	2.21	1.48	16	53
C_4H_{10}	34	58	2.42×10^{-3}		10.6	10.8	23	1.86	4.50	(46)	195

Sauli, 1977

a) i.p. = ion pairs

Primary Ionisation

Gas	Z	A	δ (g/cm³)	E_{ex}	E_i (eV)	I_0	W_i	dE/dx for MIP (MeV/g cm^{-2})	(keV/cm)	n_p (i.p./cm) a)	n_T (i.p./cm) a)
H_2	2	2	8.38×10^{-5}	10.8	15.9	15.4	37	4.03	0.34	5.2	9.2
He	2	4	1.66×10^{-4}	19.8	24.5	24.6	41	1.94	0.32	5.9	7.8
N_2	14	28	1.17×10^{-3}	8.1	16.7	15.5	35	1.68	1.96	(10)	56
O_2	16	32	1.33×10^{-3}	7.9	12.8	12.2	31	1.69	2.26	22	73
Ne	10	20.2	8.39×10^{-4}	16.6	21.5	21.6	36	1.68	1.41	12	39
Ar	18	39.9	1.66×10^{-3}	11.6	15.7	15.8	26	1.47	2.44	29.4	94
Kr	36	83.8	3.49×10^{-3}	10.0	13.9	14.0	24	1.32	4.60	(22)	192
Xe	54	131.3	5.49×10^{-3}	8.4	12.1	12.1	22	1.23	6.76	44	307
CO_2	22	44	1.86×10^{-3}	5.2	13.7	13.7	33	1.62	3.01	(34)	91
CH_4	10	16	6.70×10^{-4}		15.2	13.1	28	2.21	1.48	16	53
C_4H_{10}	34	58	2.42×10^{-3}		10.6	10.8	23	1.86	4.50	(46)	195

Sauli, 1977

a) i.p. = ion pairs

Primary Ionisation

Gas	Z	A	δ (g/cm^3)	E_{ex} (eV)	E_i (eV)	I_0 (eV)	W_i	dE/dx for MIP ($MeV/g\ cm^{-2}$)	dE/dx for MIP (keV/cm)	n_p (i.p./cm) a)	n_T (i.p./cm) a)
H_2	2	2	8.38×10^{-5}	10.8	15.9	15.4	37	4.03	0.34	5.2	9.2
He	2	4	1.66×10^{-4}	19.8	24.5	24.6	41	1.94	0.32	5.9	7.8
N_2	14	28	1.17×10^{-3}	8.1	16.7	15.5	35	1.68	1.96	(10)	56
O_2	16	32	1.33×10^{-3}	7.9	12.8	12.2	31	1.69	2.26	22	73
Ne	10	20.2	8.39×10^{-4}	16.6	21.5	21.6	36	1.68	1.41	12	39
Ar	18	39.9	1.66×10^{-3}	11.6	15.7	15.8	26	1.47	2.44	29.4	94
Kr	36	83.8	3.49×10^{-3}	10.0	13.9	14.0	24	1.32	4.60	(22)	192
Xe	54	131.3	5.49×10^{-3}	8.4	12.1	12.1	22	1.23	6.76	44	307
CO_2	22	44	1.86×10^{-3}	5.2	13.7	13.7	33	1.62	3.01	(34)	91
CH_4	10	16	6.70×10^{-4}		15.2	13.1	28	2.21	1.48	16	53
C_4H_{10}	34	58	2.42×10^{-3}		10.6	10.8	23	1.86	4.50	(46)	195

Sauli, 1977

a) i.p. = ion pairs

primary ionisation:

- ~100 e^-/cm for MIP
- not continuously distributed
- clustered along track length

Tube Counter

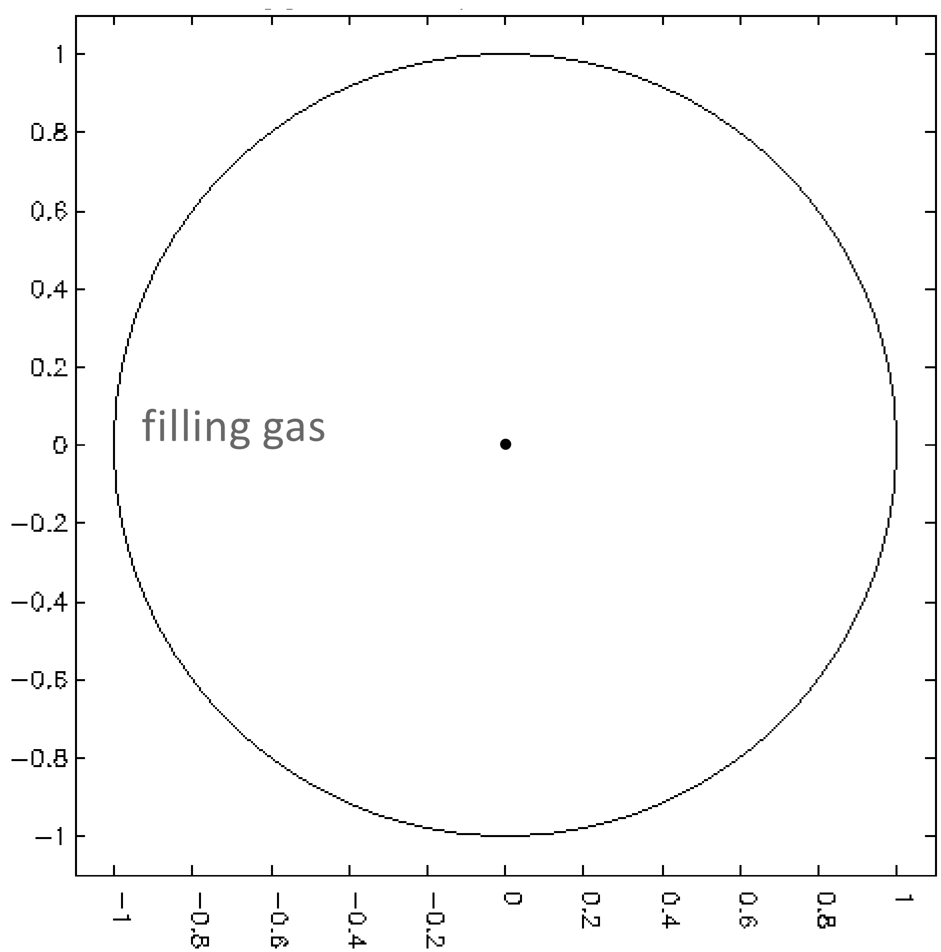

Tube Counter

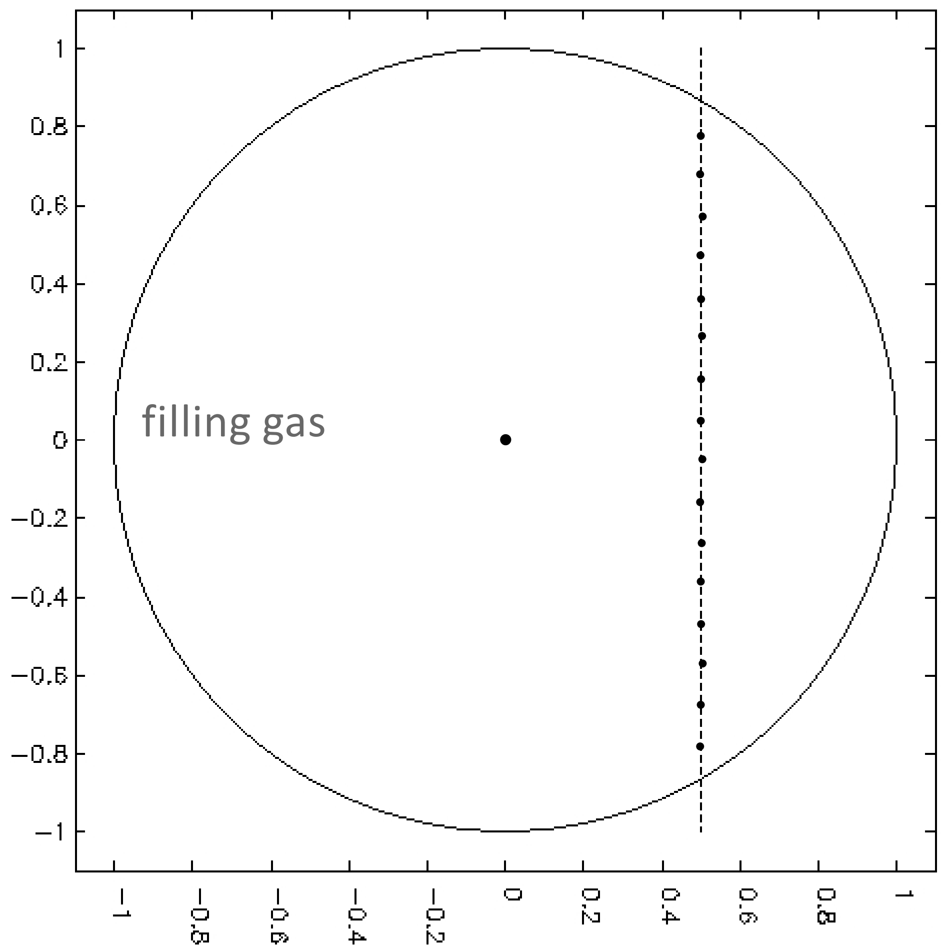

Tube Counter

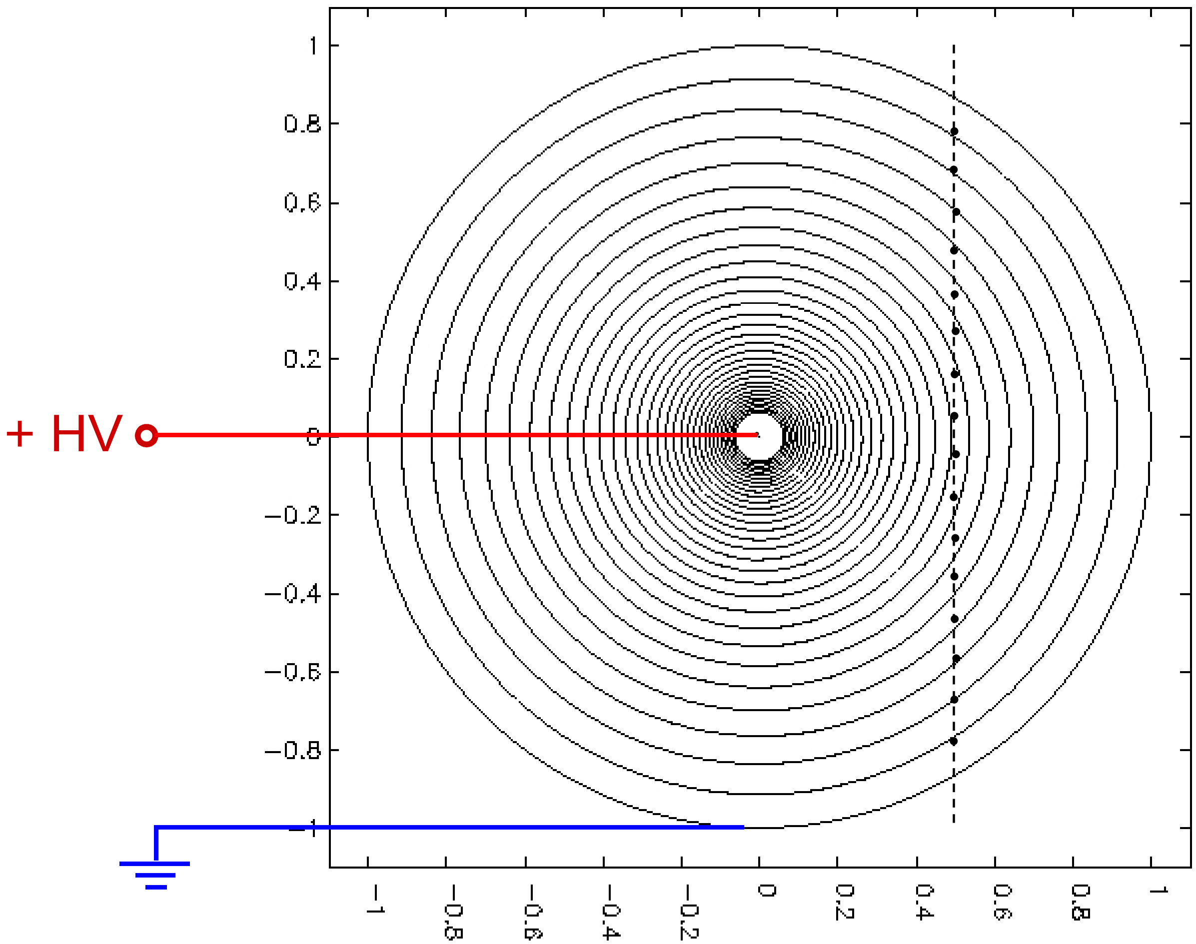

Tube Counter

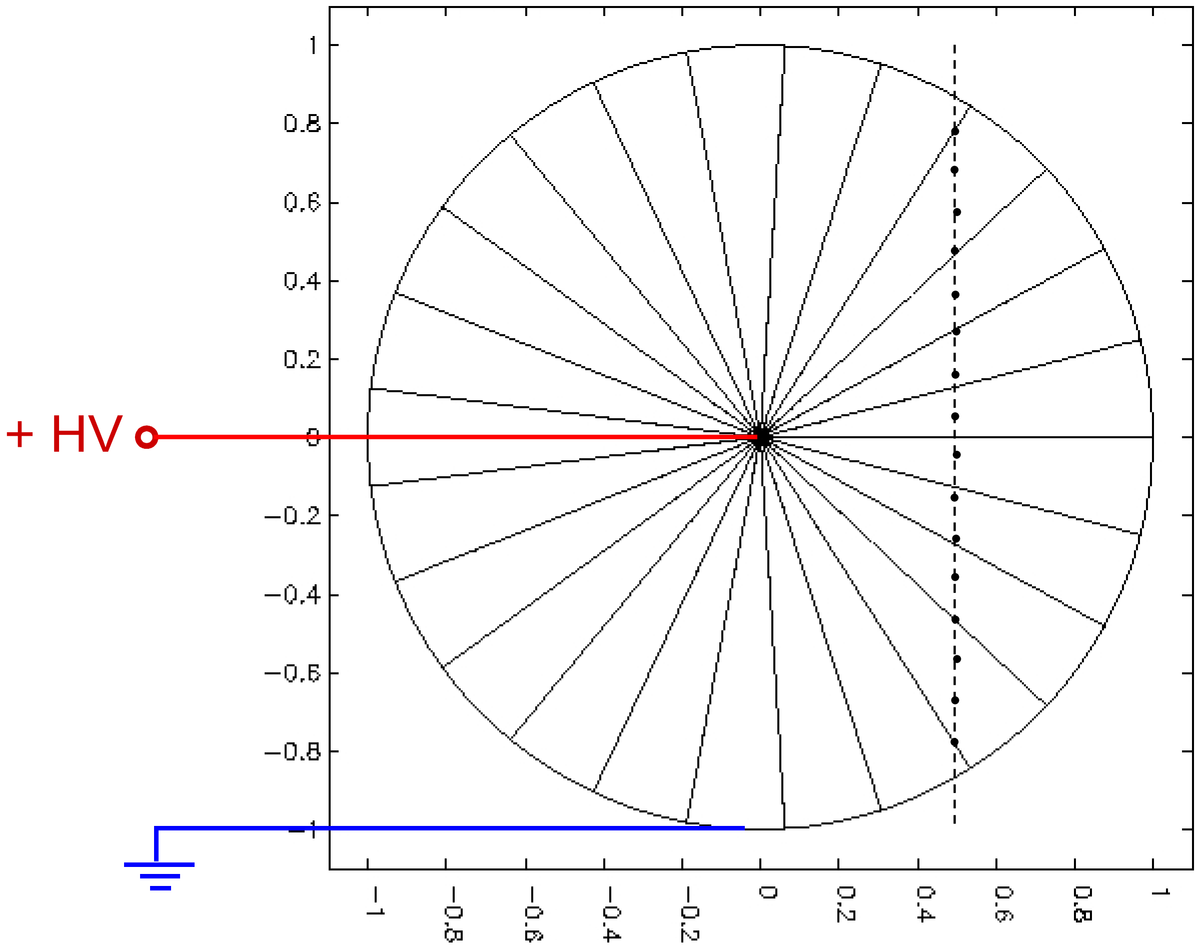

Drift of Charge

drift of charge:

- under the influence of external electric or electric and magnetic fields the electrons and positive ions drift towards their corresponding electrode
- electro-negative gas components / impurities will lead to a loss of charge due to electron attachment → loss of signal size

- equilibrium of energy loss in collisions and energy gain between collisions:
  - $v_{d,electron}$ ≈ 1-10 cm/μs
  - v_{d,ion^+} ~ 1000-times slower
    usually kT-limit → constant μ → $v_{d,ion} = \mu \cdot E$
  - D_T, D_L ≈ 100-500 μm/√1cm
  - magnetic deflection angle $\alpha_{Lorentz}$

Drift of Charge

electrons

- drift velocity

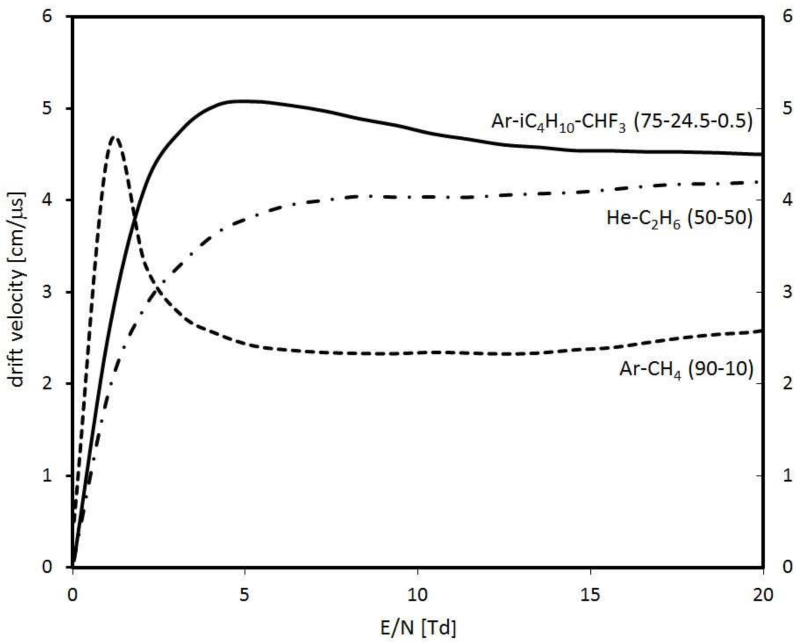

- diffusion

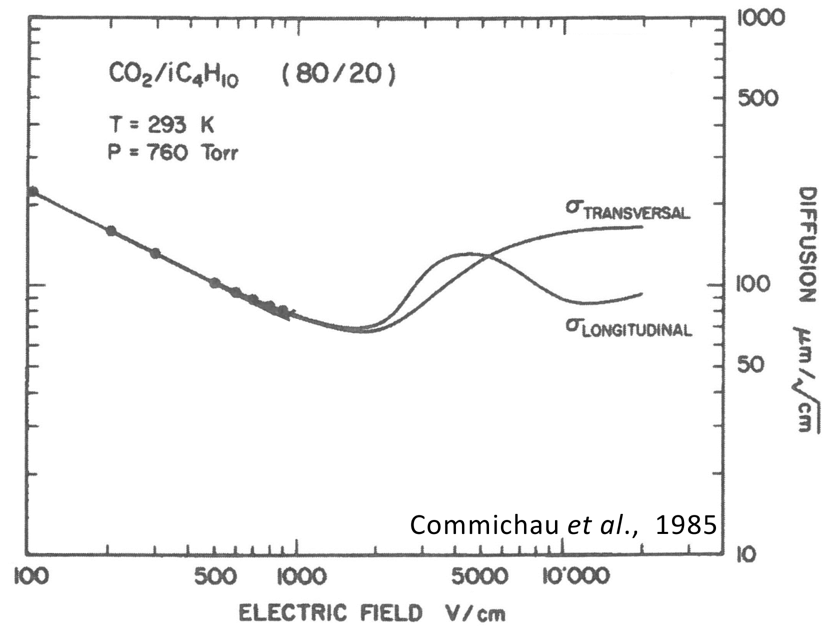

Drift of Charge

electrons ▪ drift velocity ▪ characteristic energy

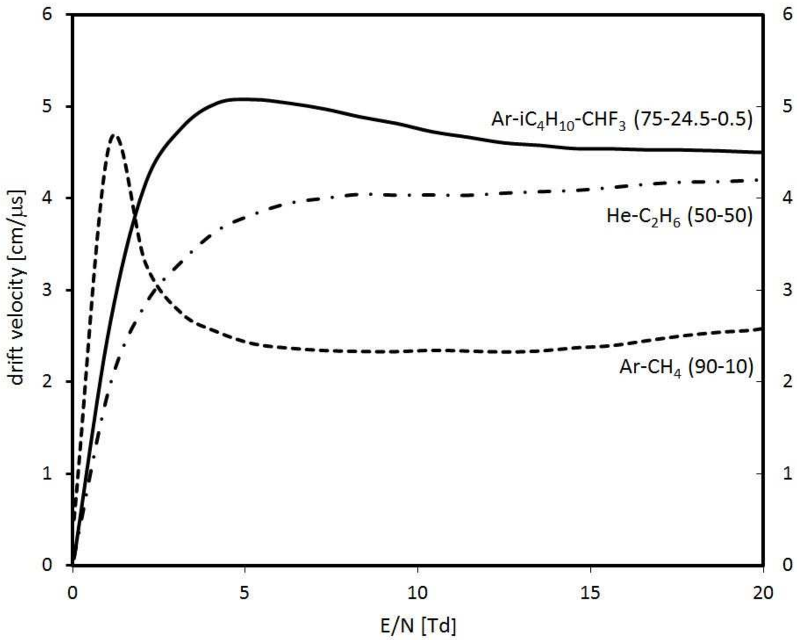

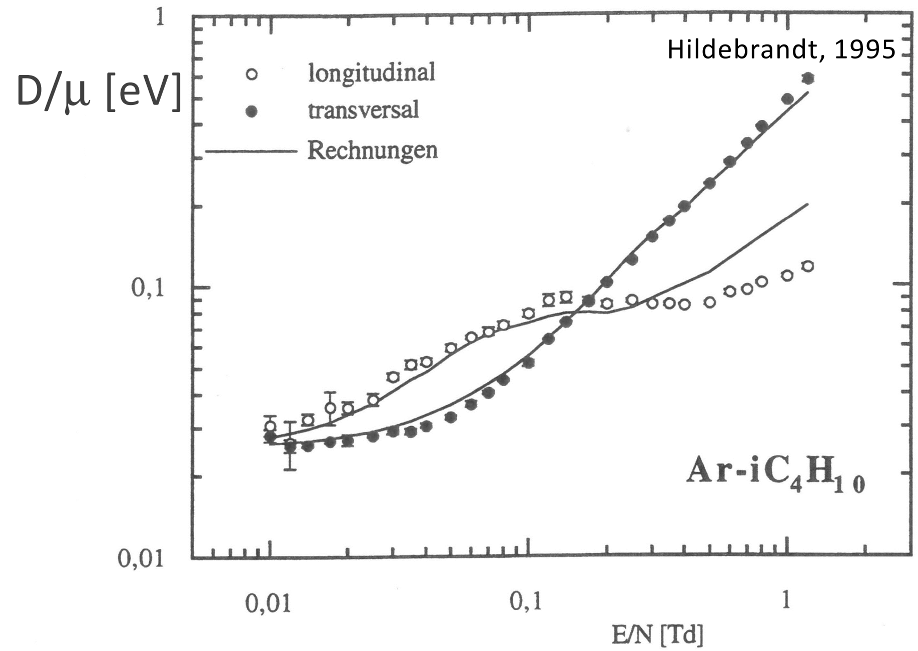

Drift of Charge

electrons ▪ drift velocity ▪ characteristic energy

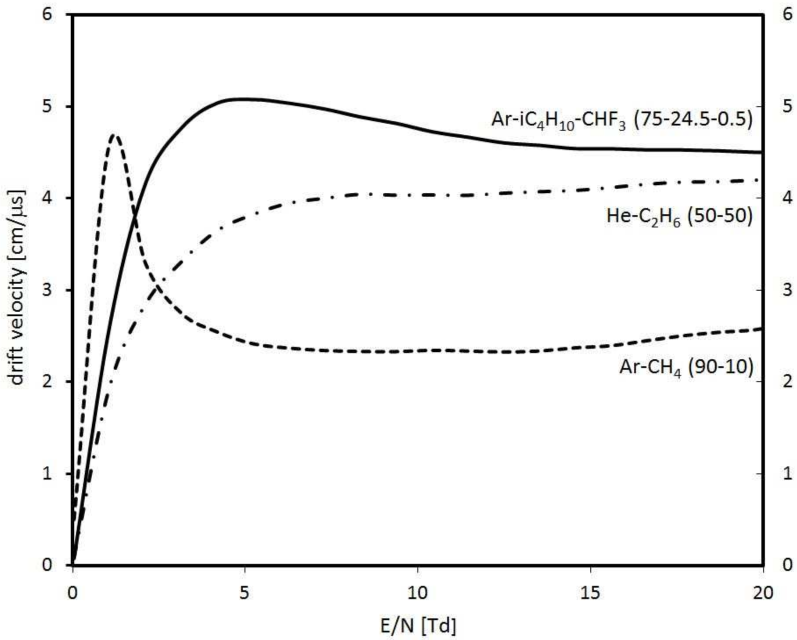

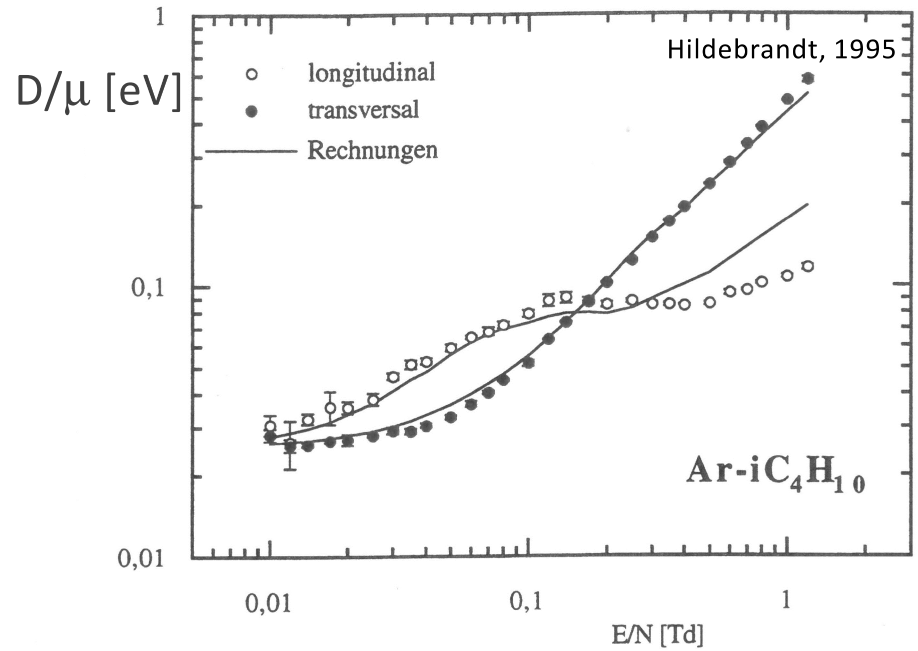

positive ions: mobility, diffusion (→ Viehland, Mason, McDaniel, Loeb, Townsend)

gas	λ_{ion}[cm]	D_{ion}[cm^2/s]	μ_{ion} $\left[\frac{cm/s}{V/cm}\right]$
H_2	$1.8 \cdot 10^{-5}$	0.34	13.0
He	$2.8 \cdot 10^{-5}$	0.26	10.2
Ar	$1.0 \cdot 10^{-5}$	0.04	1.7
O_2	$1.0 \cdot 10^{-5}$	0.06	2.2

Sauli, 1977; Grupen, 1996

Gas	Ion	Mobility [cm^2 V^{-1} s^{-1}]
Ar	Ar^+	1.54
He	He^+	10.4
CO_2	$CO_2{}^+$	1.09
Ar	$CH_4{}^+$	1.87
Ar	$C_2H_6{}^+$	2.06
Ar	$iC_4H_{10}{}^+$	2.15
Ar	$CO_2{}^+$	1.72

Tavernier, 2010

Drift of Charge

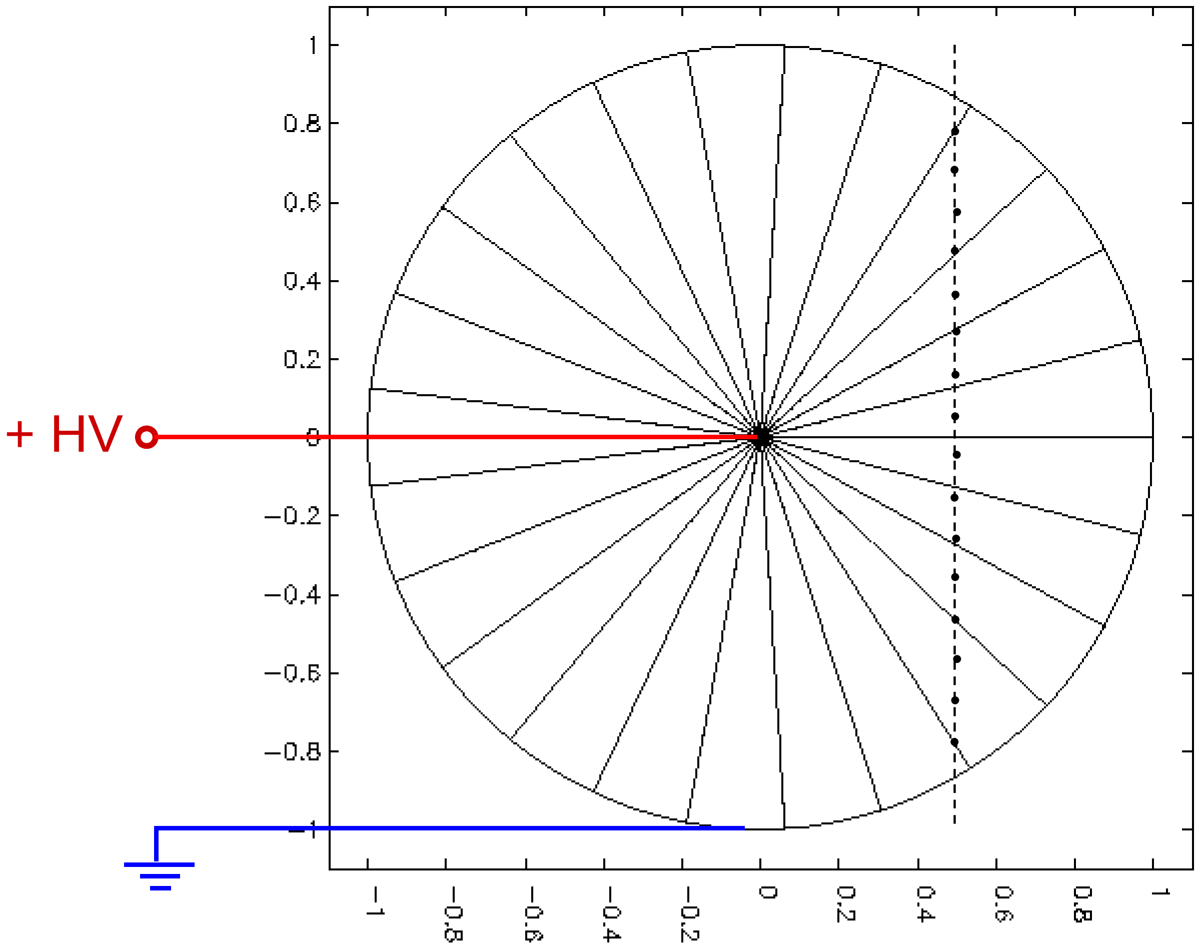

Drift of Charge

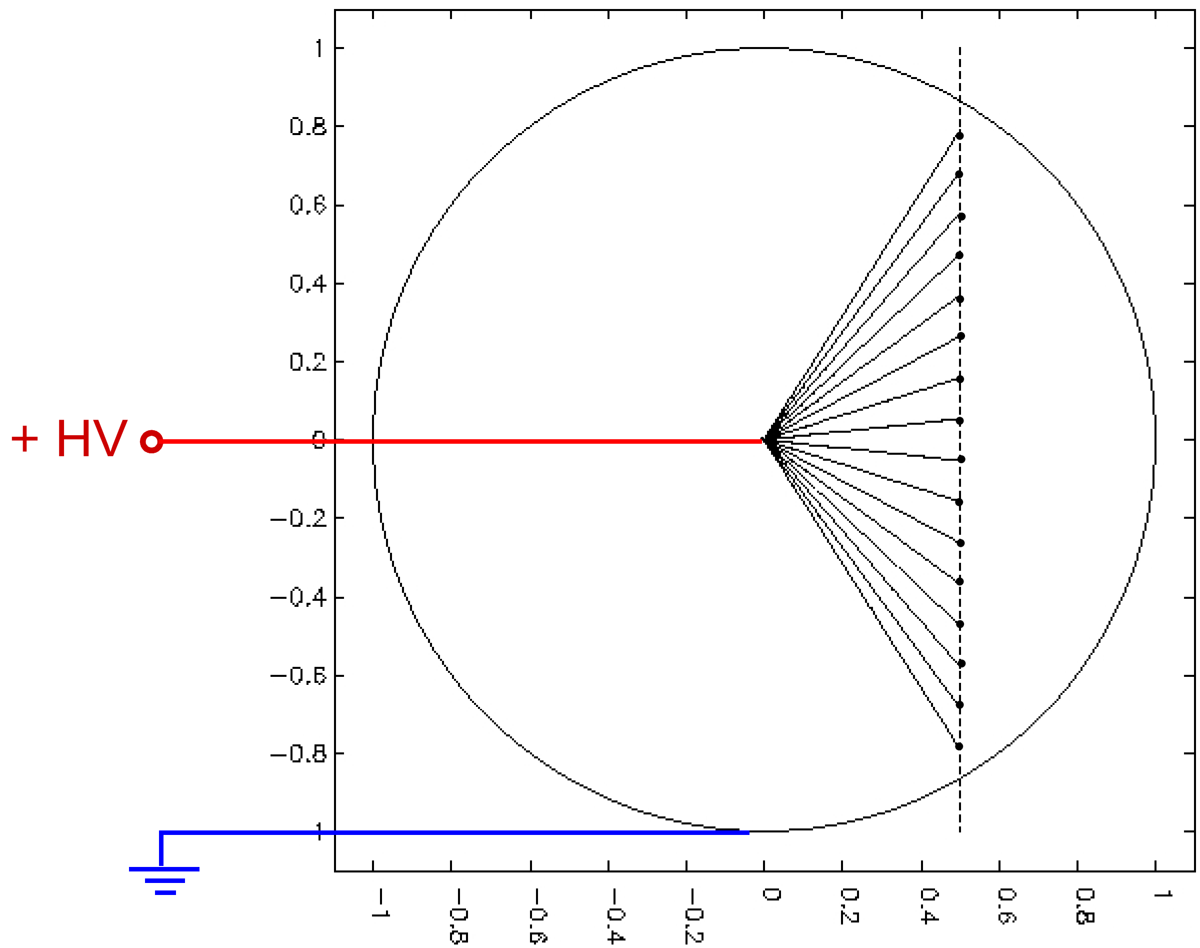

Amplification of Charge

Neither ~100 e^-/cm nor ~25 000 e^-/n-^{3}He-capture is a sufficient amount of charge
→ amplification inside gas volume before electronics is needed

amplification of charge:

- exceeds the electrical field ~10 kV/cm the drifting electron (from primary ionisation) gains sufficient energy between collisions so that $\varepsilon_{mean} < E_{ionisation}$
  → possible to create additional electron-ion pairs in collisions with neutral gas atoms or molecules
  → growing cascade forms an electron avalanche
  electron multiplication, "gas amplification", gas gain: typically ~10 – 10^6

Amplification of Charge

Neither ~100 e^-/cm nor ~25 000 e^-/n-^{3}He-capture is a sufficient amount of charge

→ amplification inside gas volume before electronics is needed

amplification of charge:

- exceeds the electrical field ~10 kV/cm the drifting electron (from primary ionisation) gains sufficient energy between collisions so that $\varepsilon_{mean} < E_{ionisation}$
  - → possible to create additional electron-ion pairs in collisions with neutral gas atoms or molecules
  - → growing cascade forms an electron avalanche
    electron multiplication, "gas amplification", gas gain: typically ~10 – 10^6
- avalanche process described by 1st Townsend coefficient, ionisation coefficient:
  - $\alpha_{Townsend}$
  - $[\alpha] = 1/\text{cm}$
  - total number of electrons: $n = n_0 \cdot e^{\alpha \cdot x}$ or $n = n_0 \cdot e^{\int \alpha(x) dx}$
  - gas gain: n/n_0

Amplification of Charge

ionisation coefficient α

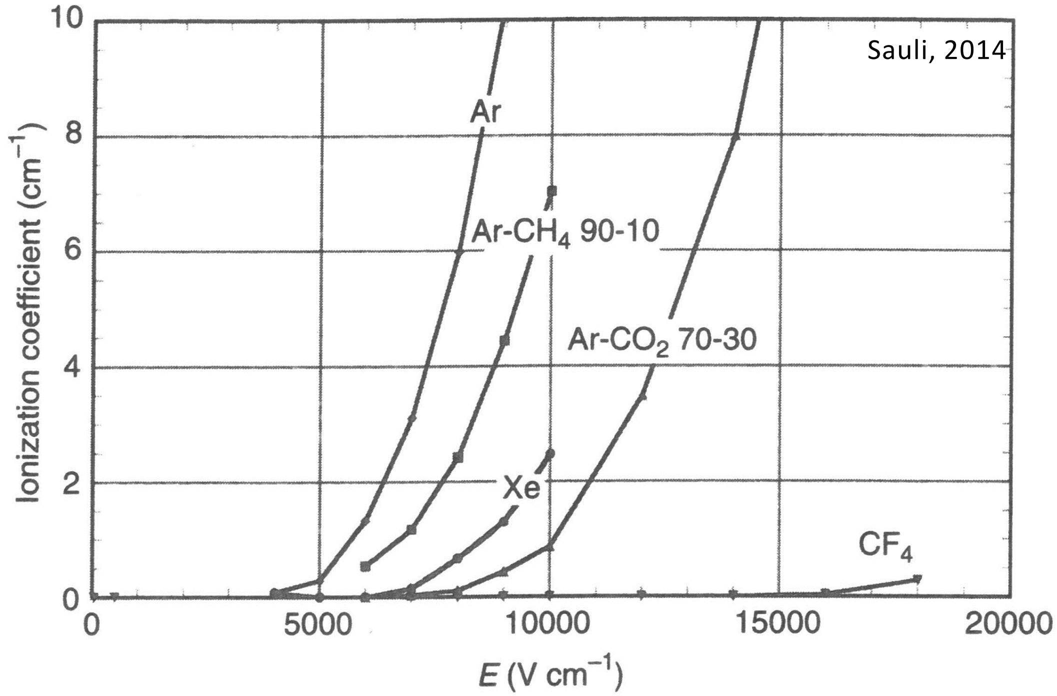

empirical formula (Korff, 1955)

$$\frac{\alpha}{p} = A \cdot e^{-\frac{Bp}{E}}$$

A, B: phenomenological constants

Gas	A ($\mathrm{cm^{-1}torr}$)	B ($\mathrm{V\,cm^{-1}torr^{-1}}$)
He	3	34
Ne	4	100
Ar	14	180
Xe	26	350
CO_2	20	466

Sauli, 2014

PAUL SCHERRER INSTITUT

Amplification of Charge

location of electron avalanche

- wire: diameter Ø ≈ 10 - 50 μm, gain ≤ 10^6

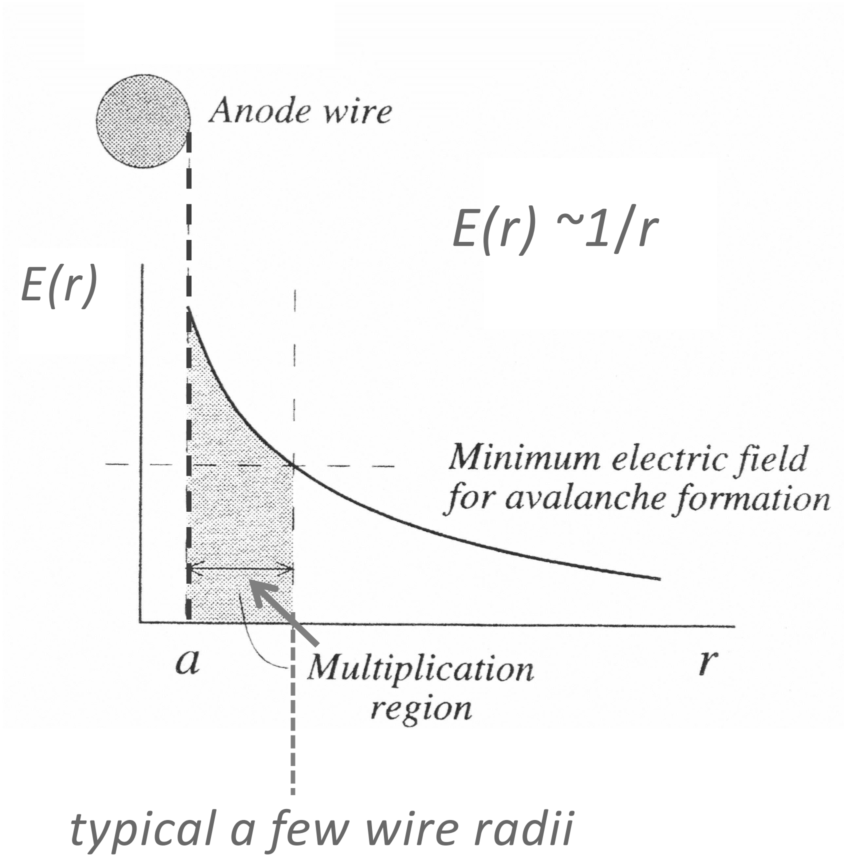

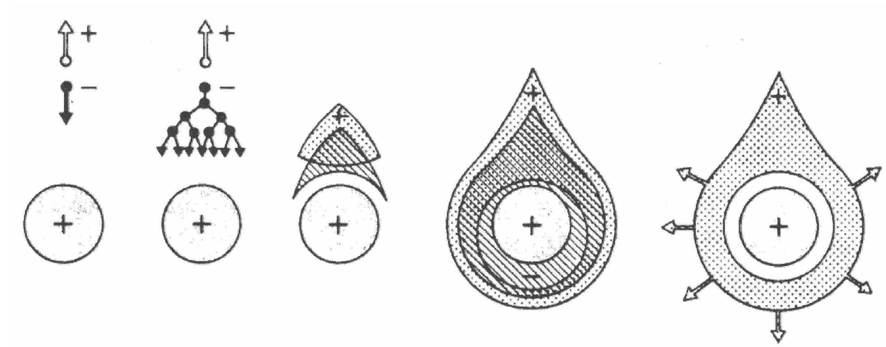

H.Raether, 1949
L.B.Loeb, 1960
G.Charpak, 1968

Amplification of Charge

location of electron avalanche

- wire: diameter Ø ≈ 10 - 50 μm, gain ≤ 10^6
- micro-strips: width ~10 μm, gain ≤ 10^4

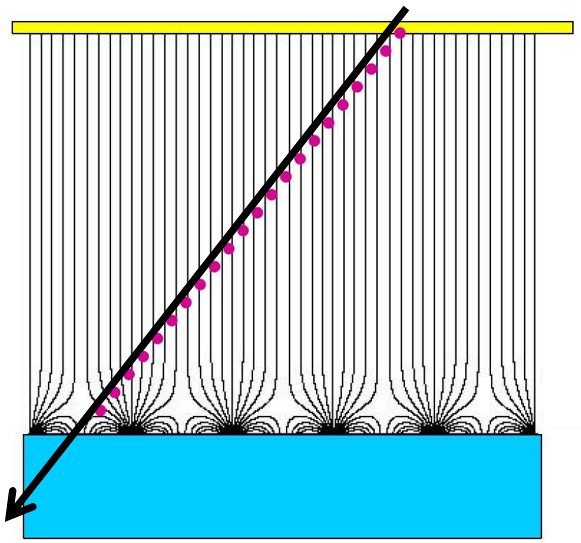

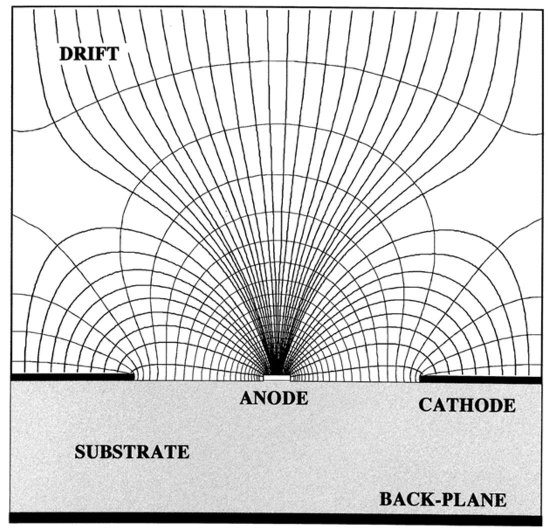

Oed, NIM A263 (1984) 351

1990's: MSGC supposed to be "all-purpose LHC tracking detector"

today: only D20 at ILL
(low gain operation)

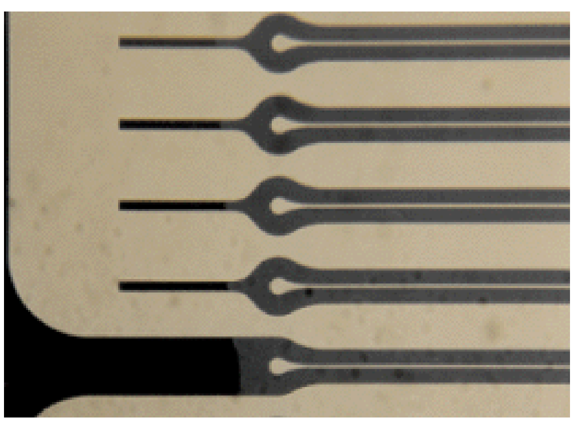

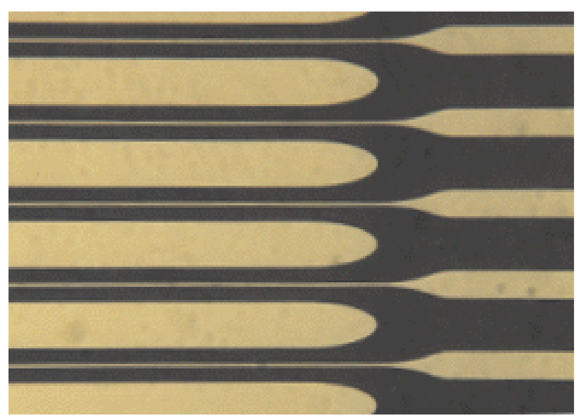

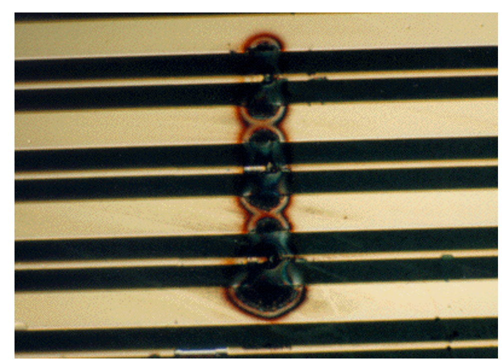

Amplification of Charge

location of electron avalanche

- wire: diameter Ø ≈ 10 - 50 μm, gain ≤ 10^6
- micro-strips: width ~10 μm, gain ≤ 10^4
- holes of Gas-Electron-Multiplier (GEM) foil: Ø ≈ 50 - 100 μm, gain ≤ 10^3

→ decoupling of amplification and charge collection

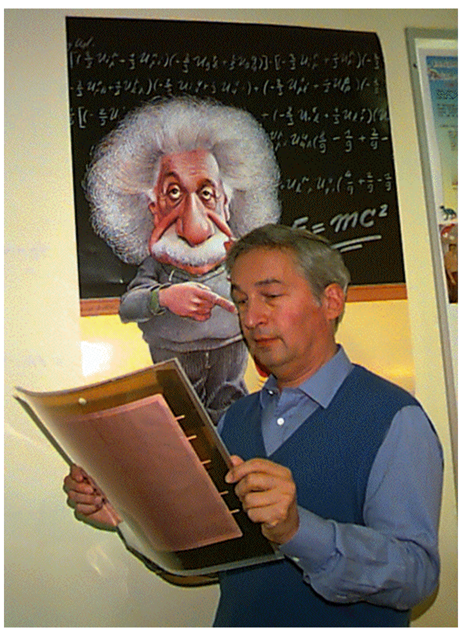

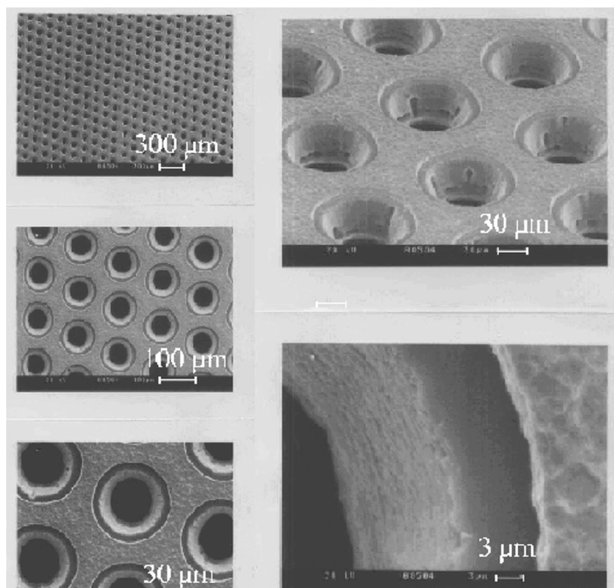

U. Werthenbach, Siegen

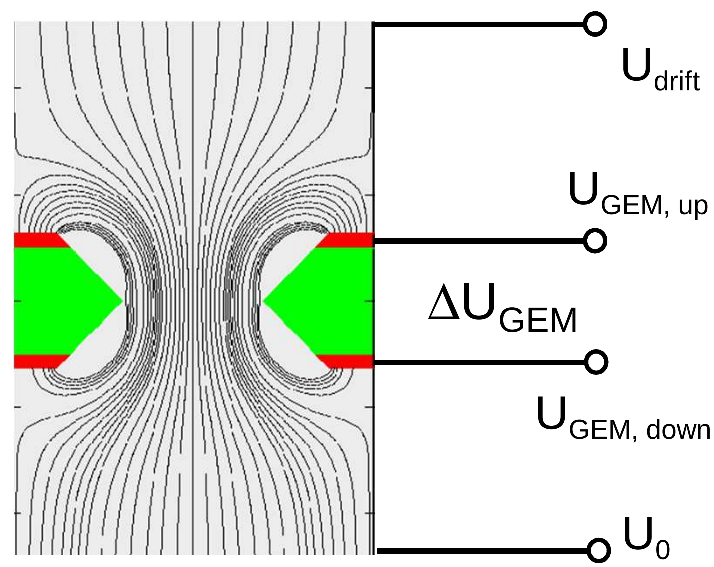

Sauli, NIM A386 (1997) 531

Amplification of Charge

location of electron avalanche

- wire: diameter Ø ≈ 10 - 50 μm, gain ≤ 10^6
- micro-strips: width ~10 μm, gain ≤ 10^4
- holes of Gas-Electron-Multiplier (GEM) foil: Ø ≈ 50- 100 μm, gain ≤ 10^3

  → combination of holes and strips: GEM-MSGC

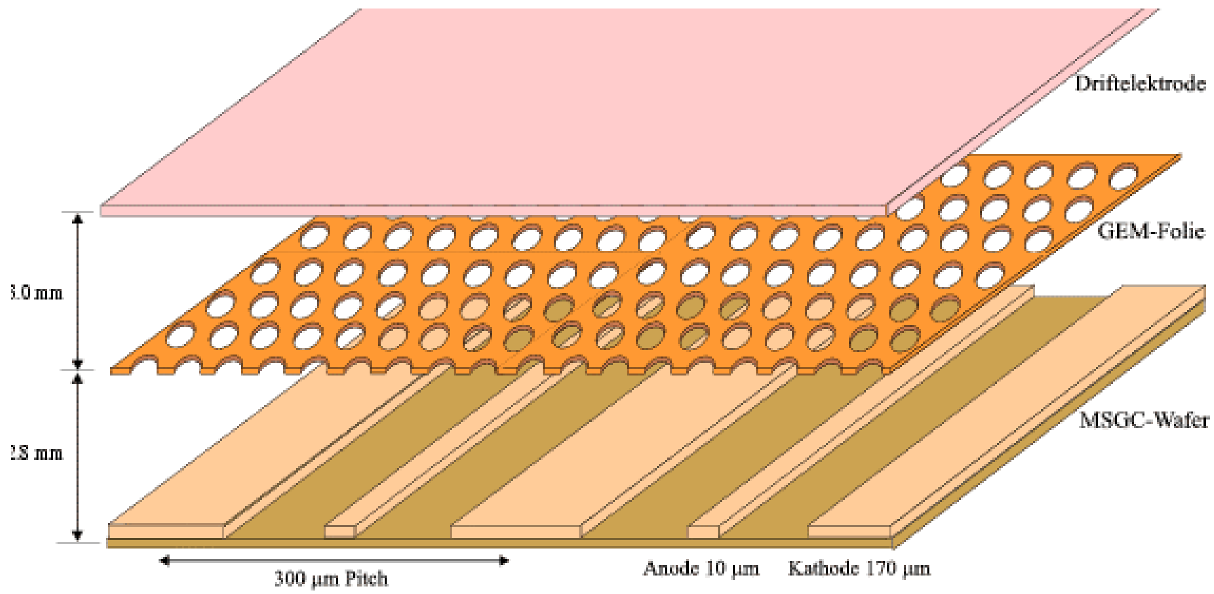

1990s: detector for Inner Tracker HERA-B

Universities Heidelberg, Siegen, Zürich and CERN

Amplification of Charge

location of electron avalanche

- wire: diameter Ø ≈ 10 - 50 μm, gain ≤ 10^6
- micro-strips: width ~10 μm, gain ≤ 10^4
- holes of Gas-Electron-Multiplier (GEM) foil: Ø ≈ 50- 100 μm, gain ≤ 10^3

  → multi-GEM detectors with dedicated readout structure

  - triple-GEM detector
    (LHCb inner tracker detector before Si)
  - 4-GEM stack
    (upgrade of ALICE TPC endplate)

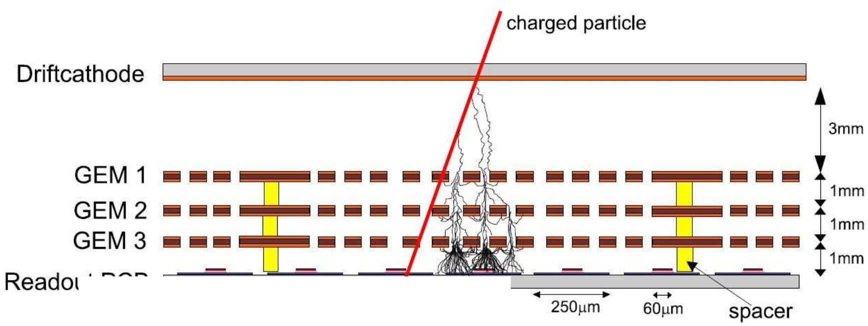

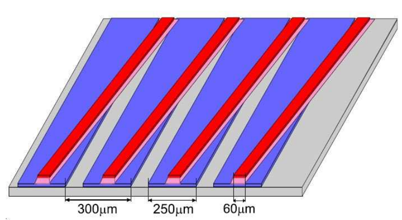

Ziegler, 2002

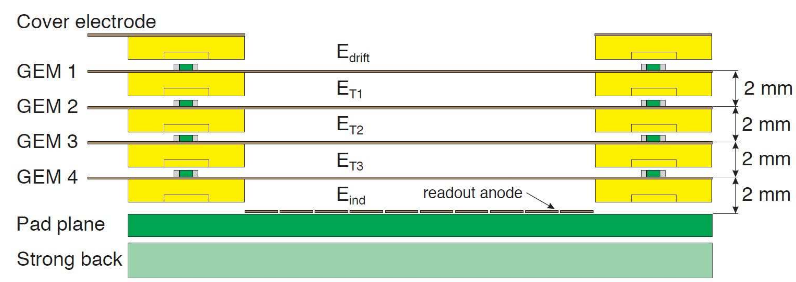

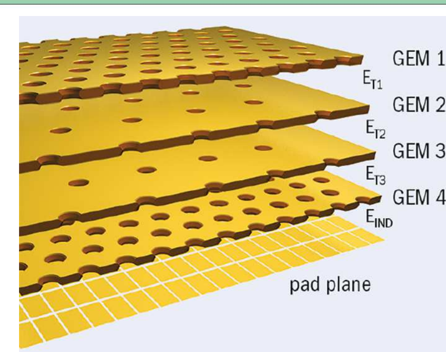

Amplification of Charge

location of electron avalanche

- wire: diameter Ø ≈ 10 - 50 µm, gain ≤ 10^6
- micro-strips: width ~10 µm, gain ≤ 10^4
- holes of Gas-Electron-Multiplier (GEM) foil: Ø ≈ 50- 100 µm, gain ≤ 10^3
- parallel-plate gap: MICRO-MEsh GAseous Structure (Micromegas), gain ≤ 10^5

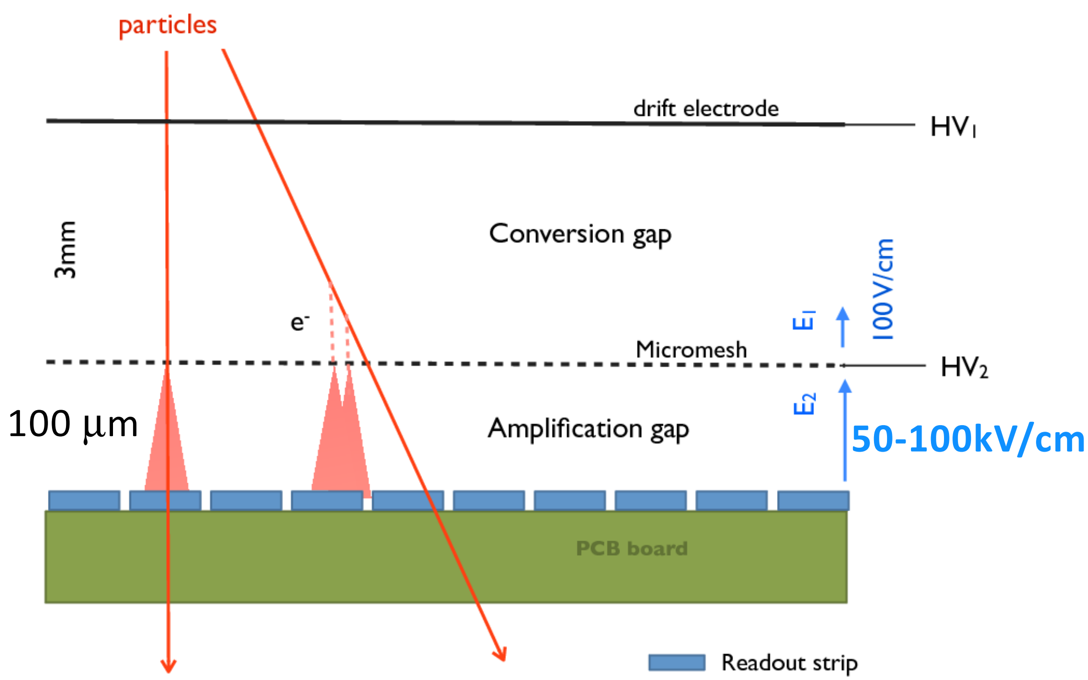

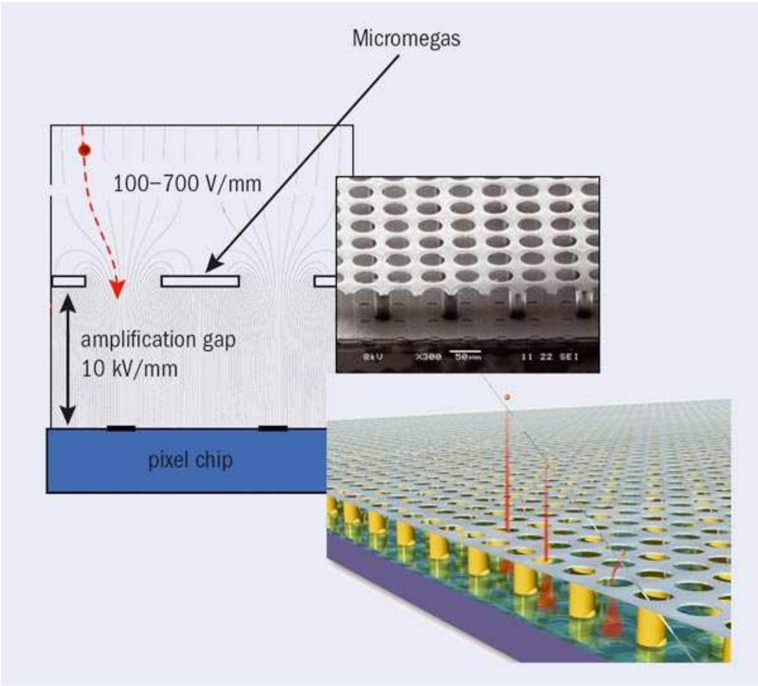

Giomataris, NIM A376 (1996) 29

Characteristics of Gaseous Detectors

operational modes of gaseous detectors:

- recombination region
- ionization region
- proportional region
- limited proportional region
- Geiger-Müller region
- discharge region

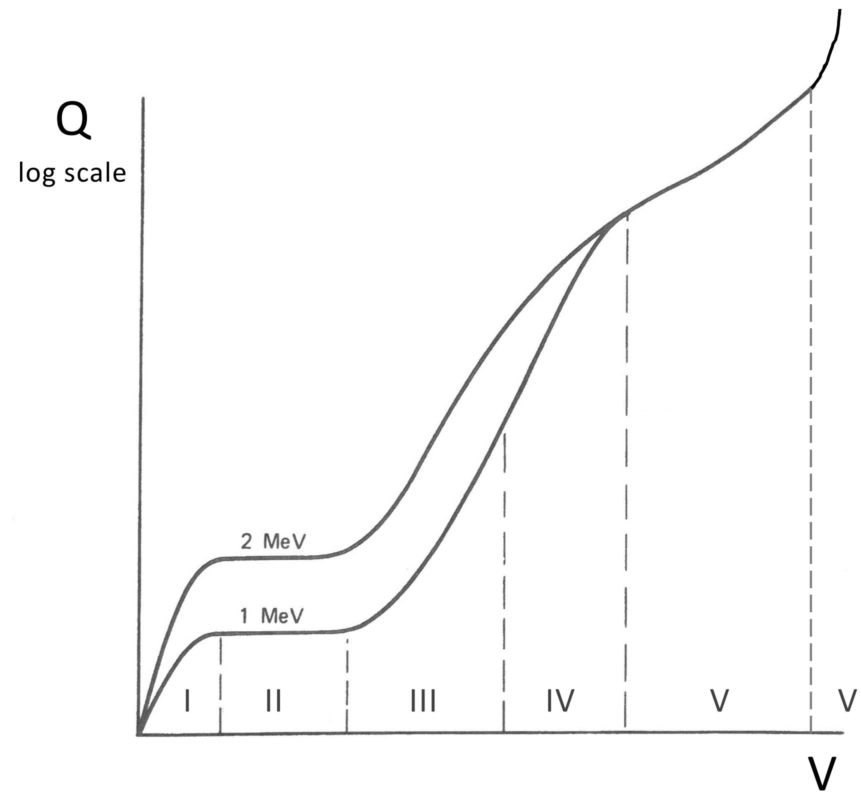

Characteristics of Gaseous Detectors

"plateau curve"

→ count rate vs voltage

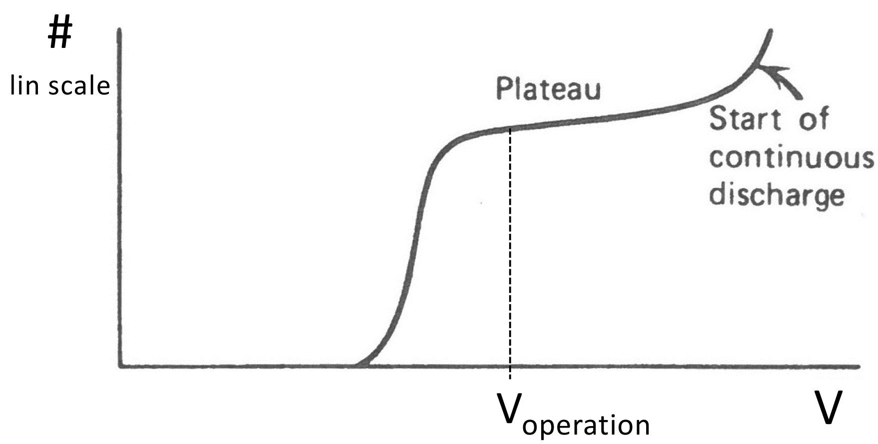

regions of operation

→ charge vs voltage

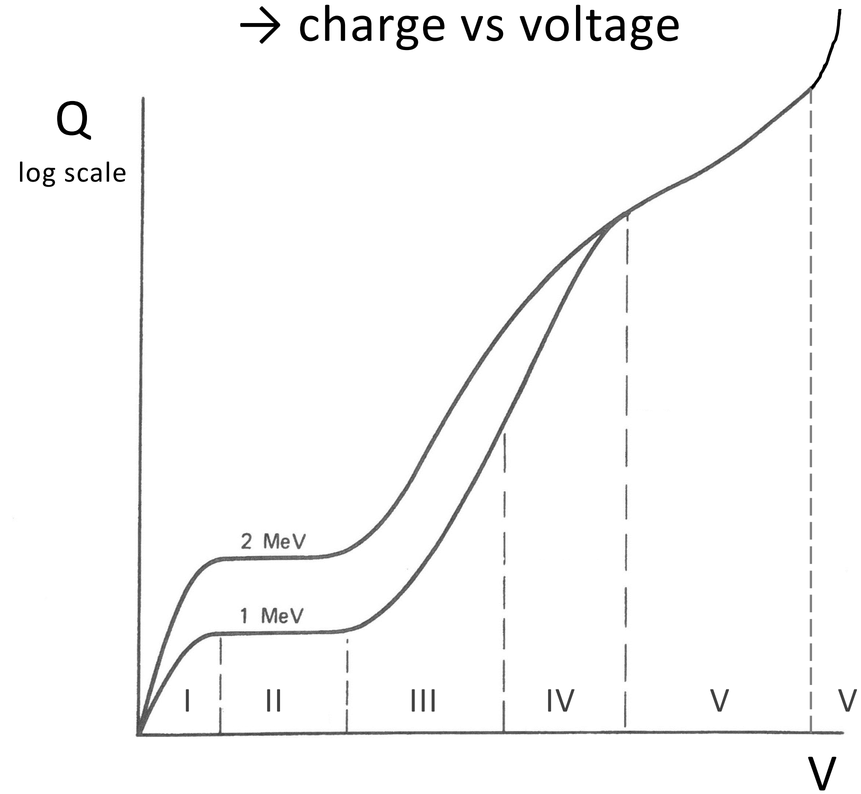

Characteristics of Gaseous Detectors

"plateau curve"

→ count rate vs voltage

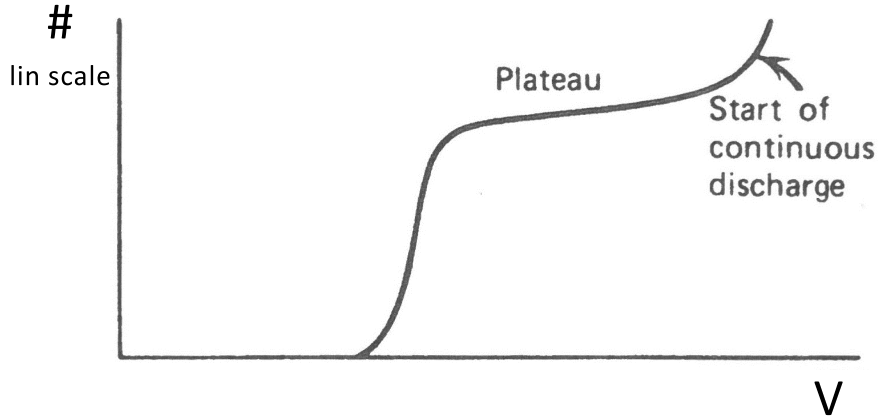

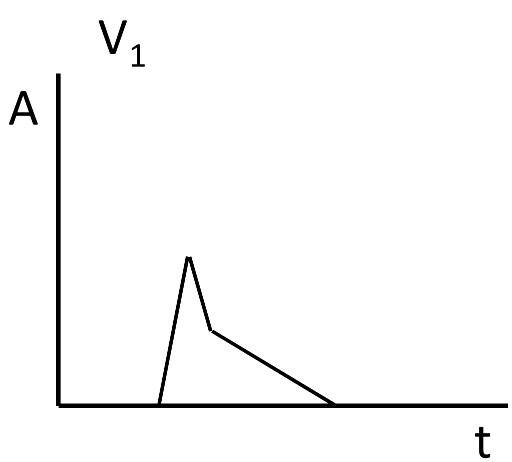

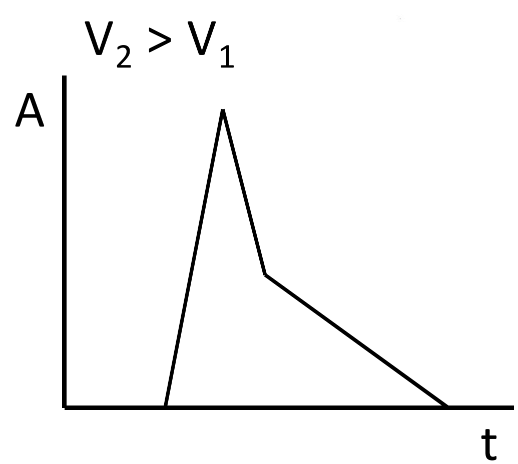

regions of operation

→ charge vs voltage

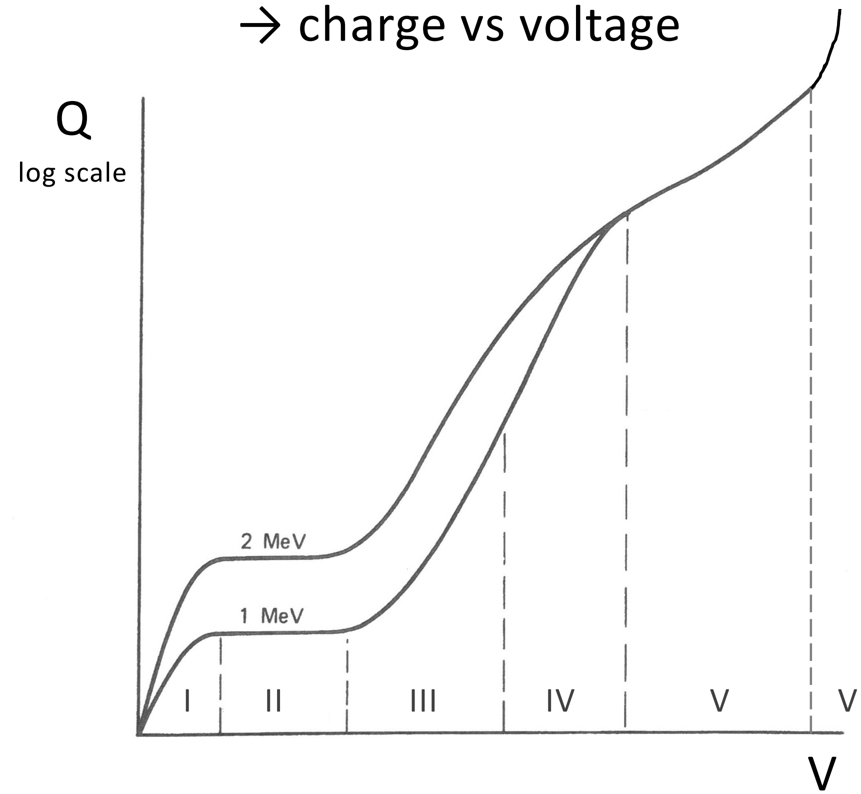

Characteristics of Gaseous Detectors

"plateau curve"

→ count rate vs voltage

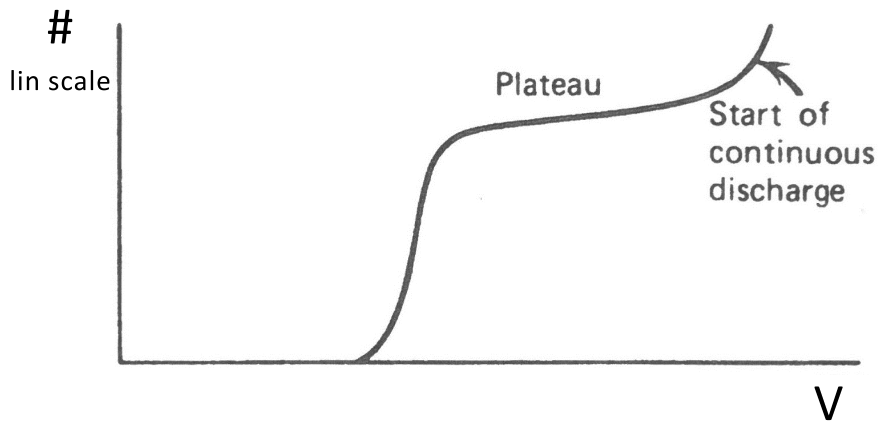

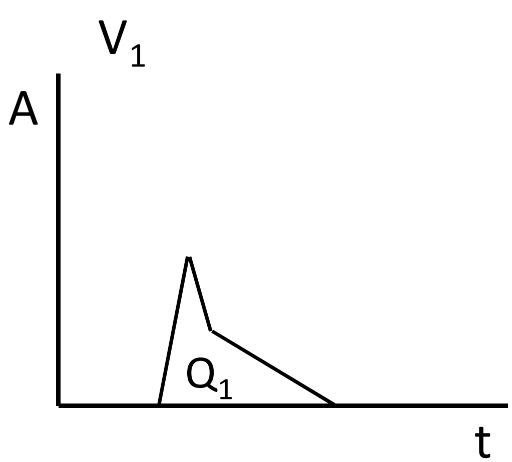

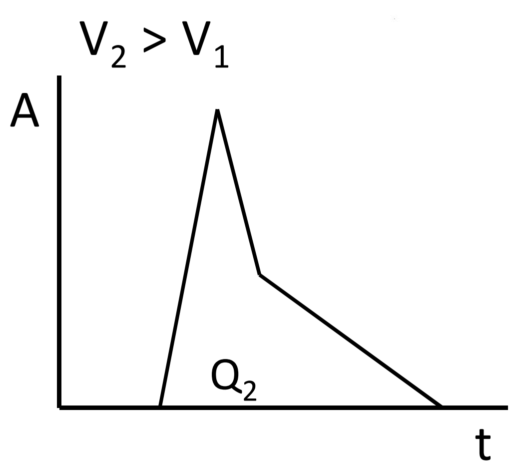

regions of operation

→ charge vs voltage

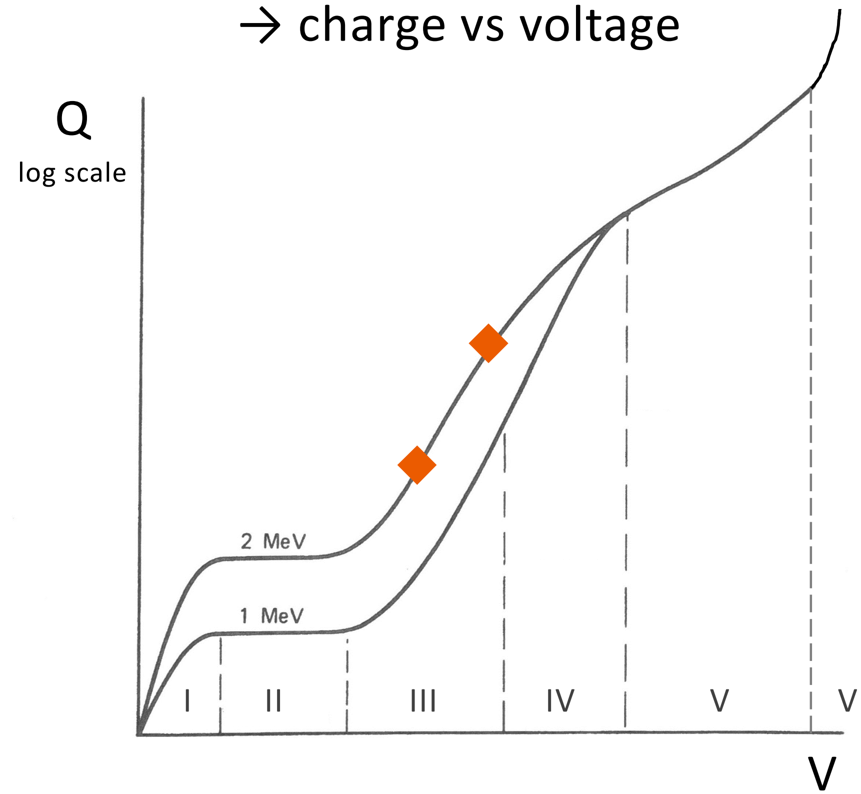

Characteristics of Gaseous Detectors

"plateau curve"

→ count rate vs voltage

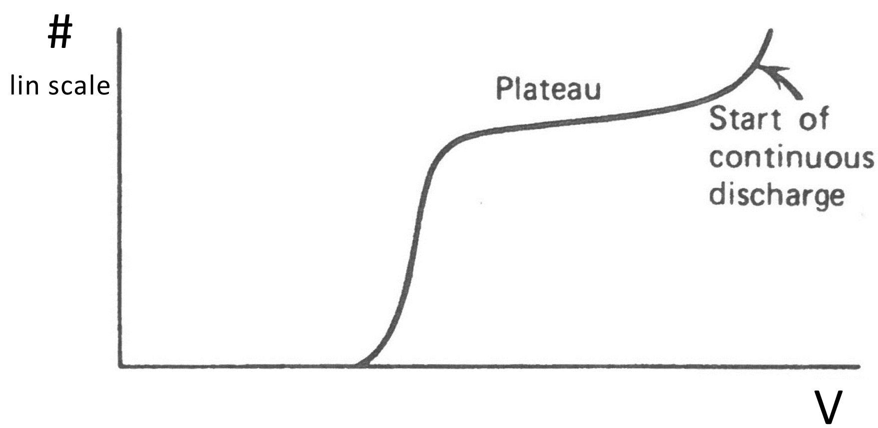

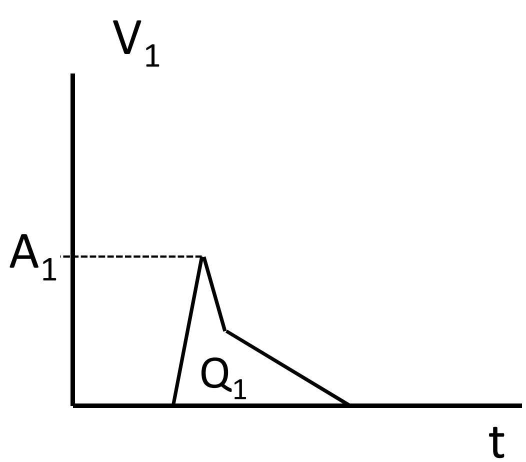

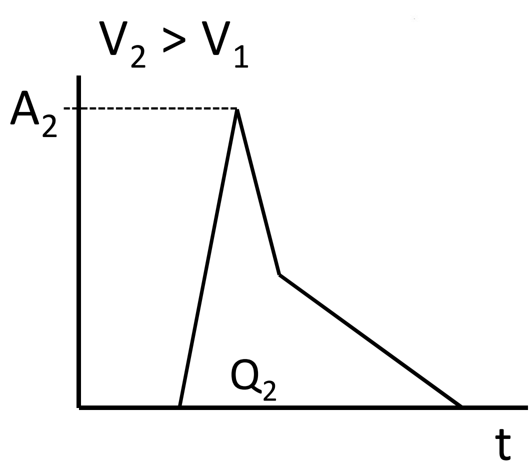

regions of operation

→ charge vs voltage

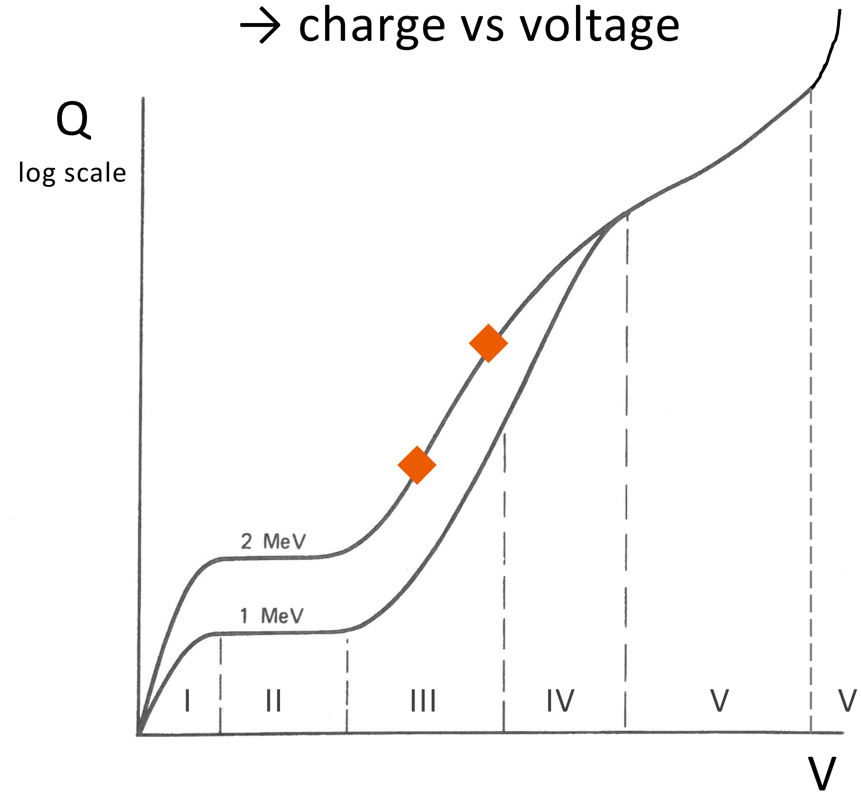

Characteristics of Gaseous Detectors

"plateau curve"

→ count rate vs voltage

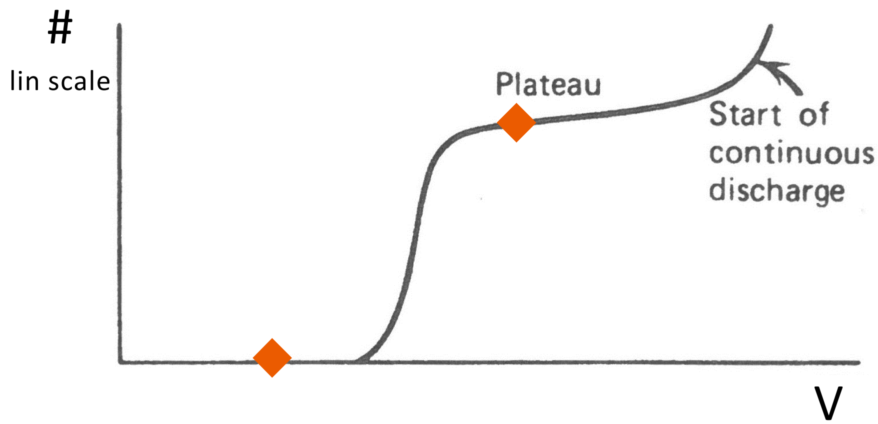

regions of operation

→ charge vs voltage

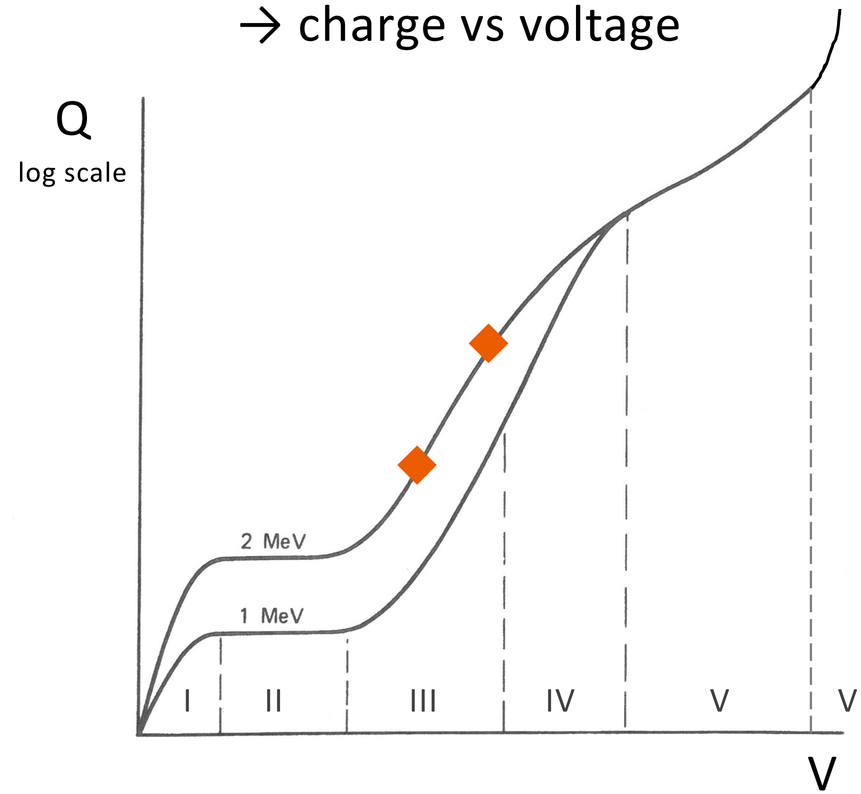

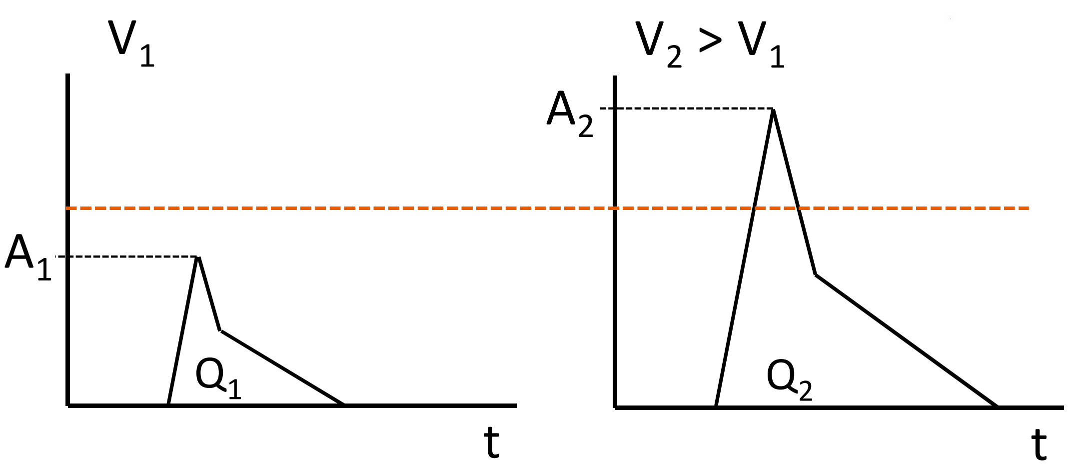

Characteristics of Gaseous Detectors

"plateau curve"

→ count rate vs voltage

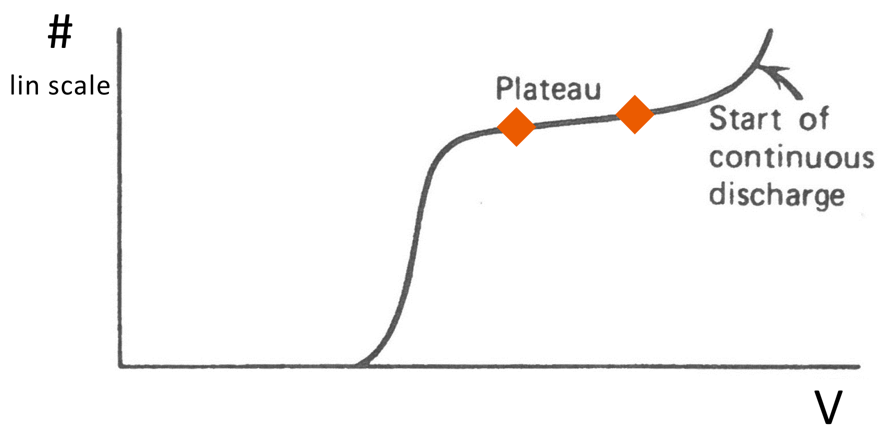

regions of operation

→ charge vs voltage

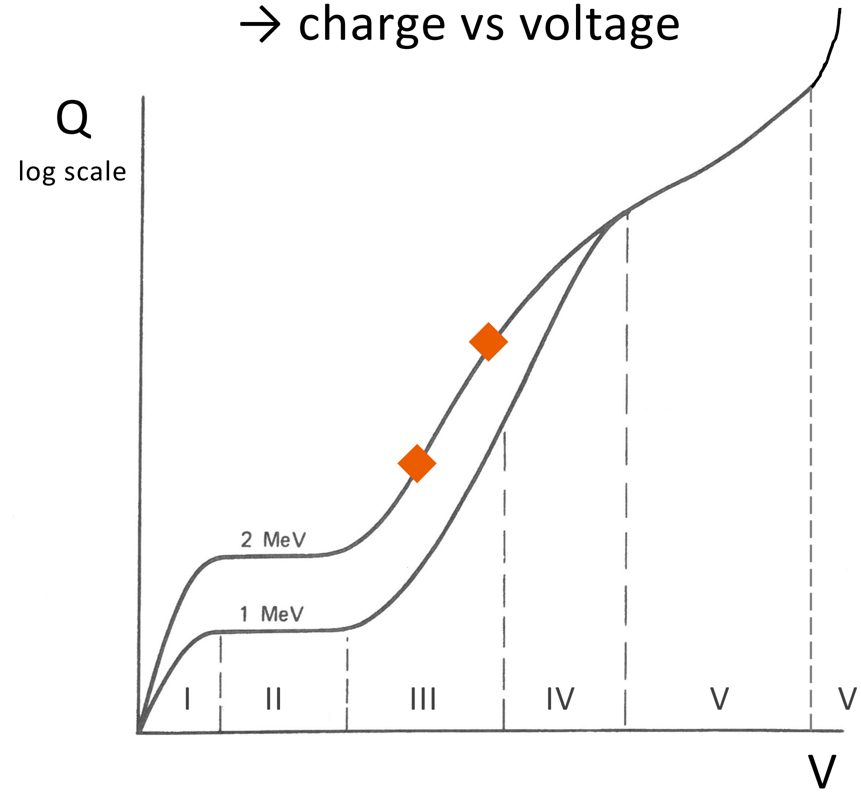

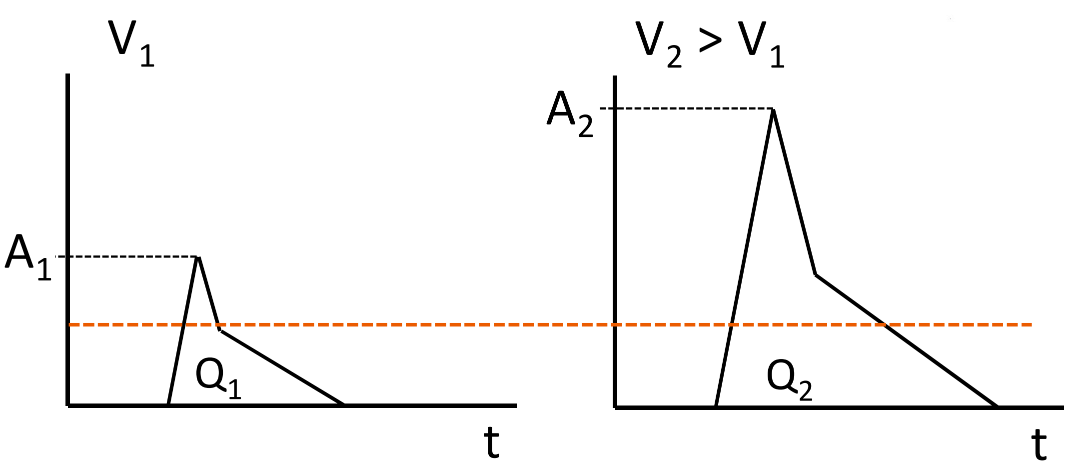

Recombination Region

region I

- applied voltage (and resulting field) very low
- electrons and ions move with relatively slow speeds
- recombination rate of electrons and ions still considerable
- as voltage (and field) increases, charges move faster
- recombination rate decreases up to point where it becomes 0

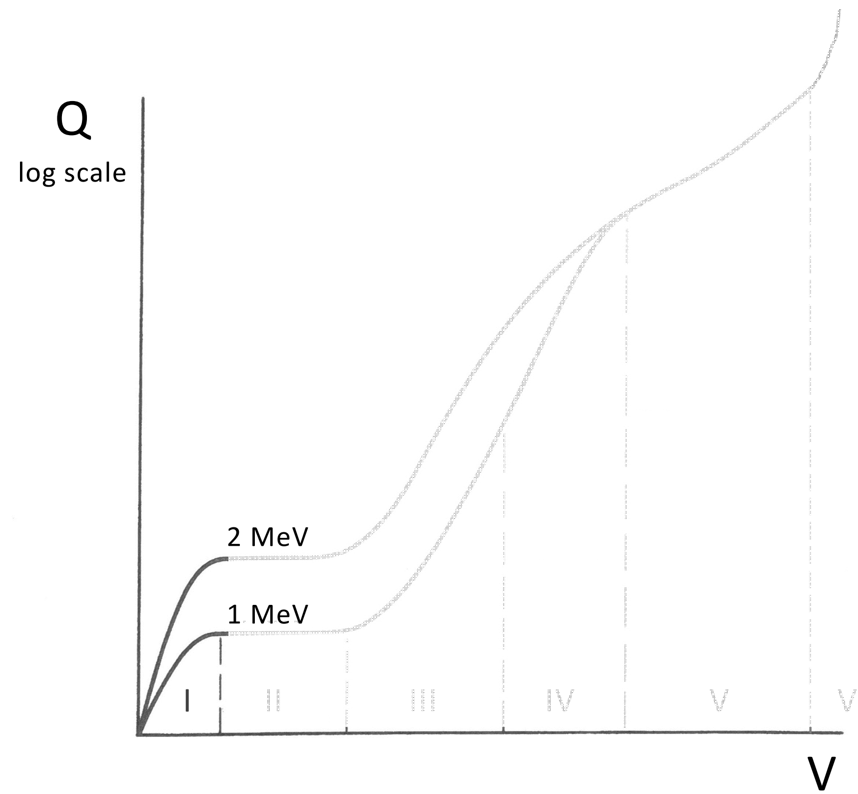

Ionization Region

region II

- recombination rate is 0 and
  no new charge is produced
- the collected charge stays constant despite a change of the applied voltage

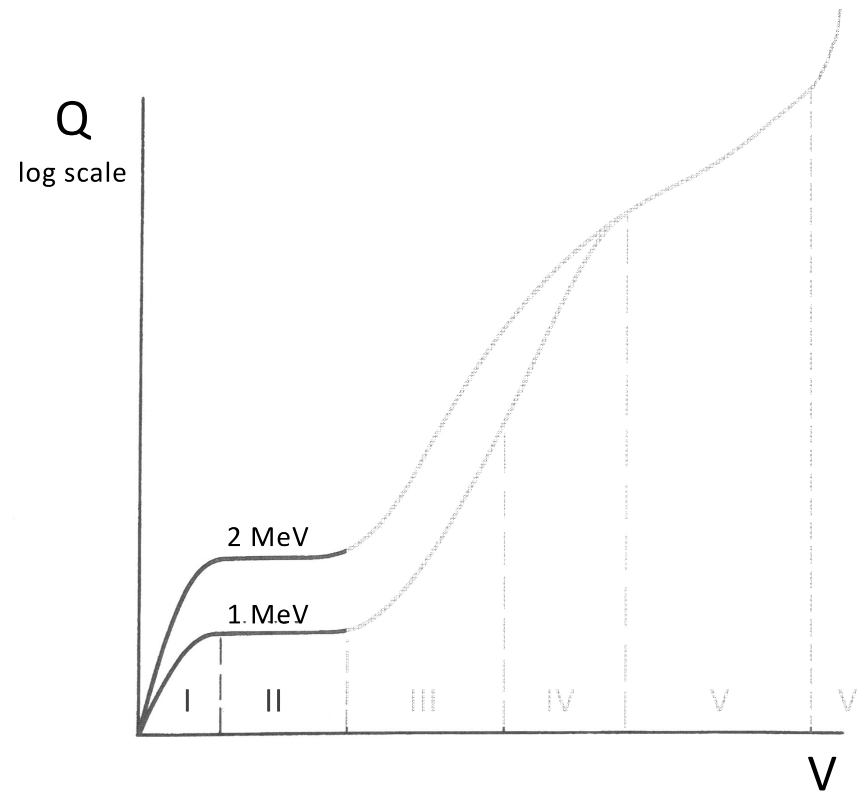

Ionization Chamber

ionization chamber placed in proton beam at proton therapy

medical proton cyclotron

- I_{proton} = 1 - 850 nA
- E_{kin} = 250 MeV

→ huge amount of primary ionisation

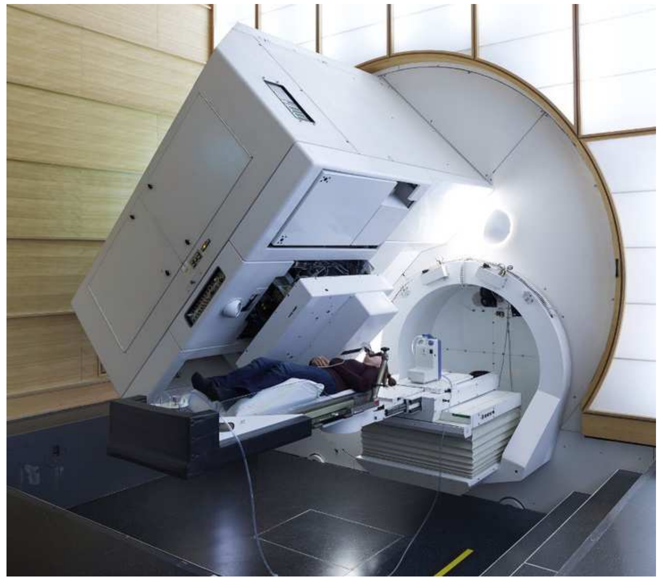

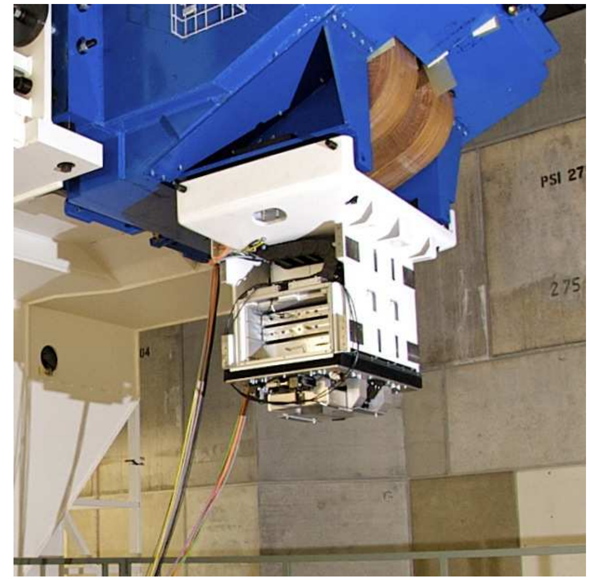

dose monitor

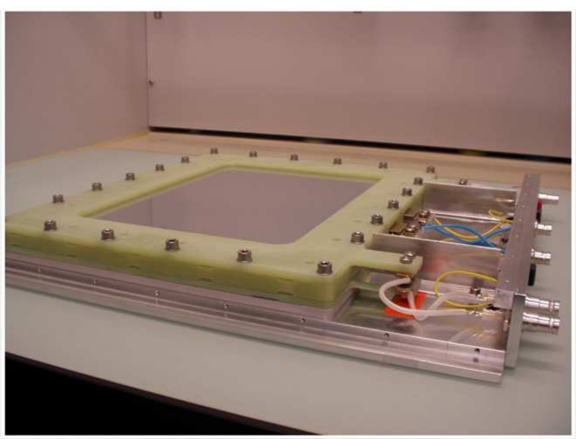

position monitor

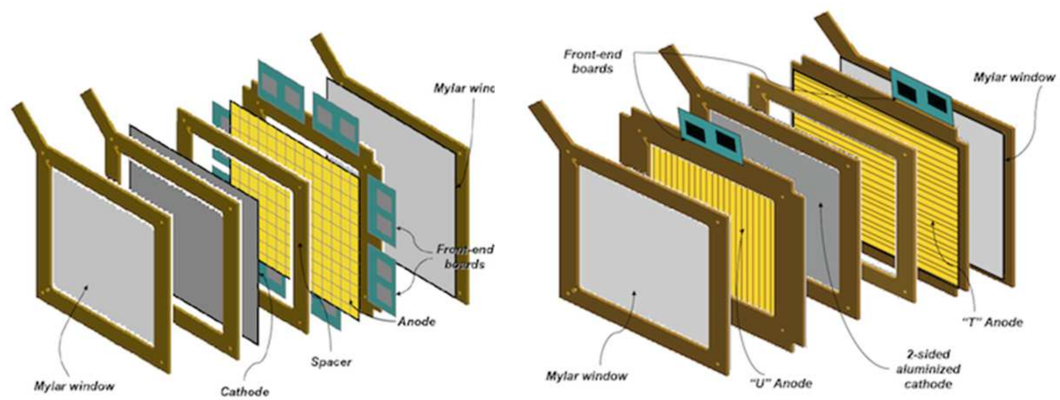

(True) Proportional Region

region III

- electric field is very strong (> ~10 kV/cm) in certain regions of the detector (e.g. wires, micro-strips, holes of GEM foil, micro-gaps)
- e^- from primary ionisation acquire sufficient energy between collisions to produce additional ionisation in e^- atom or e^- molecule collisions
- the multiplication factor (gas gain) is for a given HV independent of primary ionisation n_0

  → pulse height is proportional to n_0

  → pulse height is proportional to dissipated energy

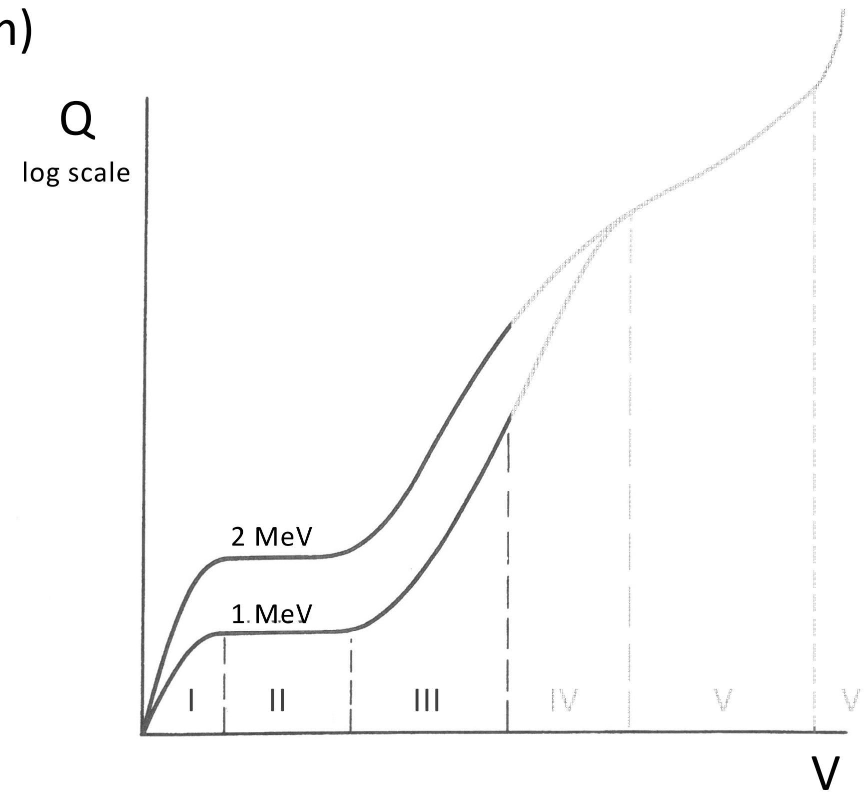

Limited Proportional Region

region IV

- free e⁻ are quickly collected, but positive ions move much slower
- each e⁻ avalanche creates a cloud of positive ions which shield the amplification region (e.g. wire) and slowly moves towards the cathode
- this space charge can significantly deteriorate the shape of the electrical field
  - → reduced "effective field" creates less gas amplification
  - → pulse height still increases with increasing number of initial ion pairs but not anymore linearly

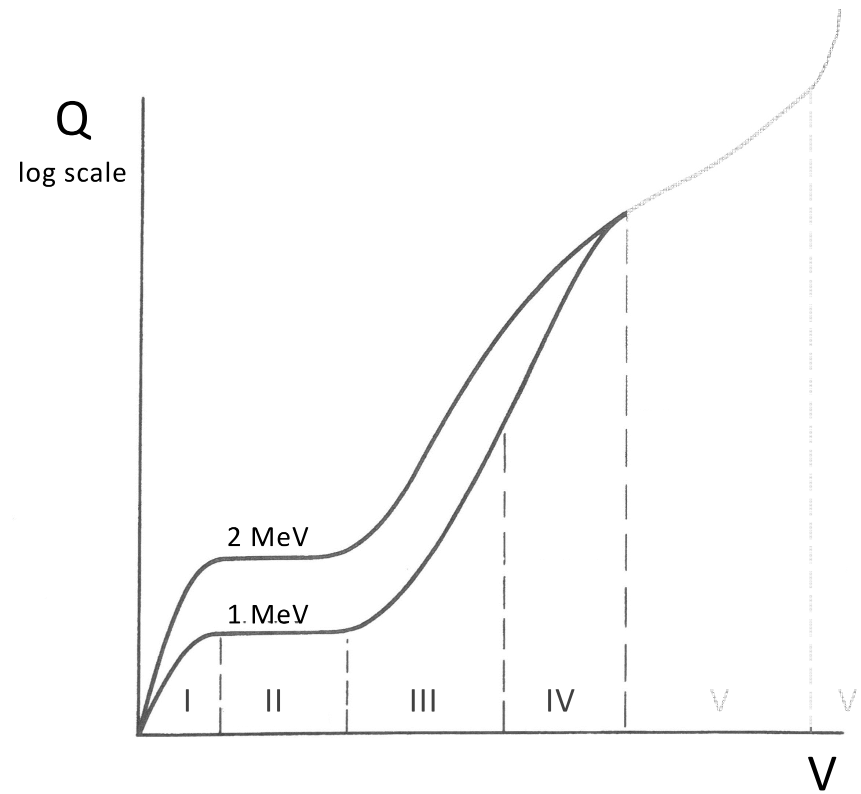

Limited Proportional Region

space charges reduces electrical field:

→ lower "effective" voltage

→ lower amplification

voltage drop ΔV

$$\Delta V = \frac{s \cdot h^2 \cdot q \cdot \Phi \cdot \ln(r_c / a)}{4 \cdot \pi \cdot \varepsilon_0 \cdot \mu \cdot V}$$

s wire spacing	h half gap
Φ rate	a wire radius
$r_c \approx$ s, h	V applied voltage

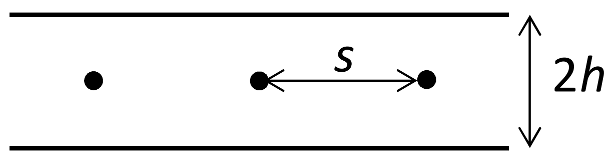

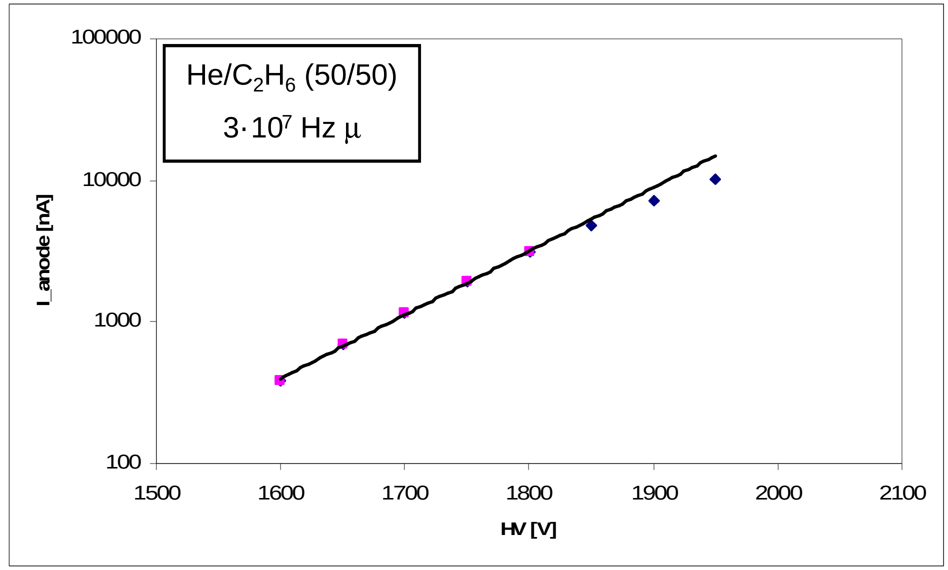

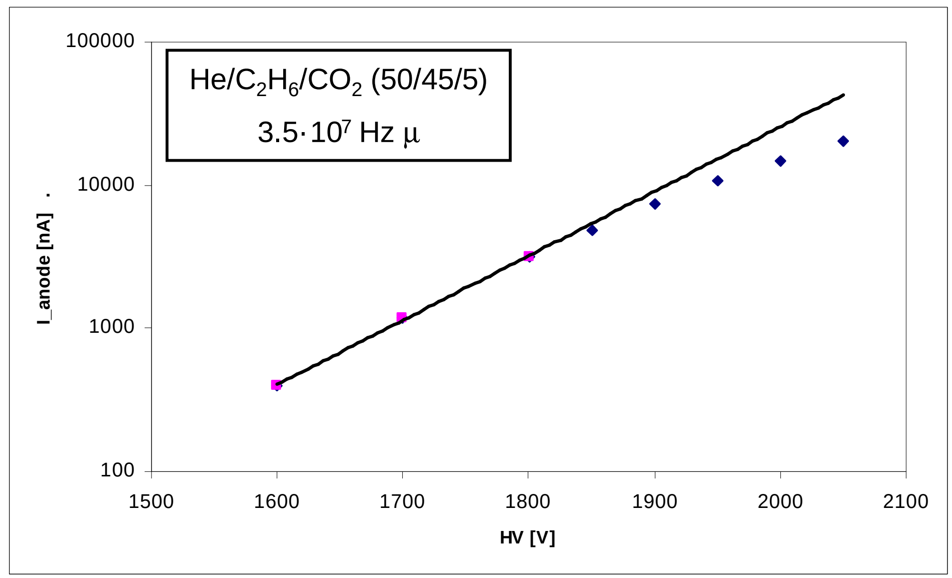

→ to reduce ΔV: reduce *s* and *h*

→ to increase rate capability: reduce cell size / increase granularity (e.g. MPGD)

Geiger-Müller Region

region V

- space charge created by positive ions becomes completely dominant
- shielding effect of amplification region increases such that the effective field decreases below the field strength were multiplication starts

→ self-limited process which will terminate when the same total amount of positive ions have been created

→ pulse shape and height are independent of primary ionisation n_0 and no longer reflect any properties of the incident radiation

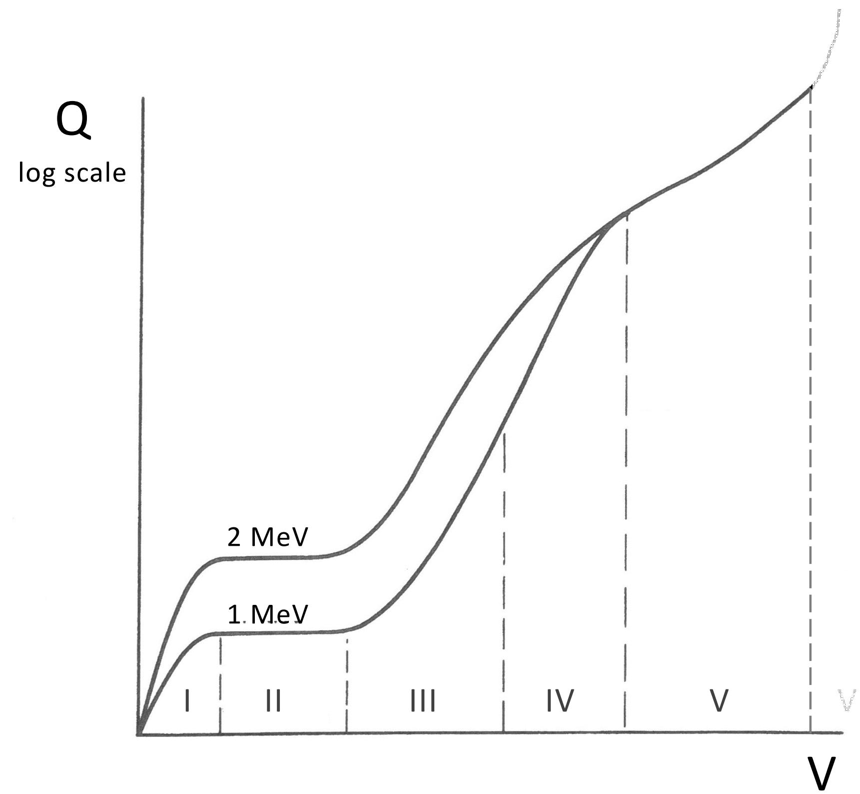

Geiger-Müller Region

region V

- depending on amount of "quencher" (photon absorber) in the gas:

  photons emitted from excited atoms and molecules in the avalanche lead to

  - additional avalanches and
  - a spread along the entire length of the wire

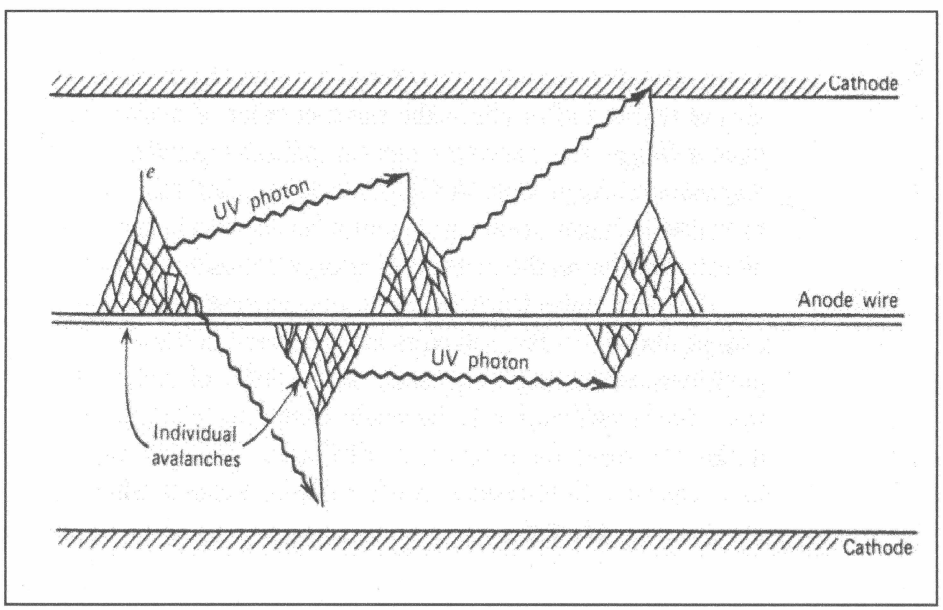

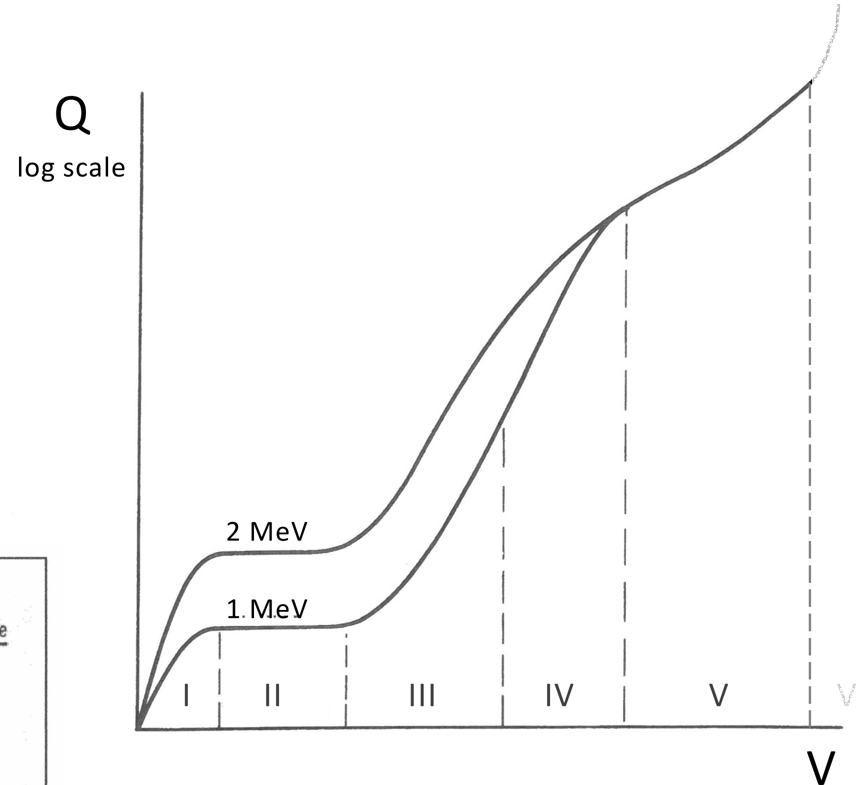

Discharge Region

region VI

- continuous breakdown with or without radiation (self-sustaining discharge)
  - → should be avoided to prevent damage to detector

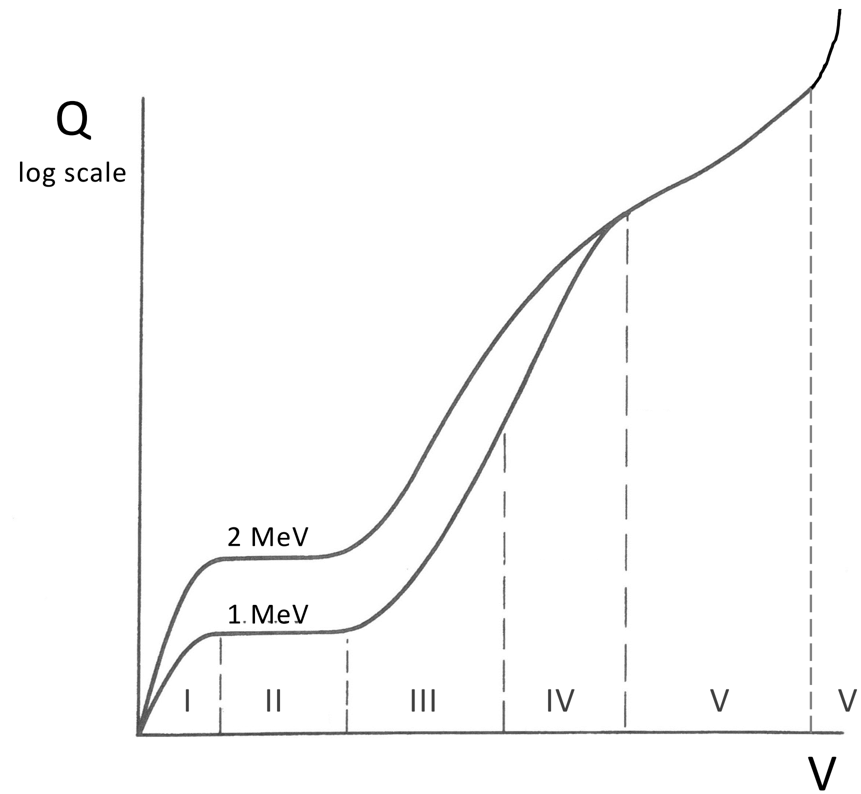

Large Area Gaseous Detectors

- 1908: first wire counter to study natural radioactivity

  E.Rutherford, H.Geiger, 1908

  Geiger, 1913

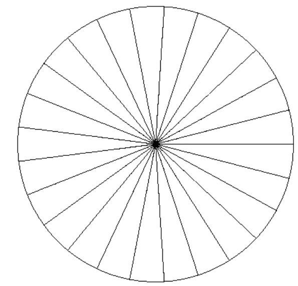

- 1928: Geiger-Müller counter with single electron sensitivity

  H.Geiger, W.Müller, 1928

  H.Geiger, W.Müller, 1928, 1929

- 1945: proportional tubes

  H.Raether, 1949

- 1968: multi-wire proportional chambers

  G.Charpak, 1968

  G.Charpak *et al.*, 1968

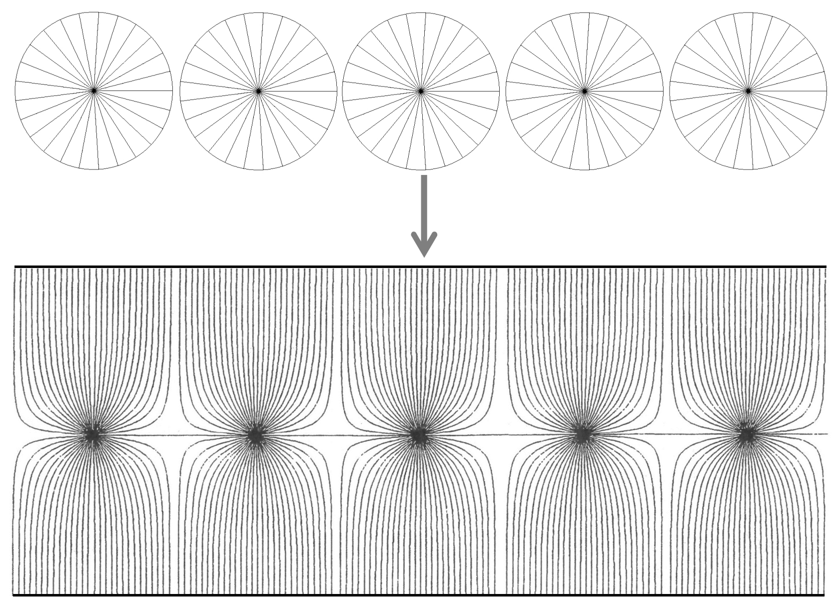

PAUL SCHERRER INSTITUT PSI

Large Area Gaseous Detectors

- 1908: first wire counter to study natural radioactivity
  E.Rutherford, H.Geiger, 1908
  Geiger, 1913
- 1928: Geiger-Müller counter with single electron sensitivity
  H.Geiger, W.Müller, 1928
  H.Geiger, W.Müller, 1928, 1929
- 1945: proportional tubes
  H.Raether, 1949
- 1968: multi-wire proportional chambers
  G.Charpak, 1968
  G.Charpak *et al.*, 1968
- 1992: Nobel Price in Physics: G.Charpak
  "…for his invention and development of particle detectors, in particular the multiwire proportional chamber."

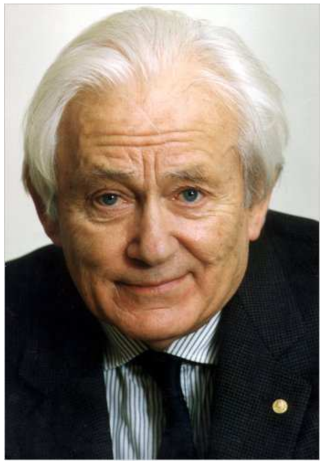

G.Charpak (1924 - 2010)

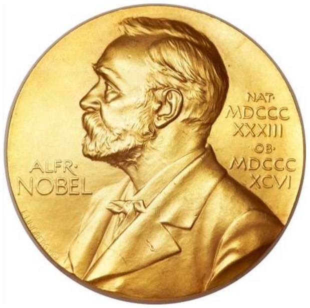

Large Area Gaseous Detectors - Limitations

multi-wire proportional chamber (MWPC):

- spatial resolution given by granularity of anode wires (several mm)
- field distortions due to (electrostatic) displacements of anode wires

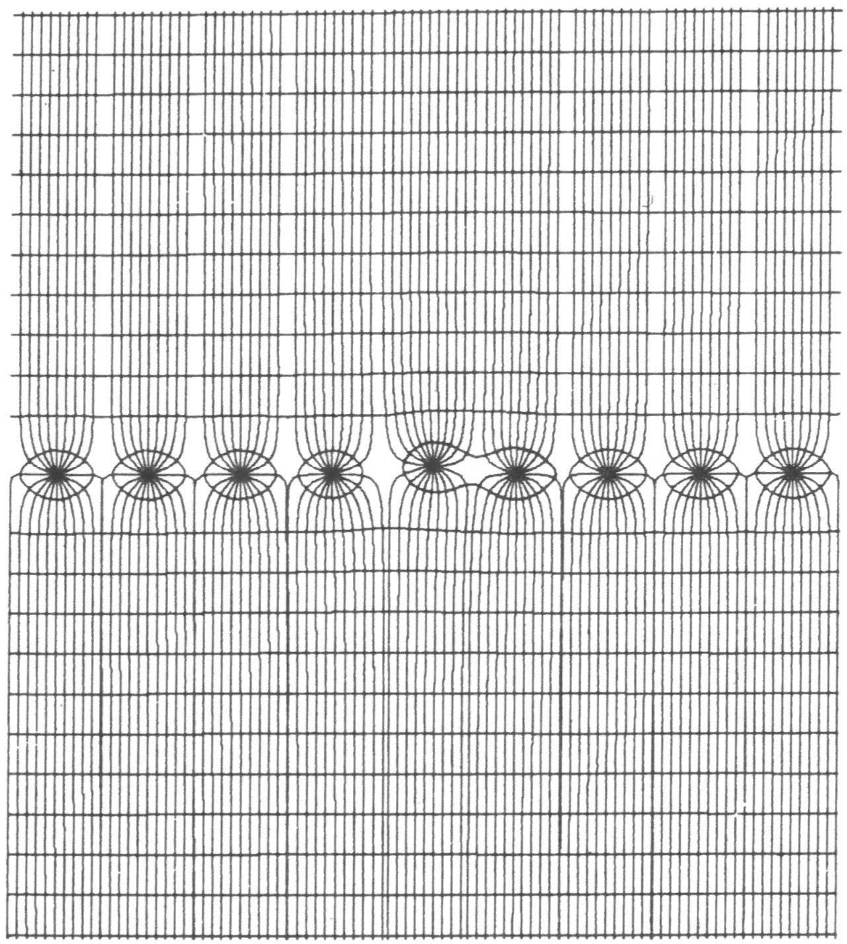

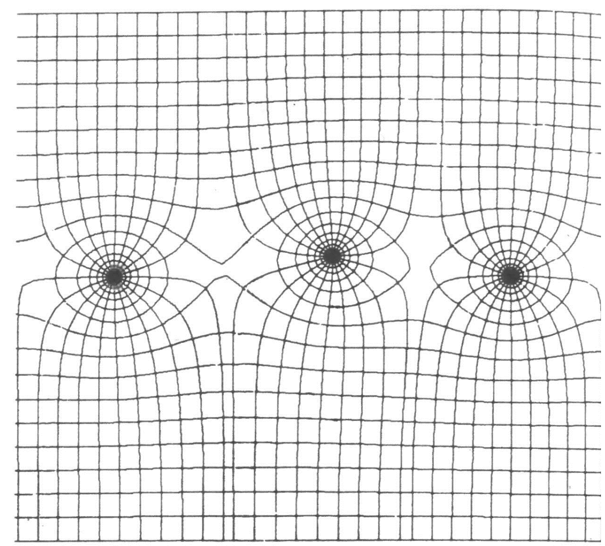

Drift Chamber - Principle

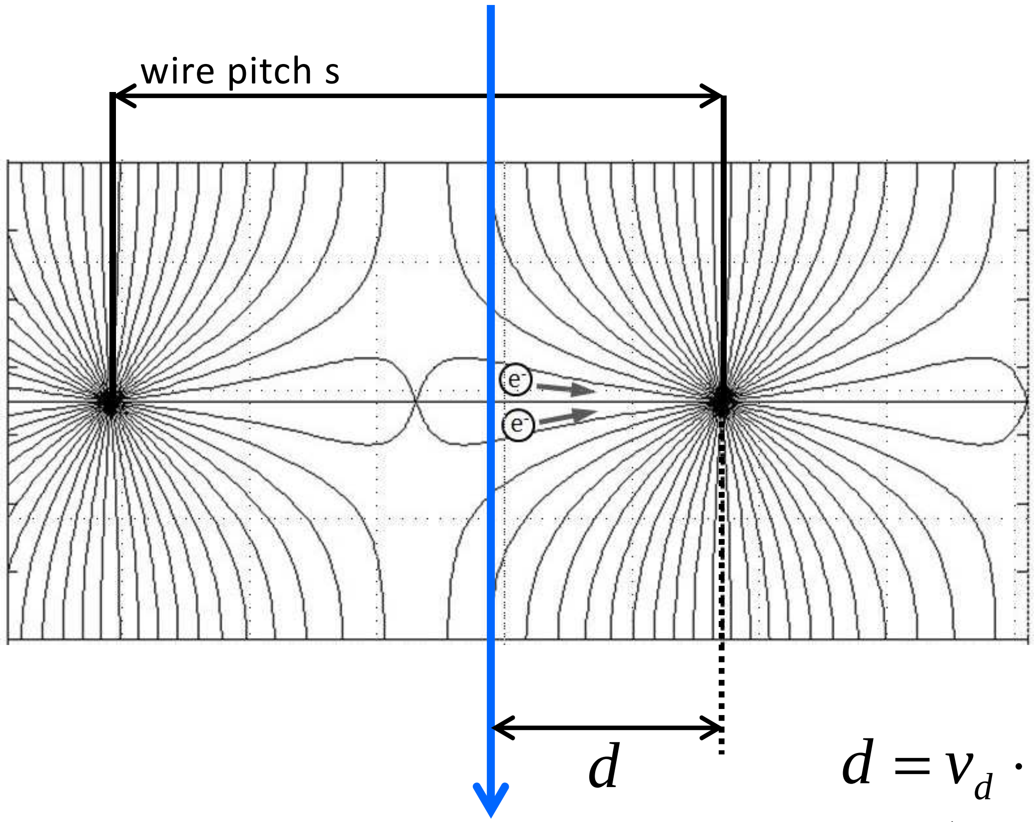

$$d = v_d \cdot t$$ in case v_d = constant

$$d = \int_{t_1}^{t_2} v_d(t)dt$$ in case $v_d = v_d(E)$

- characteristic features of drift chamber design:
  - geometry: small variations of *E* within drift cell
  - gaseous electronics, as $v_d = v_d(E)$: small Δv_d for unavoidable ΔE

Drift Chamber – Adjustment of Electrical Field

elcectrical field without and with potential wire:

- MWPC

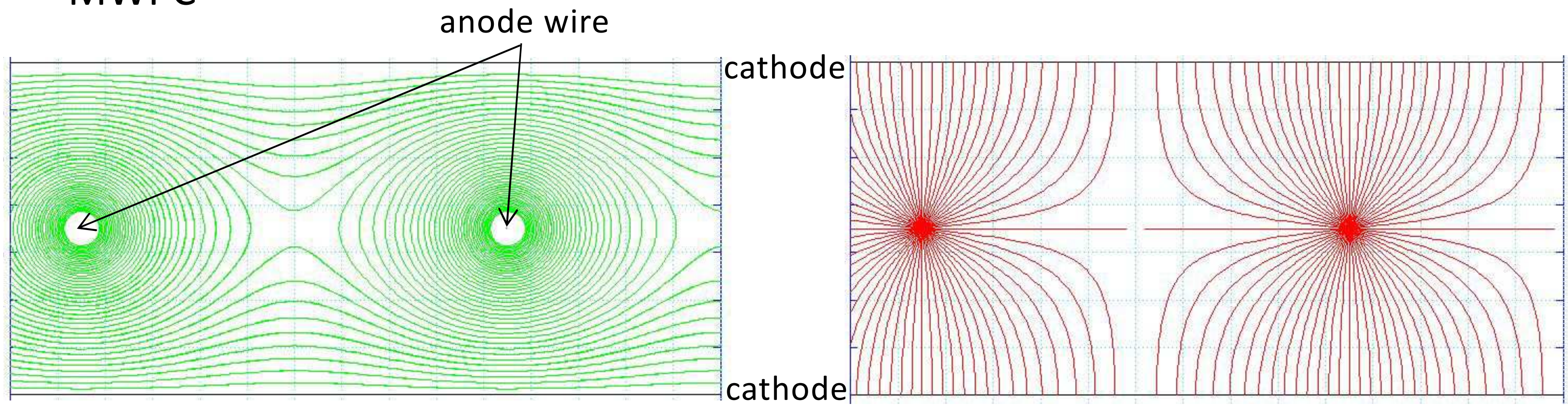

Drift Chamber – Adjustment of Electrical Field

elcectrical field without and with potential wire:

- MWPC

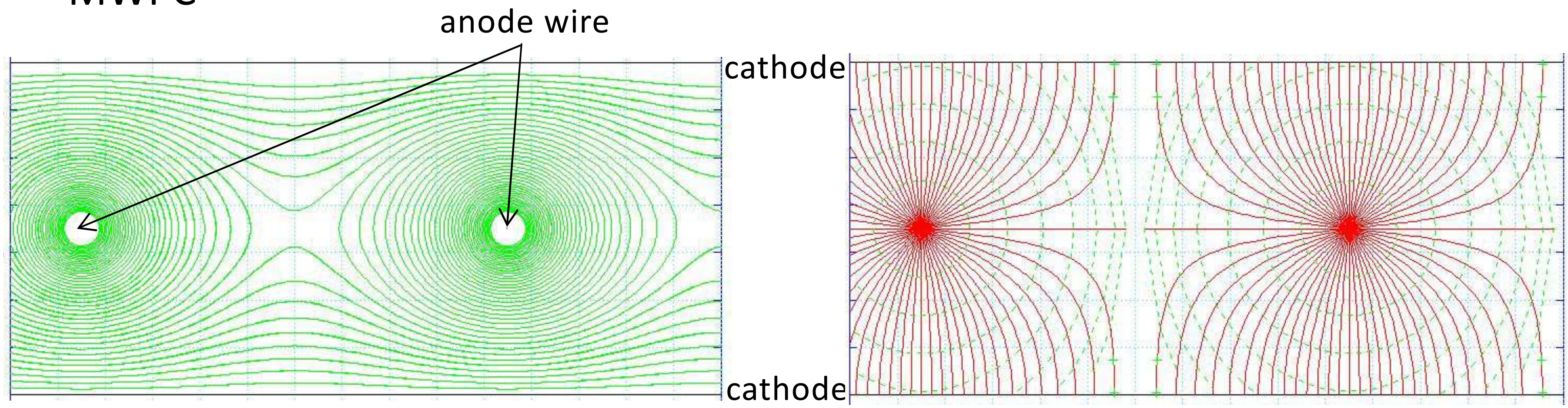

Drift Chamber – Adjustment of Electrical Field

elcectrical field without and with potential wire:

- MWPC

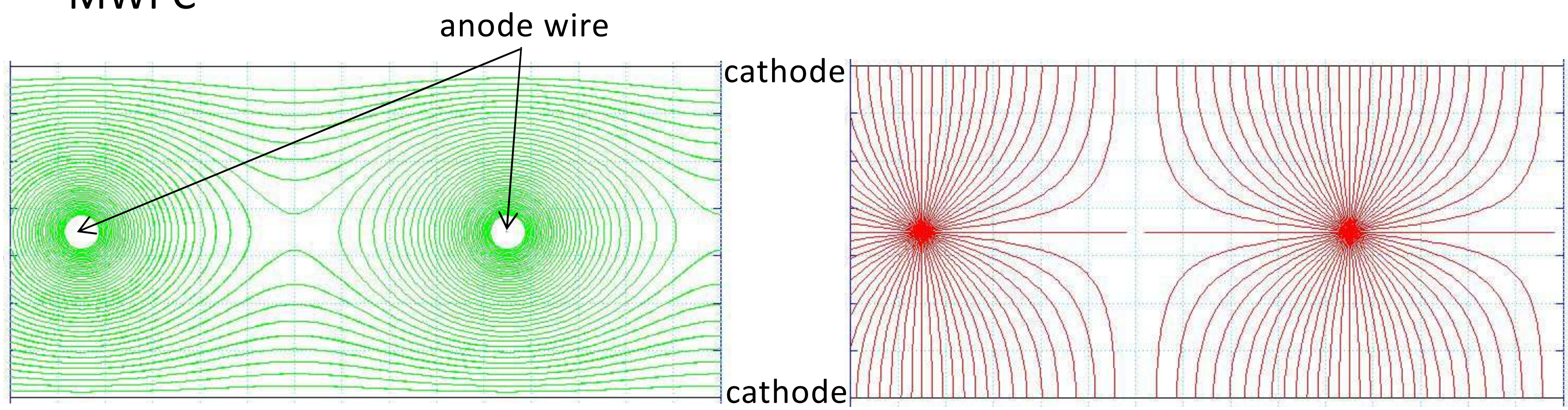

- drift chamber

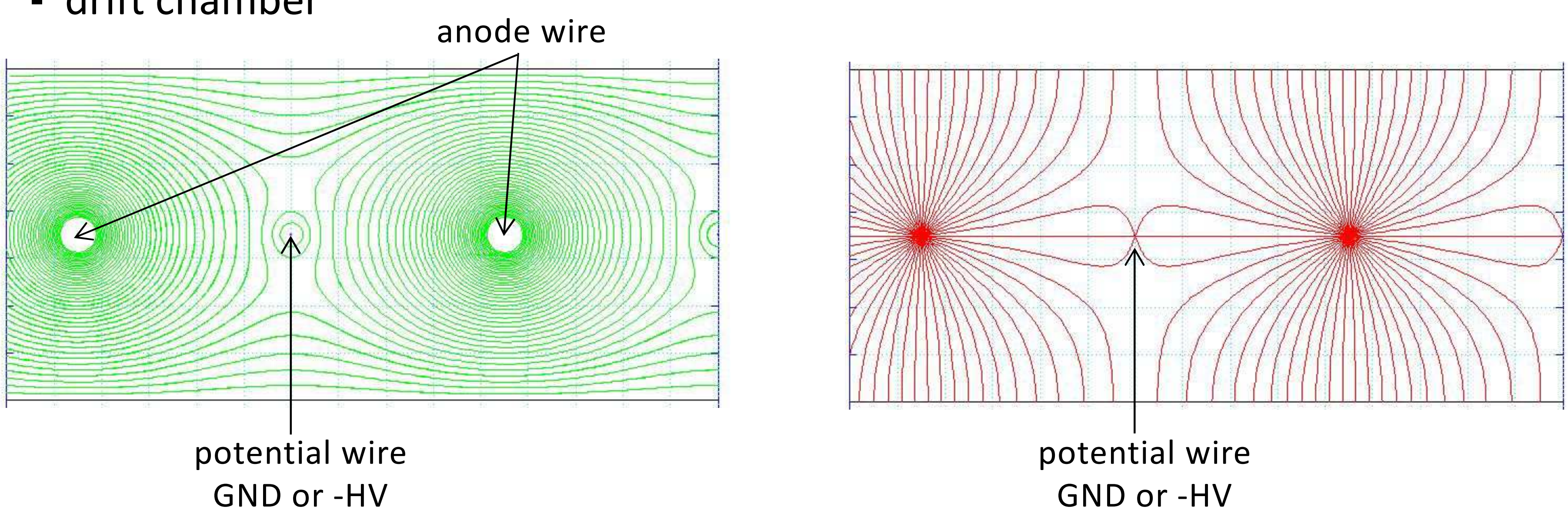

Drift Chamber – Adjustment of Electrical Field

elcectrical field without and with potential wire:

- MWPC

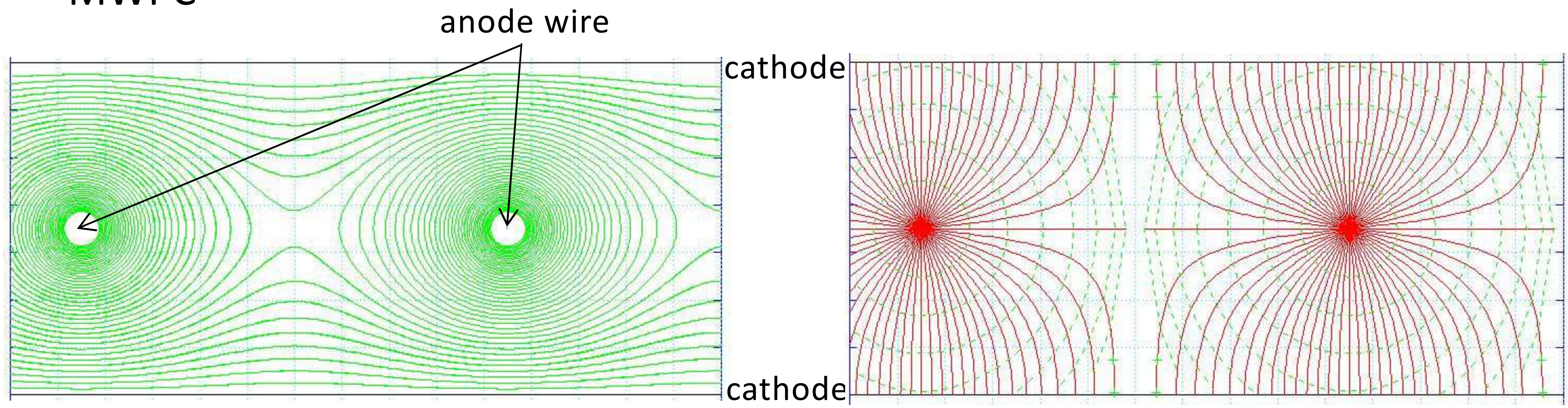

- drift chamber

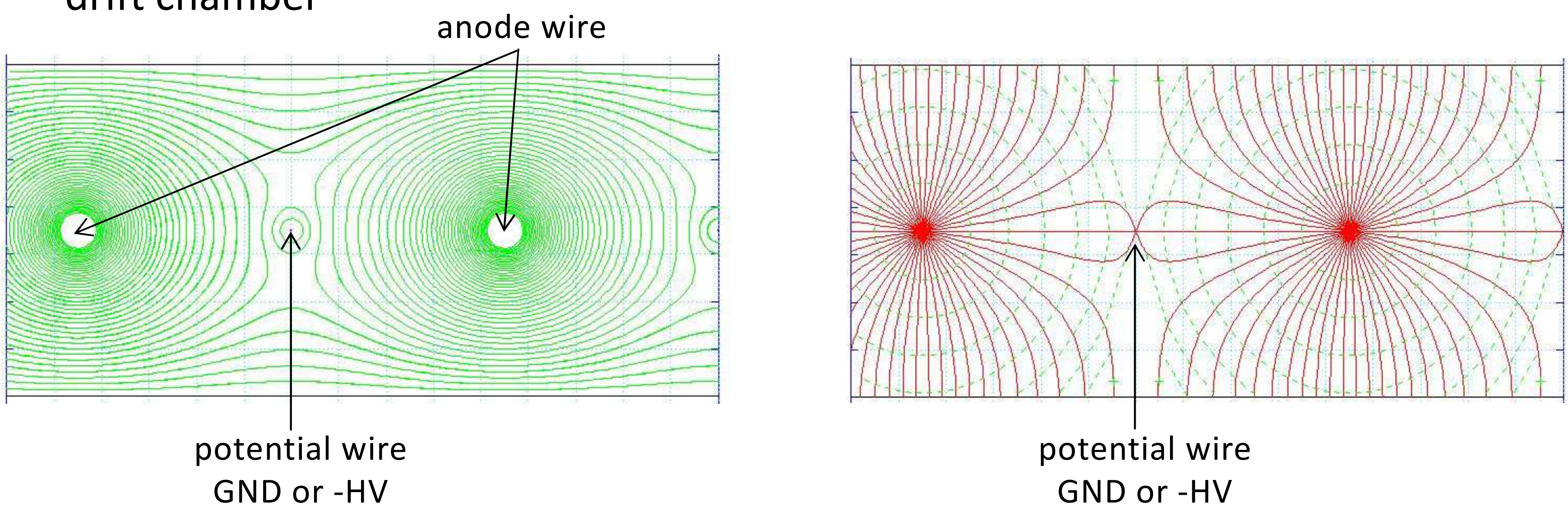

Drift Chamber – Choice of Gas

requirements for appropriate drift chamber filling gas:

- fast v_d
- v_d vs HV plateau
- small diffusion

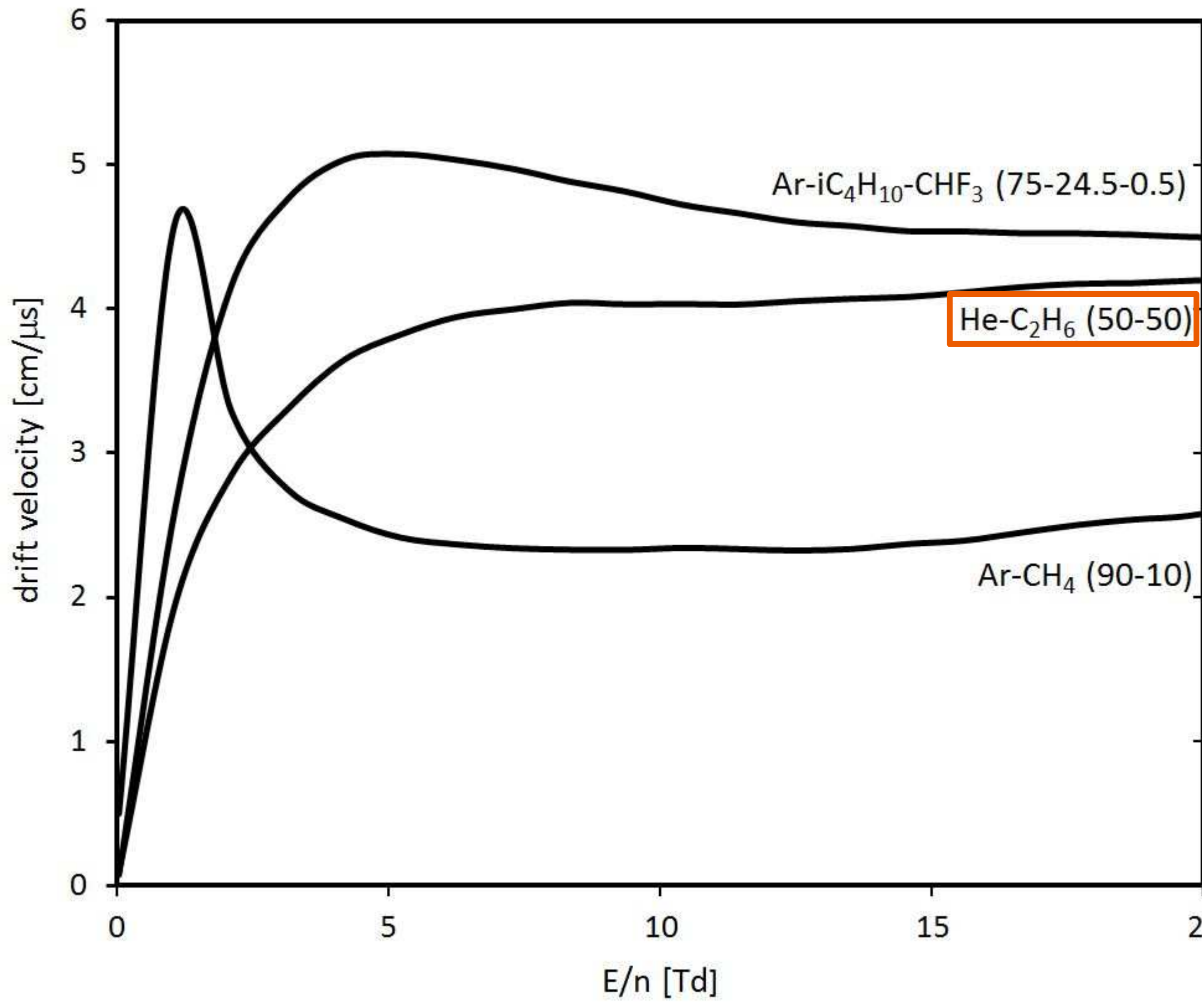

Drift Chamber

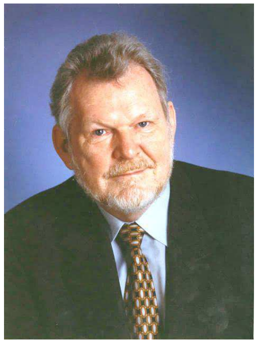

A.H.Walenta

J.Heintze

The drift chamber was "born" in Heidelberg:

- 1968/69: diploma thesis A. H. Walenta
- 1971: A. H. Walenta, J. Heintze and B. Schürlein,
  Nuclear Instruments and Methods 92 (1971) 373-380
  "The multiwire drift chamber - a new type of proportional wire chamber"
- 1972: PhD thesis A. H. Walenta: "Lokalisierung von Teilchenspuren durch Messung der Elektronendriftzeiten in grossflächigen Proportionalzählern"

NUCLEAR INSTRUMENTS AND METHODS 92 (1971) 373–380; © NORTH-HOLLAND PUBLISHING CO.

THE MULTIWIRE DRIFT CHAMBER
A NEW TYPE OF PROPORTIONAL WIRE CHAMBER*

A. H. WALENTA, J. HEINTZE and B. SCHÜRLEIN

I. Physikalisches Institut der Universität Heidelberg, Heidelberg, Germany

Received 27 November 1970

In this article a new type of proportional wire chamber is described with large wire distances and accurate position determination by drift time measurement. The electronic circuitry required has been considerably reduced while the space resolution has been improved as compared to a conventional proportional wire chamber. The limit for position accuracy seems to be at present $\sigma = 0.2$ mm.

The complete system with computer read out described in this article has a location accuracy of $\sigma = 0.47$ mm.

σ = 0.2 mm even with wire pitch ~10 mm

MEG Experiment

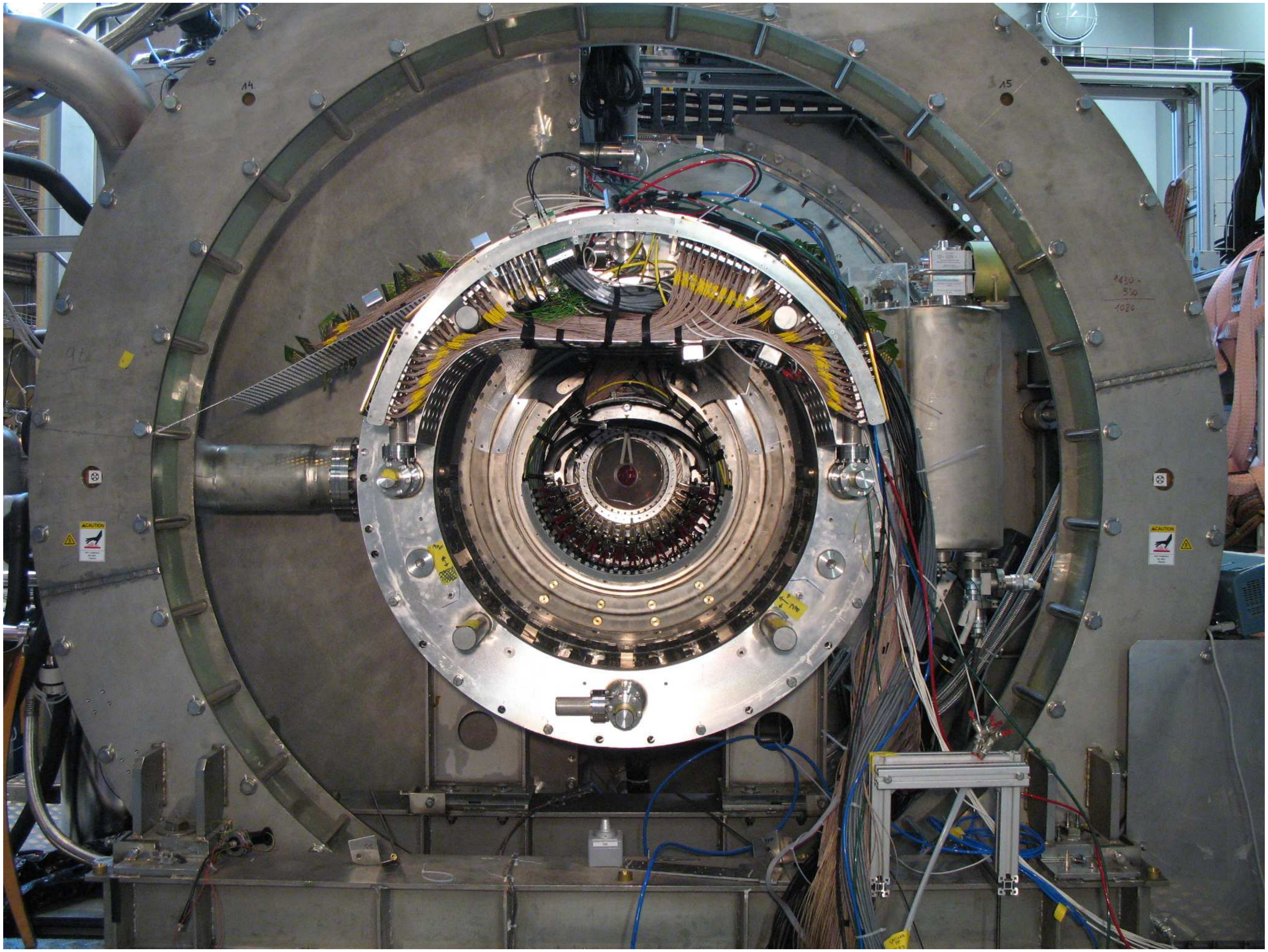

MEG and MEG II experiment

- dedicated experiments for the search for the charge lepton violating decay

  $\mu^+ \rightarrow e^+ \gamma$

  - MEG: B($\mu^+ \rightarrow e^+ \gamma$) < 4.2 · 10^{-13} (90% CL)
  - MEG II: x10 improvement in sensitivity

- positron spectrometer (tracker & timing counter) designed for precision measurement of 52.8 MeV/c e^+

- tracker system
  - high momentum resolution (< 0.4%)
  - high angular resolution (~5mrad)

  → low-mass tracker for low multiple Coulomb scattering contribution

  → very good spatial resolution in sub-mm region

→ gaseous detector: drift chamber

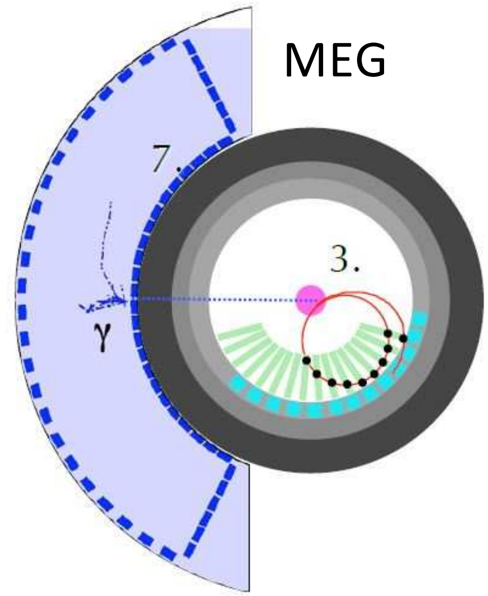

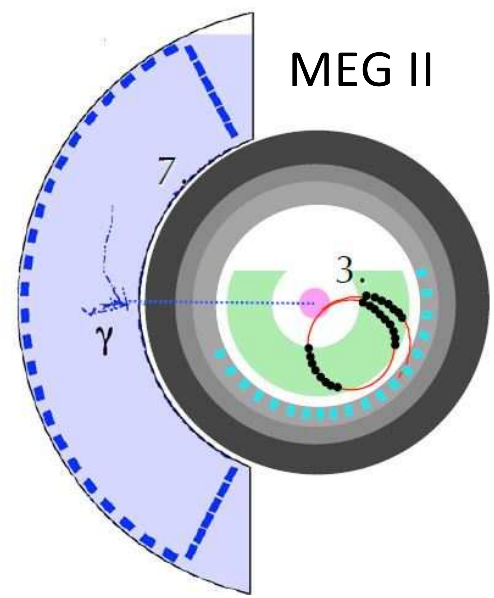

Radiation Length

MEG experiment: material budget (in units of X_0) along e^+ track

	MEG	MEG II
detector module	$2.6 \cdot 10^{-4}$	
track (7.5 modules)	$2.0 \cdot 10^{-3}$	$1.1\text{-}1.2 \cdot 10^{-3}$

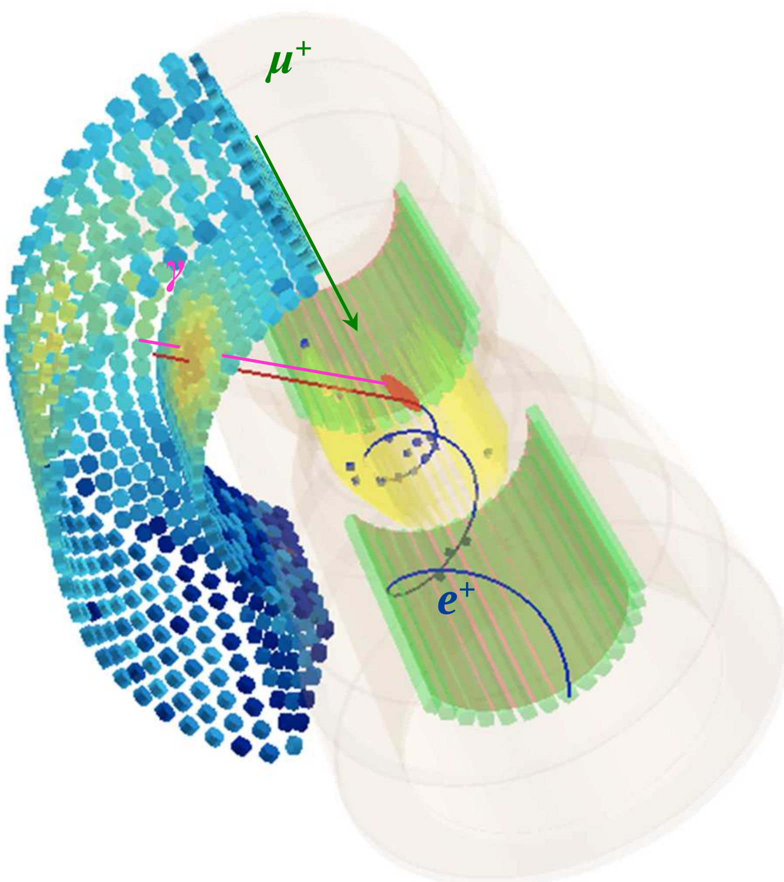

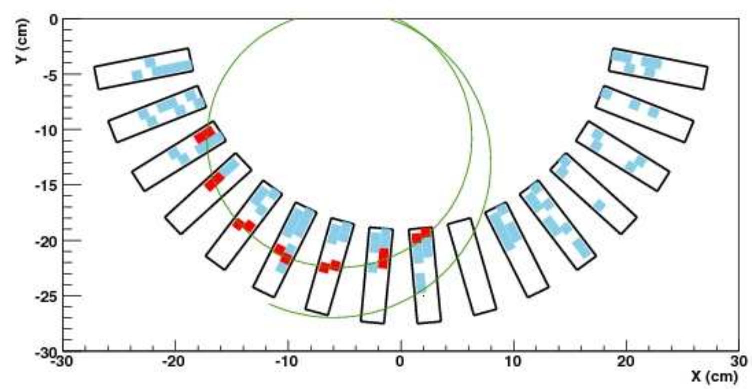

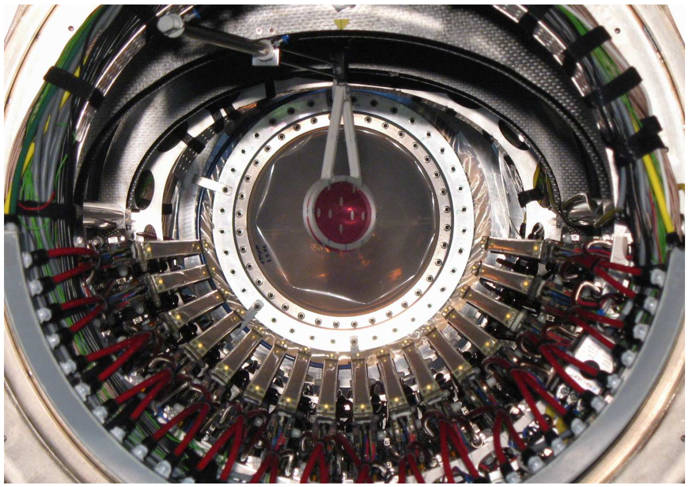

Radiation Length

MEG experiment: material budget (in units of X_0) along e^+ track

	MEG	MEG II	300µm Si	50µm Si
detector module	$2.6\cdot10^{-4}$		$32\cdot10^{-4}$	$5.3\cdot10^{-4}$
track (7.5 modules)	$2.0\cdot10^{-3}$	$1.1\text{-}1.2\cdot10^{-3}$	$24\cdot10^{-3}$(?)	$4.0\cdot10^{-3}$(?)

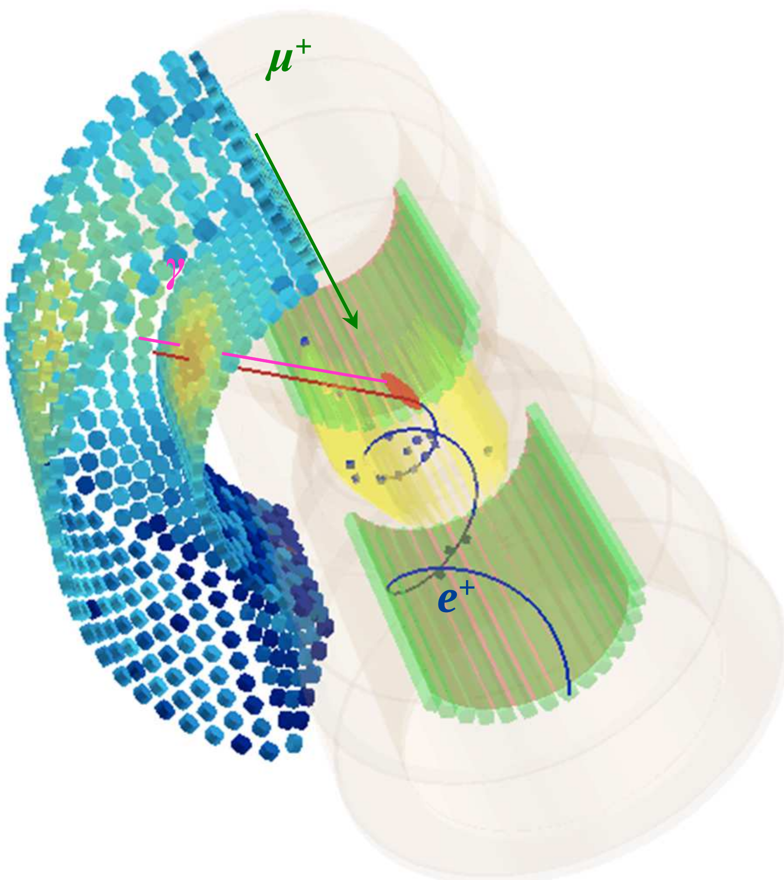

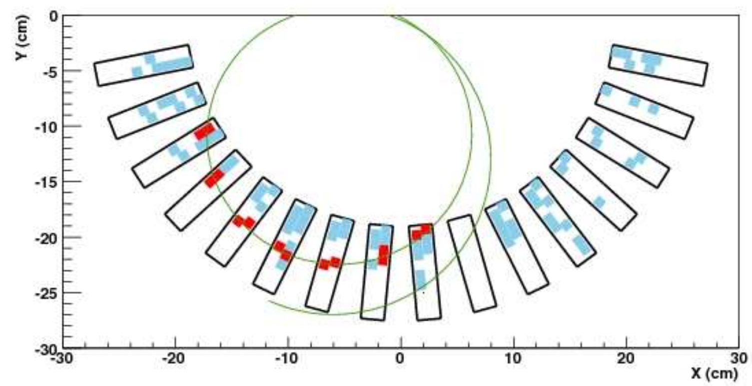

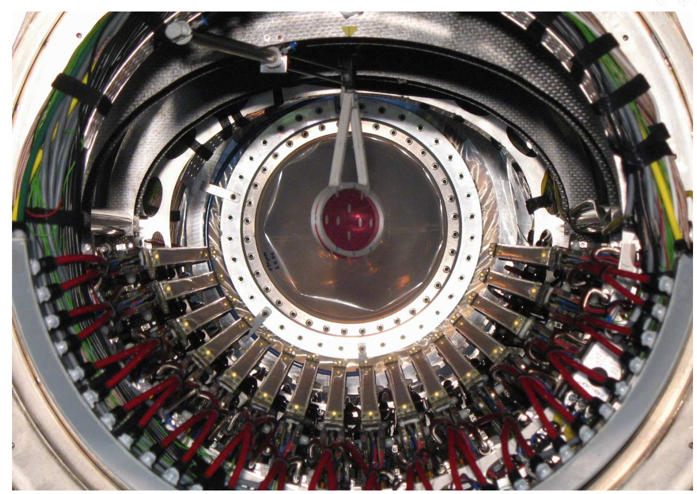

MEG Drift Chamber

- V shaped frame → "no" material in sensitive area
- DC module consists of detector two planes
- middle cathode/cathode hood

  12.5 μm polyimid foil, 250 nm Al deposition
- two wire planes: alternating anode and potential wires
- wires planes shifted by $d_{anode\text{-}pot.wire}$

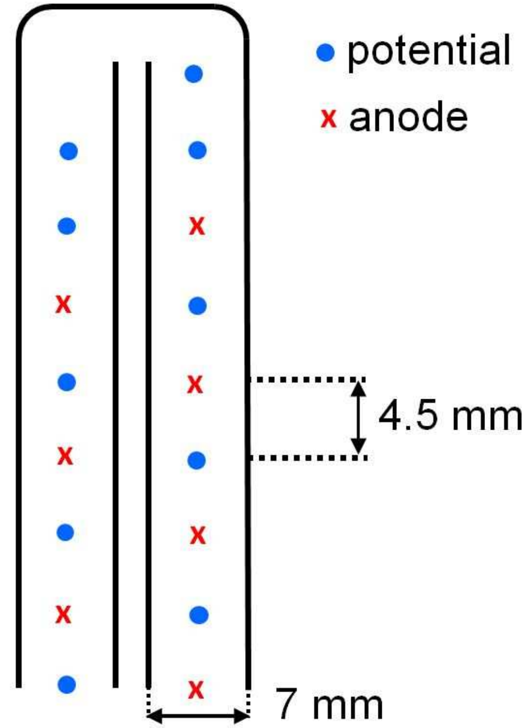

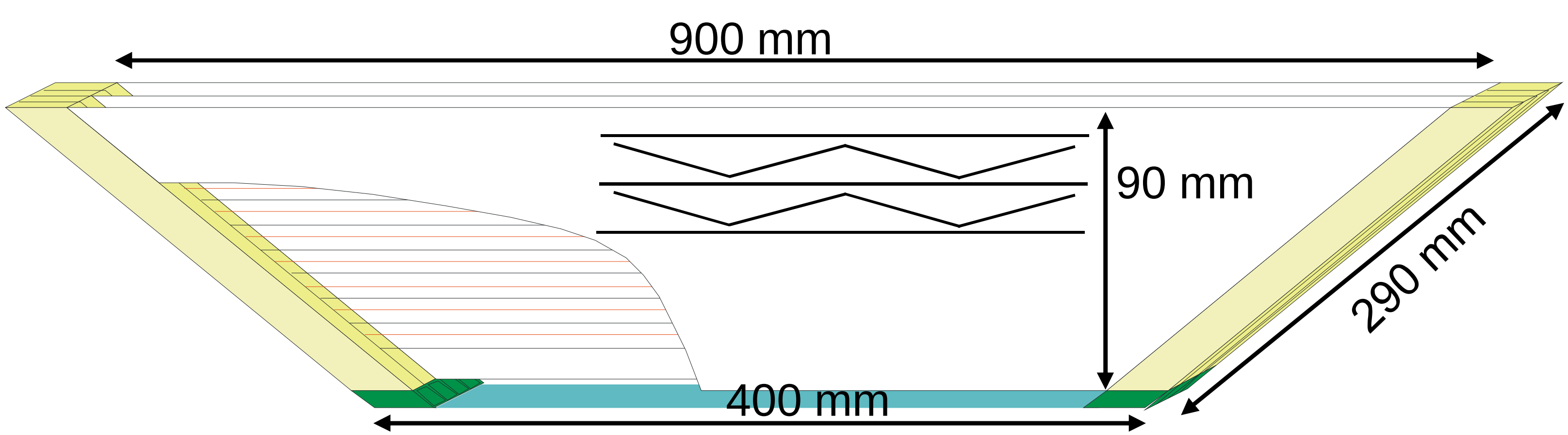

MEG Drift Chamber

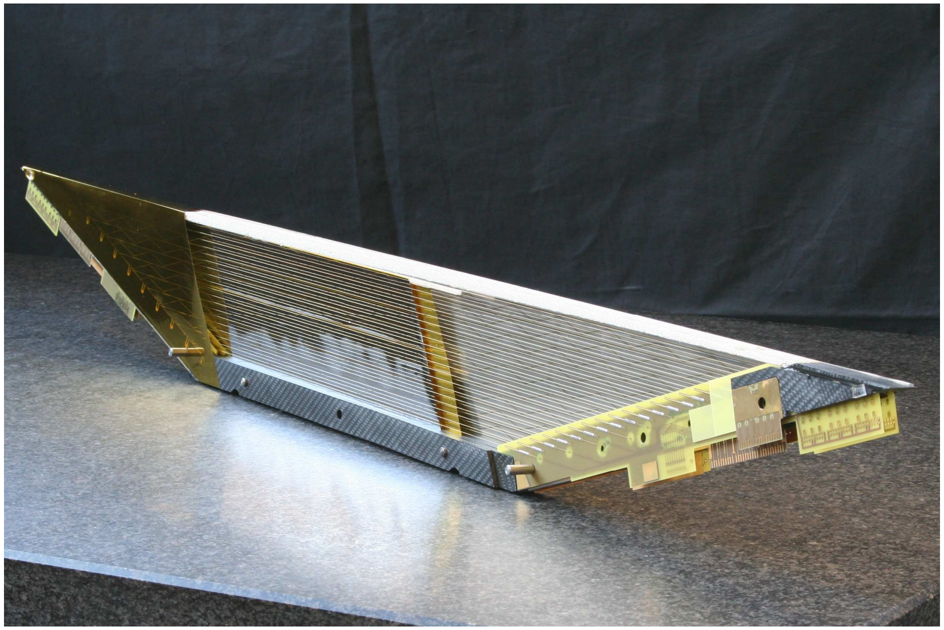

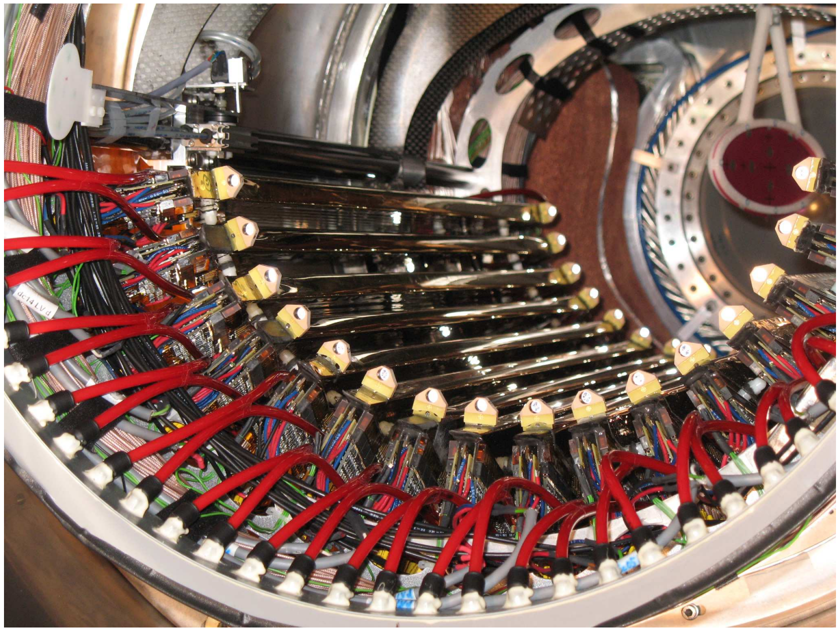

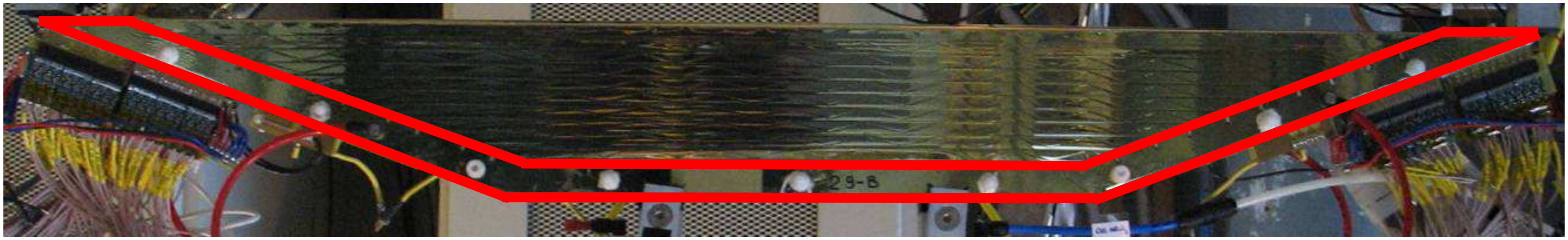

MEG Drift Chamber – Characteristics I

- field geometry:

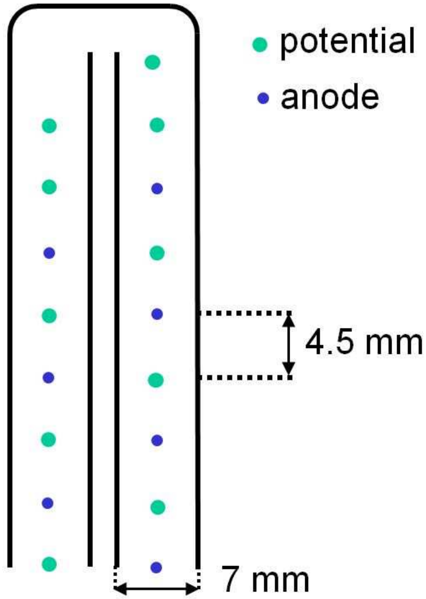

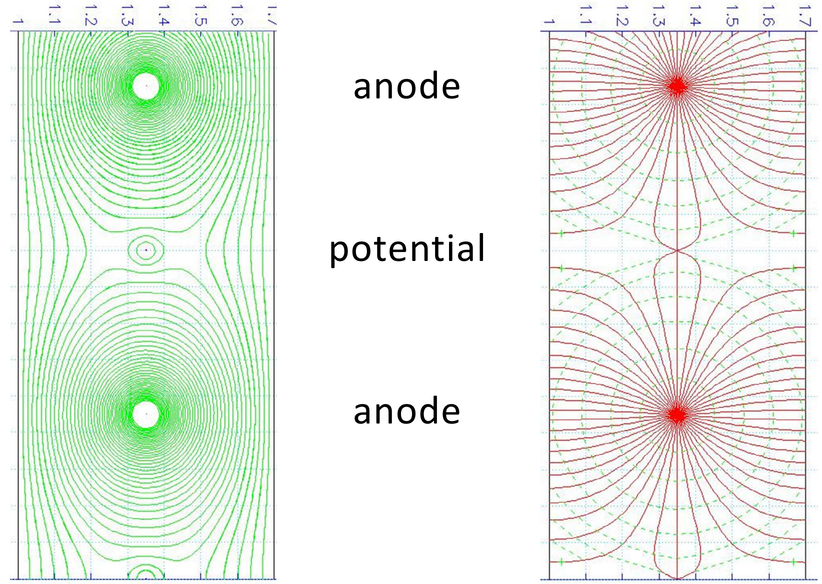

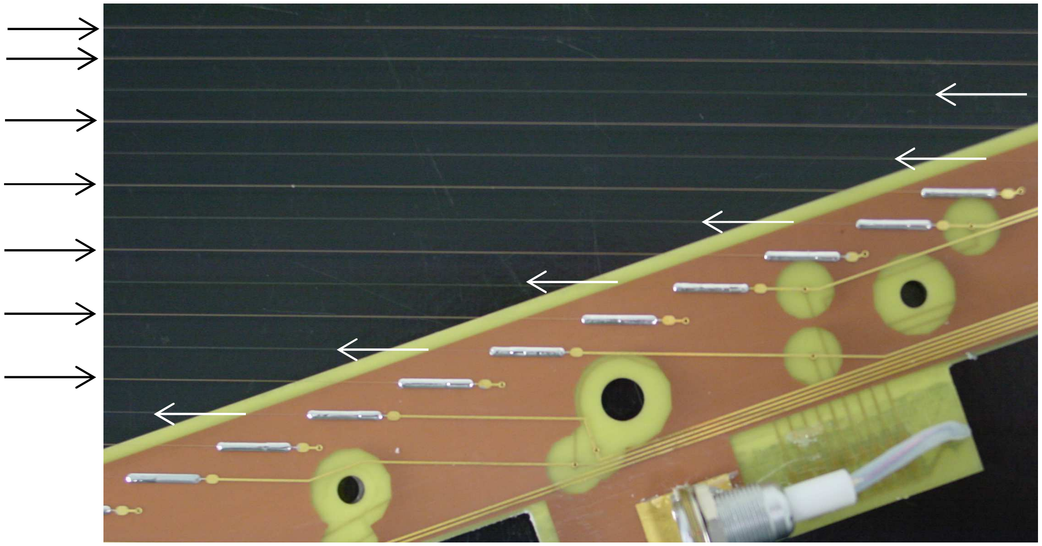

potential wires
Cu 98/Be 2
Ø 50 μm

anode wires
Ni 80/Cr 20
Ø 25 μm

MEG Drift Chamber – Characteristics II

- filling gas He-C_2H_6 (50-50)
  - quite high v_d
  - v_d vs HV plateau
  - long radiation length due to He
  - good HV stability due to C_2H_6

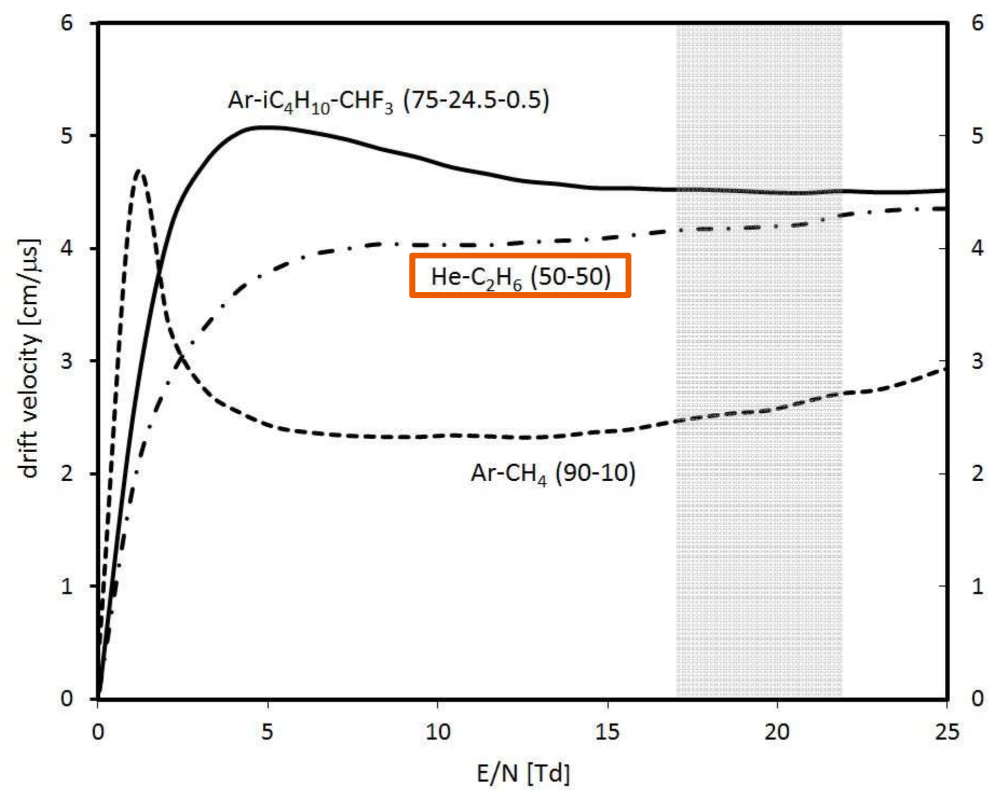

"P10": Ar-CH_4 (90-10)

"magic gas": Ar-iC_4H_{10}-CHF_3 (75-24.5-0.5)

MEG II Cylindrical Drift Chamber

- based on drift chamber of KLOE experiment at DAΦNE (INFN Frascati)
- single, cylindrical volume (L ~200 cm, $Ø_{outer}$ 60 cm)
- wires with stereo angle and U - V views → determination of hit position along wire
- small drift cell sizes (7 mm)
- ~1400 anode wires (gold-plated W, Ø 20 μm) ~7500 cathode/guard wires (silver-plated Al, Ø 40/50 μm)

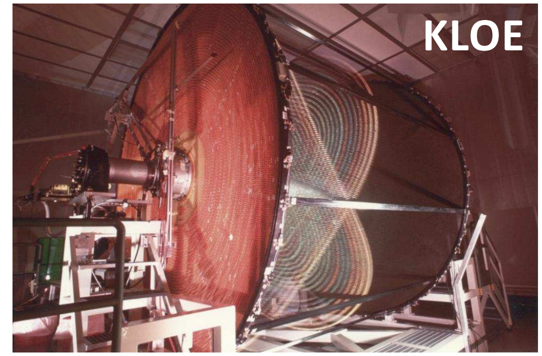

L=3.3m, Ø 4m, 52140 wires

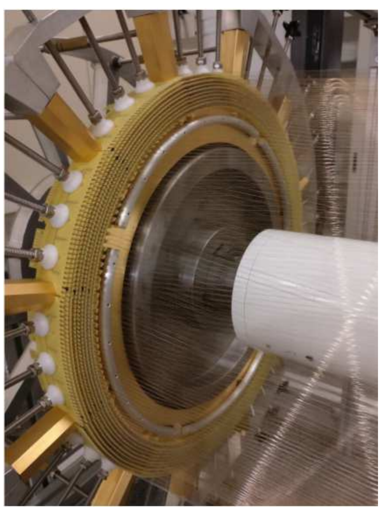

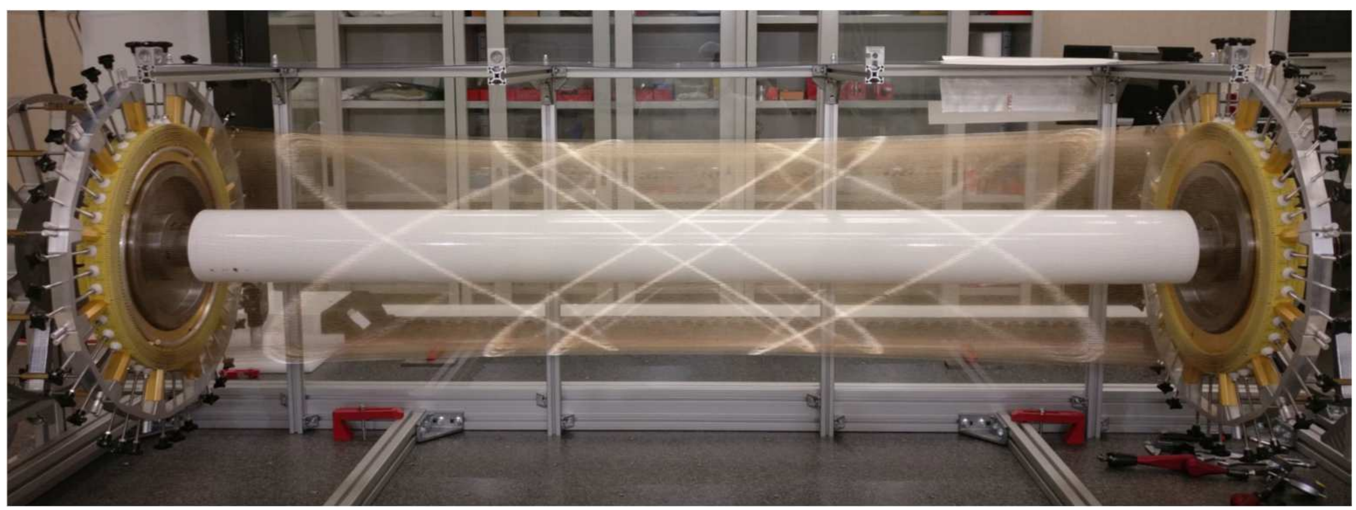

MEG II Cylindrical Drift Chamber

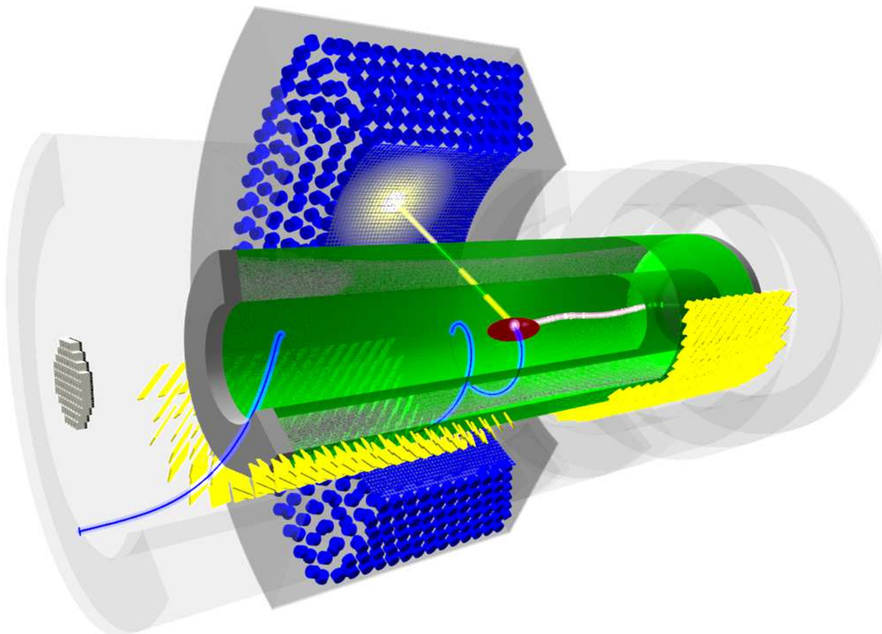

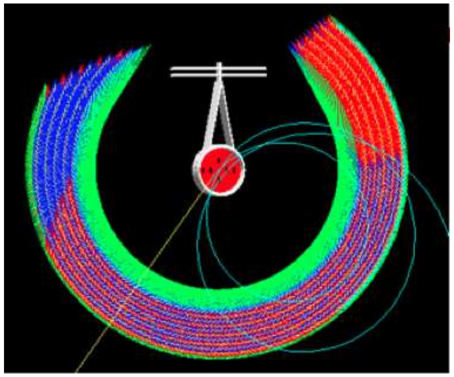

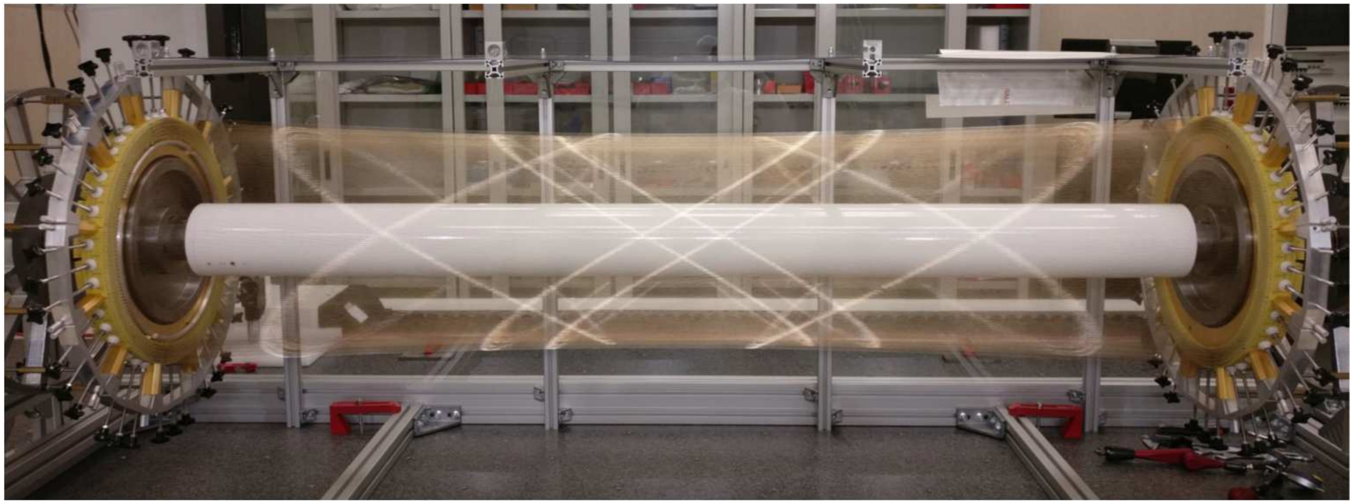

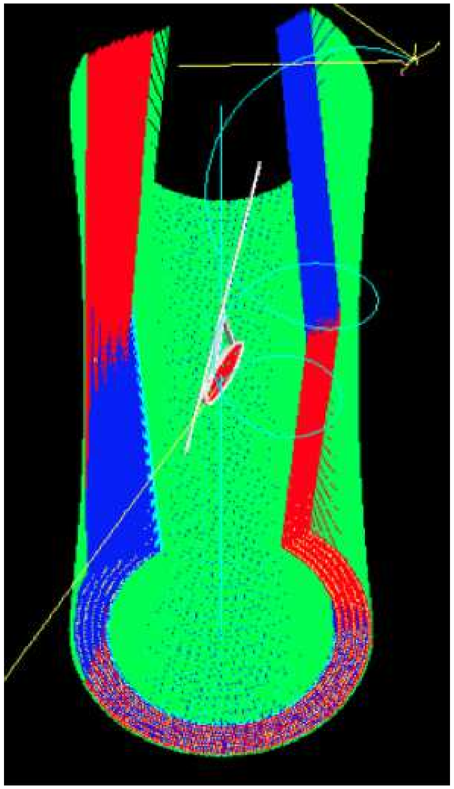

MEG II Cylindrical Drift Chamber

- drift cell geometry (MEG)

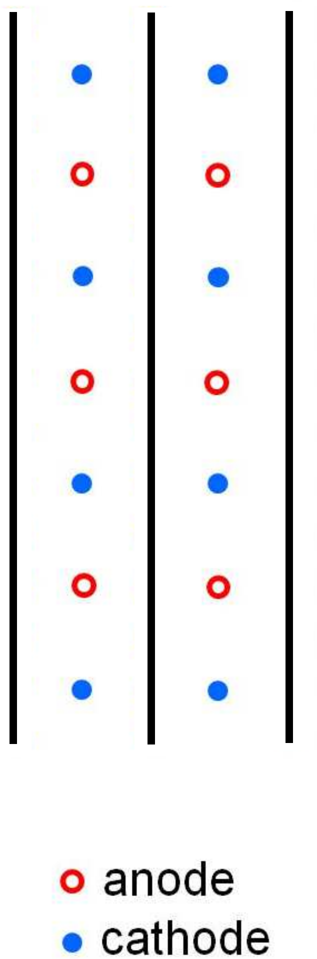

MEG II Cylindrical Drift Chamber

- drift cell geometry

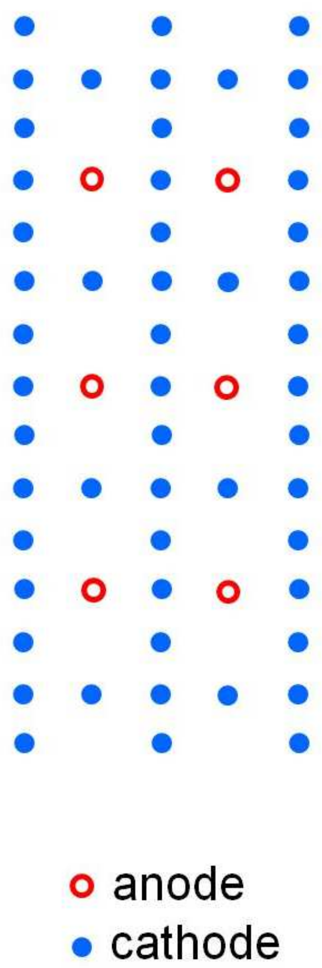

MEG II Cylindrical Drift Chamber

- drift cell geometry

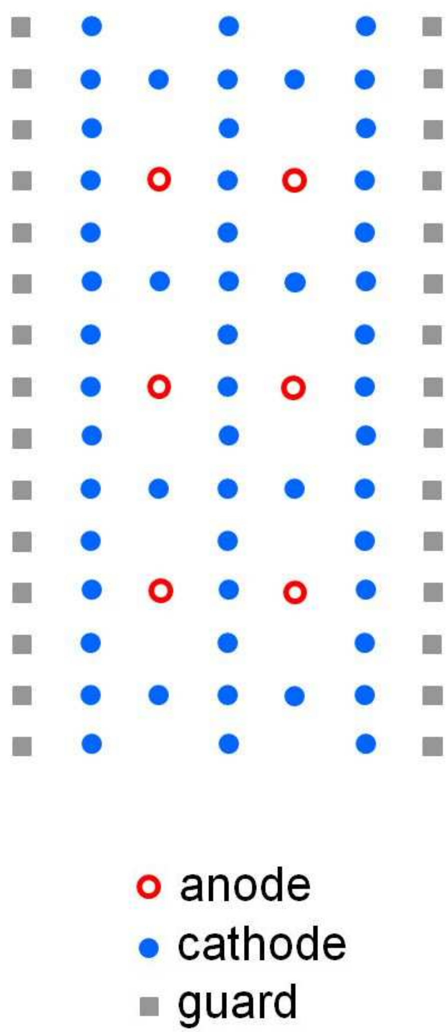

MEG II Cylindrical Drift Chamber

- drift cell geometry

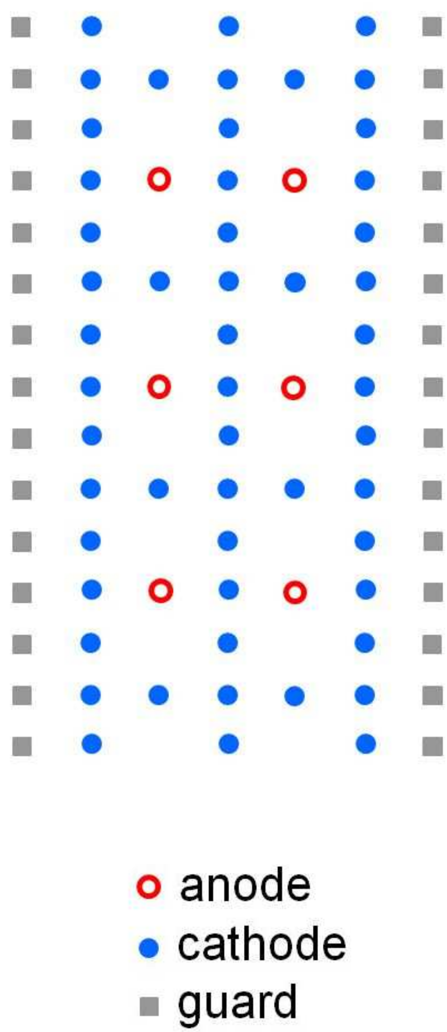

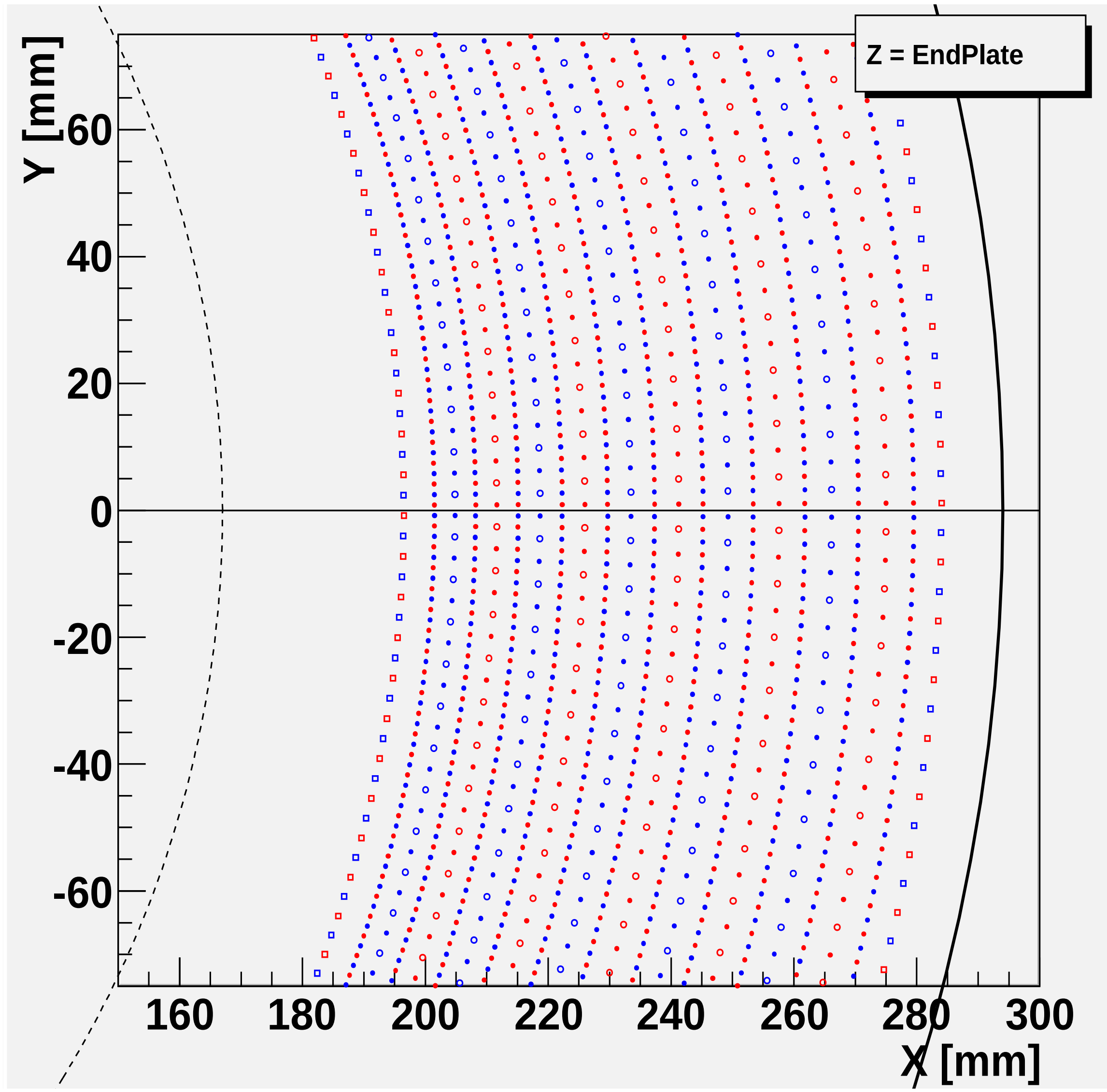

MEG II Cylindrical Drift Chamber

- filling gas He-iC_4H_{10} (85-15 or 90-10)
  - long radiation length due to high He fraction → low multiple scattering, good momentum resolution
  - slow v_d, no v_d vs HV plateau, large diffusion
  - small number of primary ionisation clusters ~13/cm (MEG: He-C_2H_6 50-50: ~35/cm) → large spacing between clusters

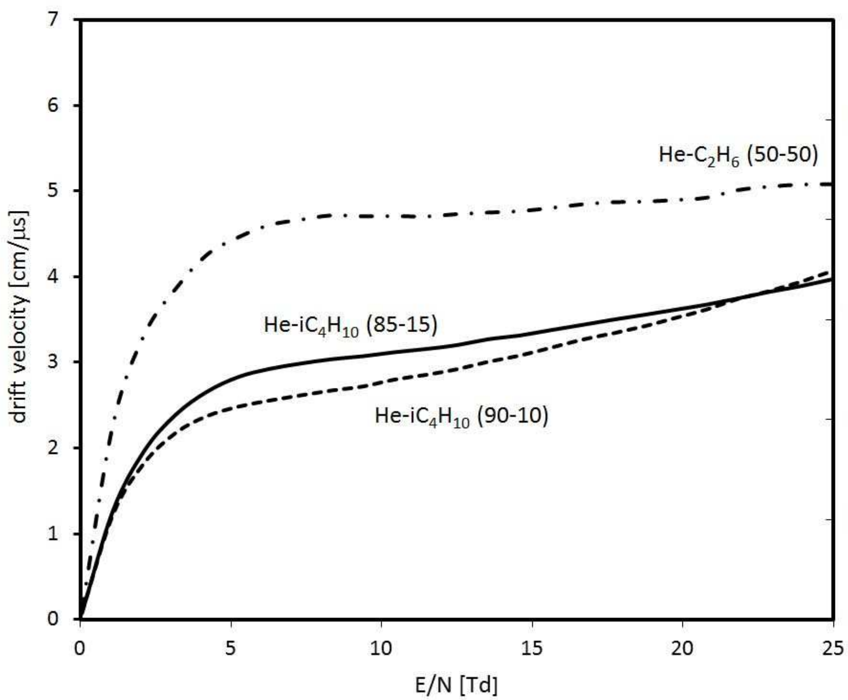

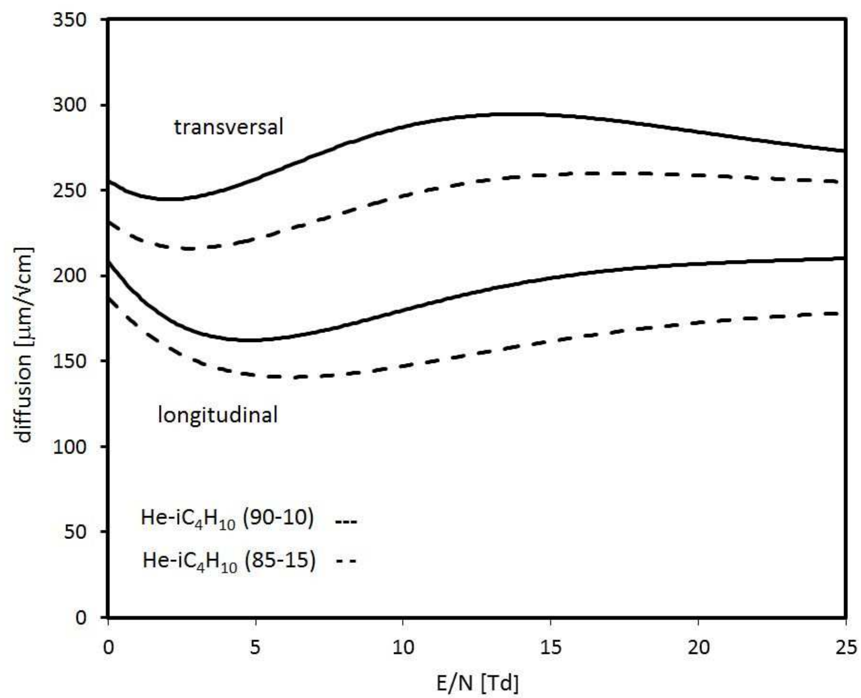

Cluster Counting Technique – in a very tiny nutshell

- MEG: He-C_2H_6 (50-50): ~35 e^-cluster/cm

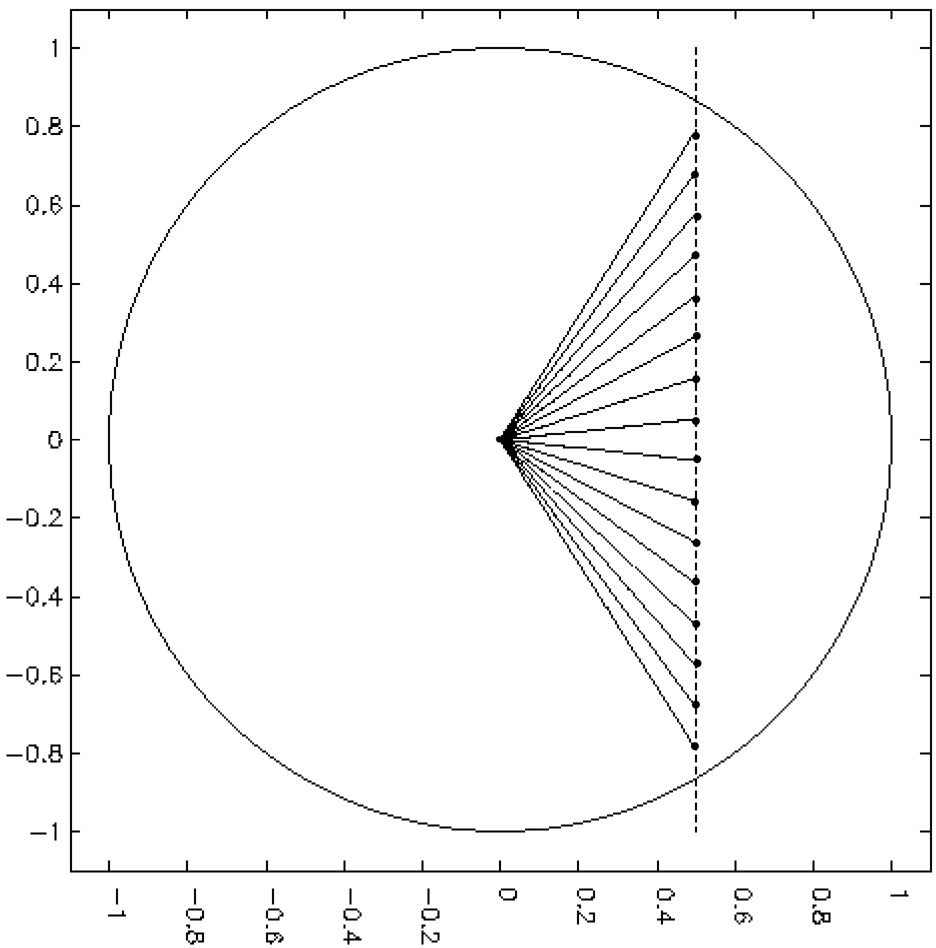

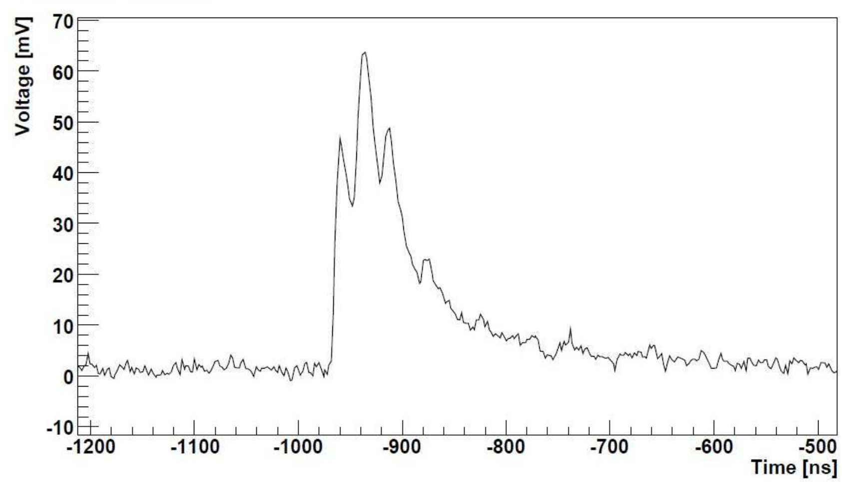

Cluster Counting Technique – in a very tiny nutshell

- MEG: He-C_2H_6 (50-50): ~35 e^-cluster/cm

in reality

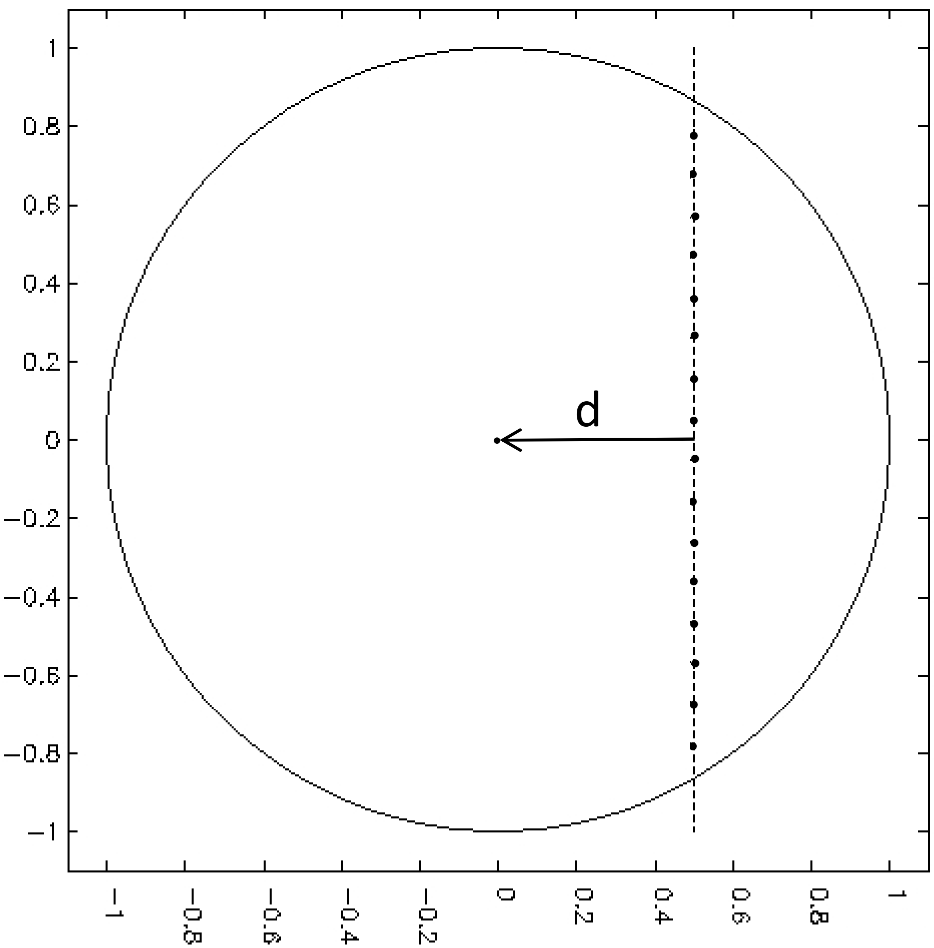

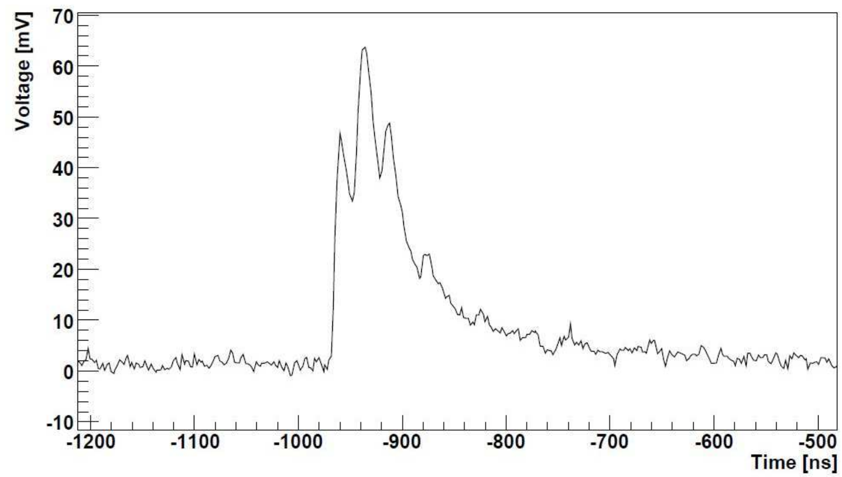

Cluster Counting Technique – in a very tiny nutshell

- MEG II: He-iC_4H_{10} (85-15 or 90-10): ~13 e^-cluster/cm

increased number of "supporting points" along trajectory of incident particle in single drift cell → improvement in
  - ▫ track fitting accuracy and
  - ▫ determination of particle momentum

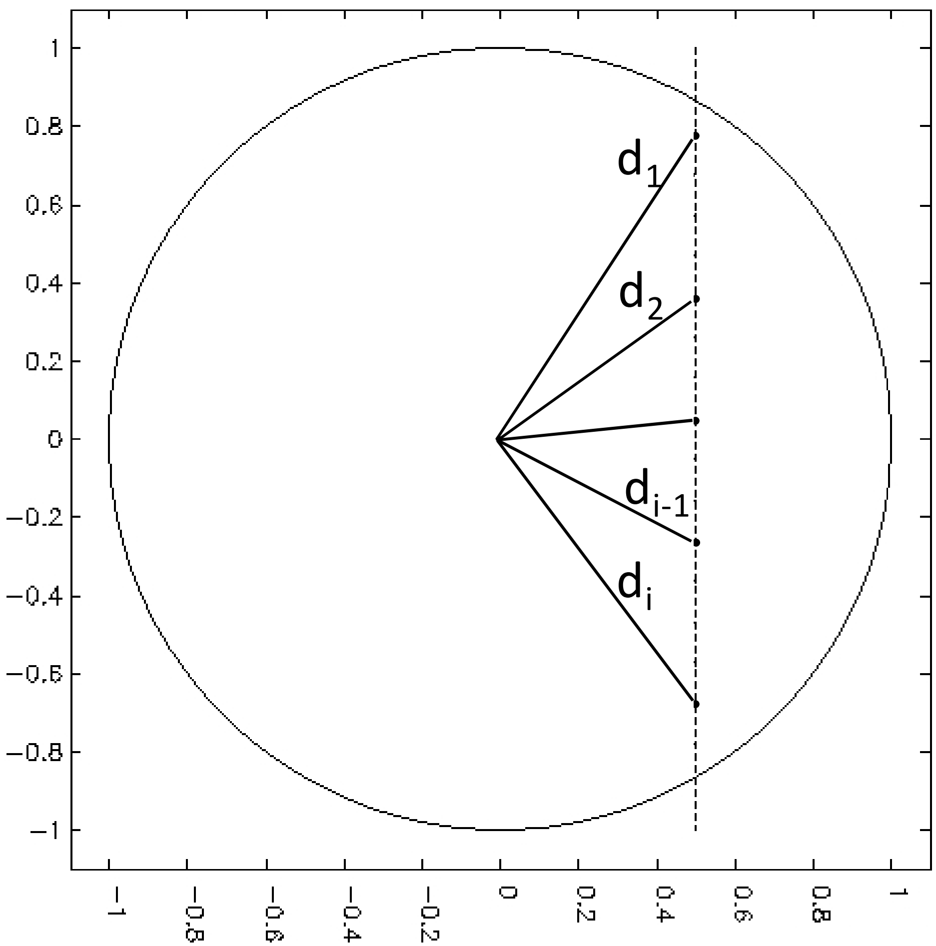

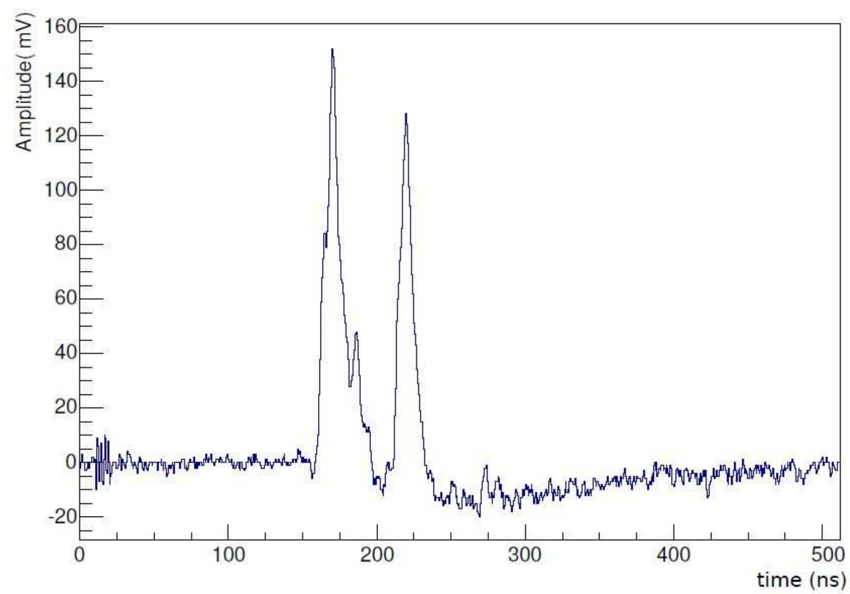

MEG Drift Chambers - Performances

	single hit	resolution (σ) momentum	angular
MEG drift chamber Adam *et al.*, Eur.Phys.J. C (2013) 73:2365	r 210 μm z 800 μm	~330 keV (0.6%)	θ 9.4 mrad ϕ 8.4 mrad
MEG II drift chamber PhD thesis M.Venturini, 2017	r ~110 μm (prototype)	~100 keV (0.2%) (MC)	θ ~6 mrad ϕ ~7 mrad (MC)

Magic Octagon – the Choice of the Filling Gas

quantities in gaseous electronics, like:

- primary ionisation n_0
- drift velocity v_d
- longitudinal, transversal diffusion D_L, D_T
- magnetic deflection angle $\alpha_{Lorentz}$
- size of electron avalanche ($\alpha_{Townsend}$)
- radiation length X_0
- HV stability, breakdown voltage
- sensitivity to radiation induced degradation

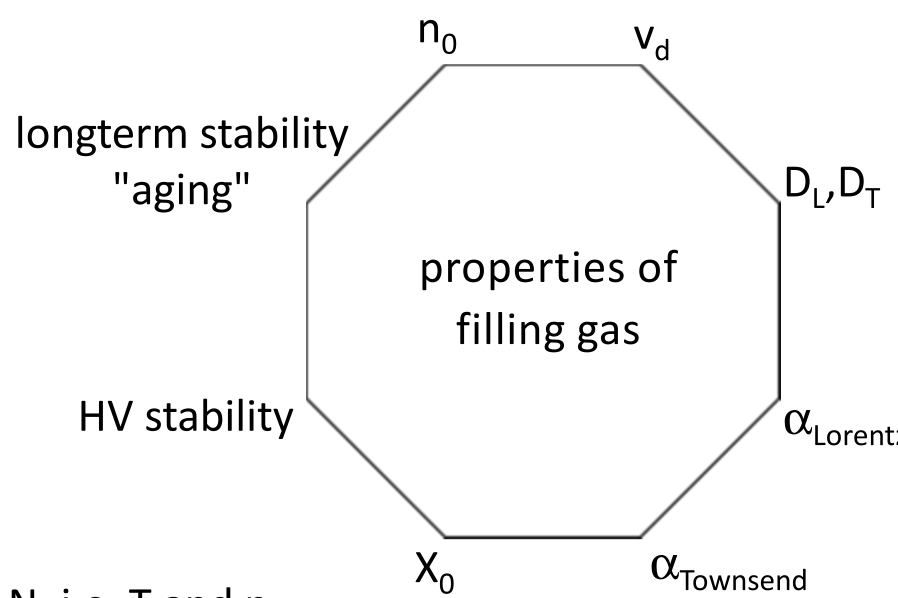

are a function of:

- particle number density N, i.e. T and p
- gas components and mixing ratios
- electrical and/or magnetic fields
- rate environment

and the characteristics of the quantities are connected to each other!

Magic Octagon – the Choice of the Filling Gas

corners of "magic Octagon" are interconnected with elastic bands
→ improving one quantity may worsen another

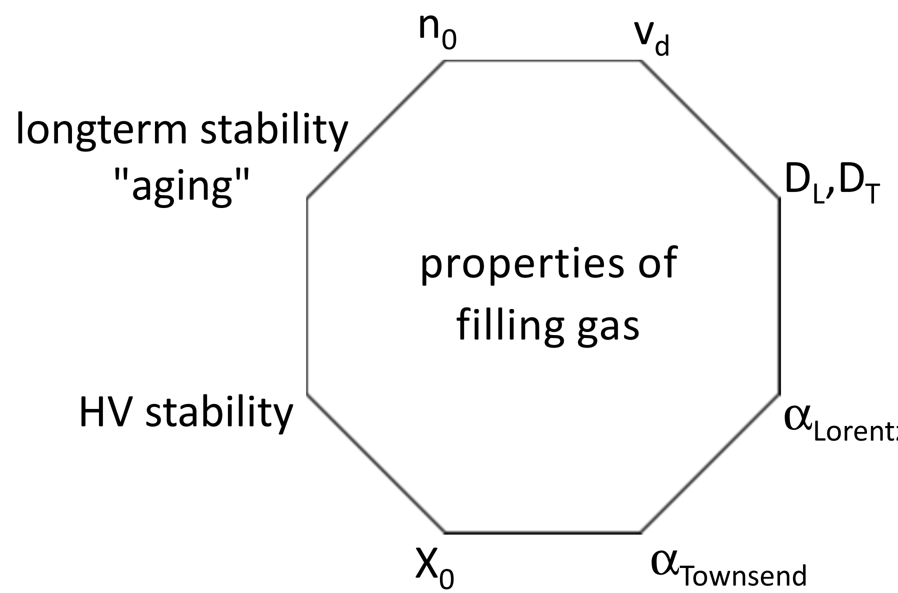

- He:
  - long radiation length X_0
    → good momentum resolution
  - high w-value (41 eV)
    → low primary ionisation
  - large diffusion
    → reduced spatial resolution
  - low breakdown voltage
- hydrocarbons:
  - small w-value (~25 eV)
    → high primary ionisation
  - good HV stability
  - short radiation length X_0
    → reduced momentum resolution
  - bad longterm stability (polymerisation of C-chains)

Magic Octagon – the Choice of the Filling Gas

quantities in gaseous electronics, like:

- primary ionisation n_0
- drift velocity v_d
- longitudinal, transversal diffusion D_L, D_T
- magnetic deflection angle $\alpha_{Lorentz}$
- size of electron avalanche ($\alpha_{Townsend}$)
- radiation length X_0
- HV stability, breakdown voltage
- sensitivity to radiation induced degradation

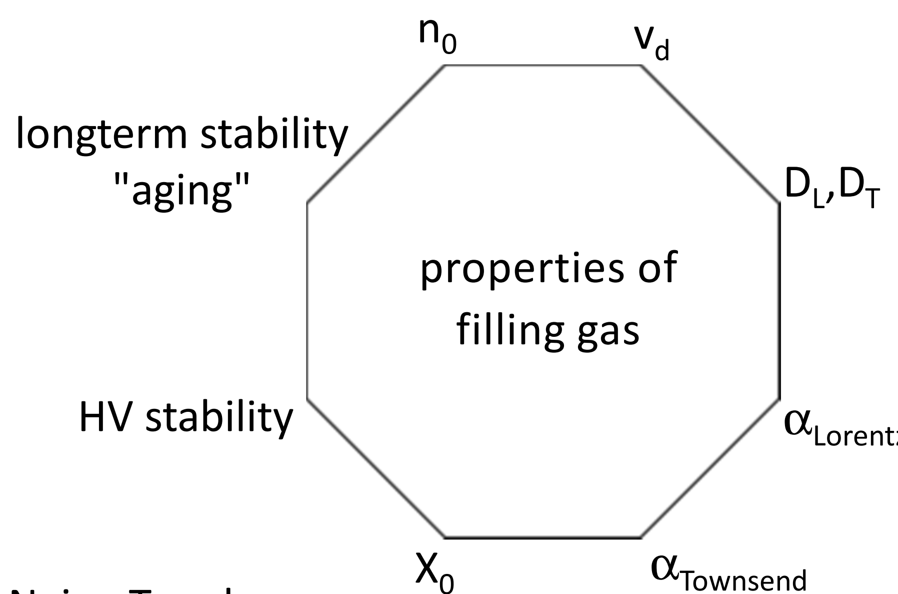

are a function of:

- particle number density N, i.e. T and p
- gas components and mixing ratios
- electrical and/or magnetic fields
- rate environment

and the characteristics of the quantities are connected to each other!

→ The choice of a counting gas is a complicated task with many compromises and weighing up of advantages, disadvantages and risks and
one always has to look at the overall picture!

Wir schaffen Wissen – heute für morgen

Summary:

Milestones in History

- 1908: first wire counter to study natural radioactivity

  E.Rutherford, H.Geiger, Proc. Roy. Soc. A81 (1908) 141-161
  „An Electrical Methode of Counting the Number of α-Particles from Radio-Active Substances"

  H.Geiger, Verh. d. Deutsch. Phys. Ges. 15 (1913) 534-539
  „Über eine einfache Methode zur Zählung von α- und β-Teilchen"

- 1928: Geiger-Müller counter with single electron sensitivity

  H.Geiger, W.Müller, Naturwissenschaften 16 (1928) 617-618
  „Elektronenzählrohr zur Messung schwächster Aktivitäten"

  H.Geiger, W.Müller, Phys. Zeits. 29, 839 (1928) and 30, 489 (1929) and 30, 523 (1929)
  „Das Elektronenzählrohr – Wirkungsweise und Herstellung eines Zählrohrs"

- 1945: proportional tubes

  H.Raether, Ergeb. Exakt. Naturwiss., Band 22 (1949) 73-120
  „ Die Elektronenlawine und ihre Entwicklung"

- 1968: multi-wire proportional chambers

  G.Charpak, Proc.Int.Symp.Nuclear Electronics, Versailles 10-13 Sep 1968

  G.Charpak *et al.*, Nucl. Inst. and Meth. 62 (1968) 262-268
  „ The use of multiwire proportional counters to select and localize charged particles"

Milestones in History

- 1971: drift chamber

  A.H.Walenta, J.Heintze, B.Schürlein, Nucl. Inst. and Meth. 92 (1971) 373-380
  „The multiwire drift chamber a new type of proportional wire chamber“

- 1974: Time Projection Chamber

  D.R.Nygren, LBL Internal report (Feb 1974); D.R.Nygren PEP 198 (1975)

  A.R.Clark *et al.*, „A Proposal for a PEP Facility Based of the Time Projection Chamber“

  D.R.Nygren, Physica Scripta Vol.23 (1981) 584-598, „Future Prospects of the TPC idea“

- 1983:

  GASEOUS DETECTORS FOR PARTICLE PHYSICS: A STILL BLOOMING SOURCE OF NEW INSTRUMENTS

  G. CHARPAK
  CERN, Geneva, Switzerland

  Nuclear Instruments and Methods 217 (1983) 5–7
  North-Holland Publishing Company

- 1986:

  Section I. plenary talks

  WILL GASEOUS DETECTORS SURVIVE THE RAPID PROGRESS IN THE COMPETING TECHNIQUES?

  G. CHARPAK
  CERN, Geneva, Switzerland

  Nuclear Instruments and Methods in Physics Research A252 (1986) 131–136
  North-Holland, Amsterdam

Milestones in History

- 1988: micro-strip gas chamber (MSGC)

  A.Oed, Nucl. Instr. and Meth. A263 (1988) 351-359
  „Position-sensitive detector with micro-strip anode for electron multiplication with gases“

- 1990‘s: huge variety of Micro-Pattern Gaseous detectors (MPGD)

  micro-strip gas chamber, gas electron multiplier, micro-mesh-gaseous structure, micro groove detector, micro gap detector, conteur a trous, micro dot avalanche chamber, micro slit gas detector, …

- 1996: MICRO-MEsh-GAseous Structure (MICROMEGAS)

  Y.Giomataris et al., Nucl. Instr. and Meth. A376 (1996) 29-35
  „MICROMEGAS: a high-granularity position-sensitive gaseous detector for high particle-flux environment“

- 1997: gas electron multiplier (GEM)

  F.Sauli, Nucl. Instr. and Meth. A386 (1997), 531-534
  „GEM: A new concept for electron amplification in gas detectors“

remark:	1978-1998:	Wire Chamber Conference WCC in Vienna
	since 2001:	Vienna Conference on Instrumentation VCI